

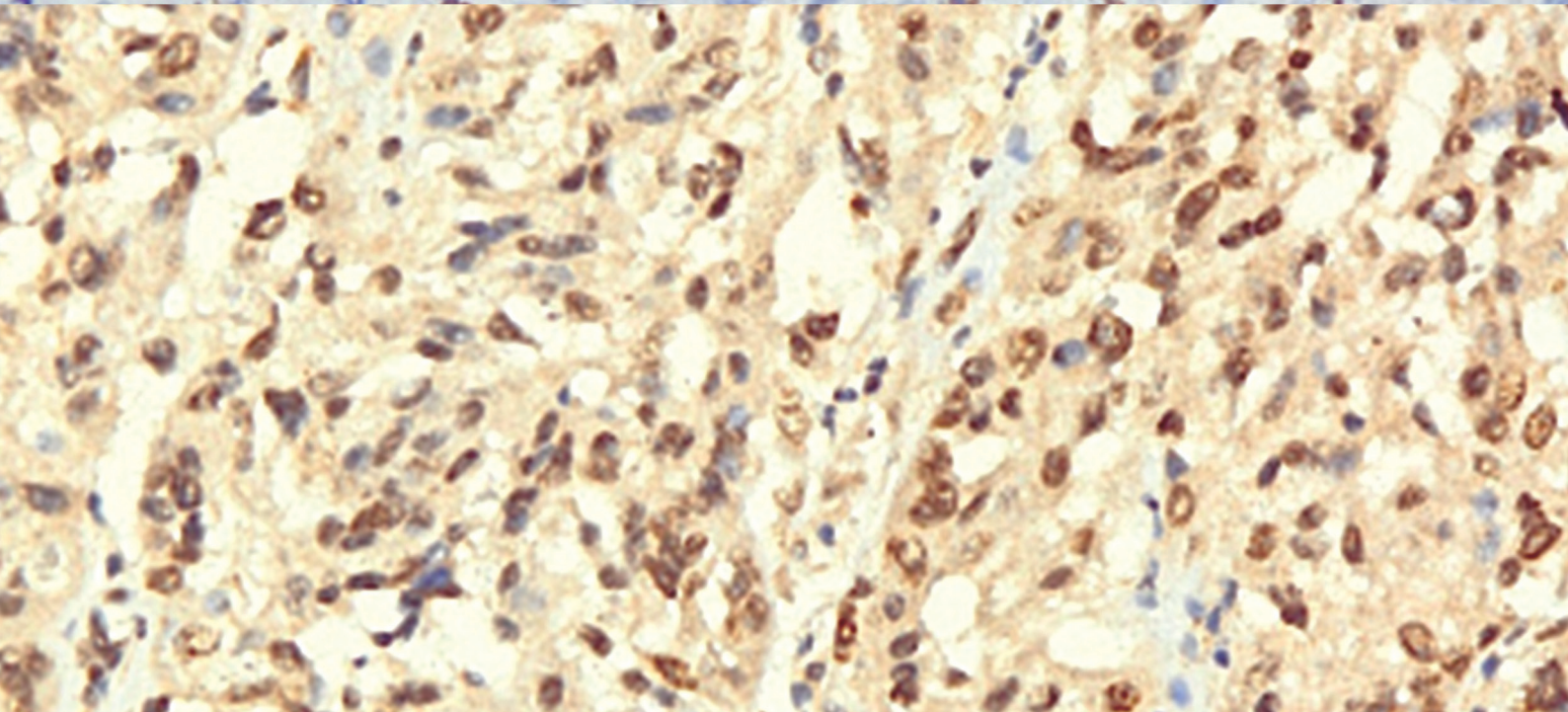
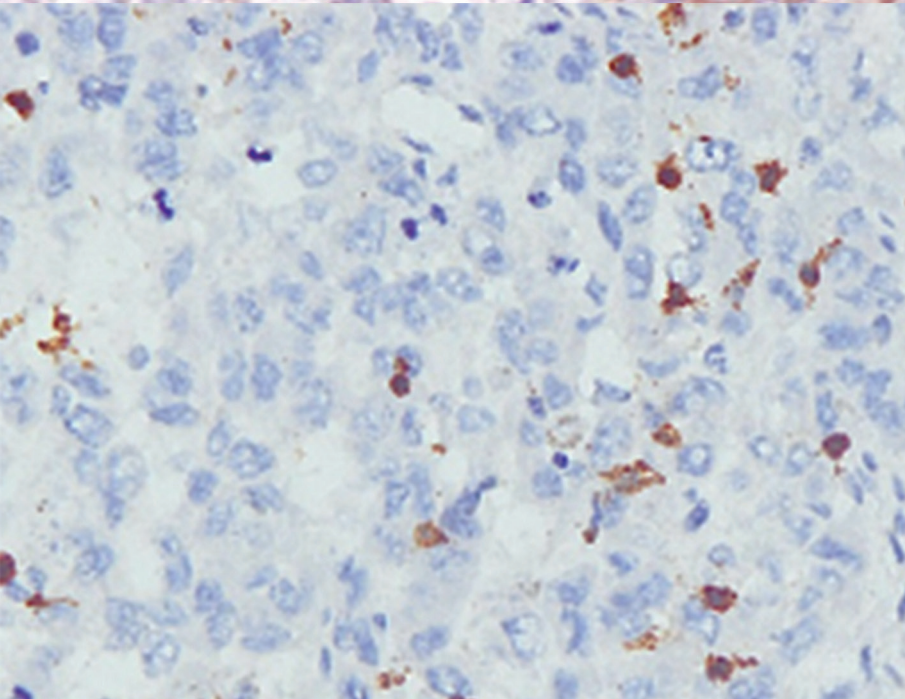
JPTM

Journal of Pathology
and Translational Medicine

May 2018
Vol. 52 / No.3
jpatholm.org
pISSN: 2383-7837
eISSN: 2383-7845



*Let Archived Paraffin
Blocks Be Utilized
for Research with Waiver
of Informed Consent*



Aims & Scope

The *Journal of Pathology and Translational Medicine* is an open venue for the rapid publication of major achievements in various fields of pathology, cytopathology, and biomedical and translational research. The Journal aims to share new insights into the molecular and cellular mechanisms of human diseases and to report major advances in both experimental and clinical medicine, with a particular emphasis on translational research. The investigations of human cells and tissues using high-dimensional biology techniques such as genomics and proteomics will be given a high priority. Articles on stem cell biology are also welcome. The categories of manuscript include original articles, review and perspective articles, case studies, brief case reports, and letters to the editor.

Subscription Information

To subscribe to this journal, please contact the Korean Society of Pathologists/the Korean Society for Cytopathology. Full text PDF files are also available at the official website (<http://jpathol.tn.org>). *Journal of Pathology and Translational Medicine* is indexed by Emerging Sources Citation Index (ESCI), PubMed, PubMed Central, Scopus, KoreaMed, KoMCI, WPRIM, Directory of Open Access Journals (DOAJ), and CrossRef. Circulation number per issue is 700.

Editors-in-Chief

Hong, Soon Won, MD (*Yonsei University, Korea*)

Kim, Chong Jai, MD (*University of Ulsan, Korea*)

Associate Editors

Jung, Chan Kwon, MD (*The Catholic University of Korea, Korea*)

Park, So Yeon, MD (*Seoul National University, Korea*)

Shin, Eunah, MD (*CHA University, Korea*)

Kim, Haeryoung, MD (*Seoul National University, Korea*)

Editorial Board

Ali, Syed Z. (*Johns Hopkins Hospital, U.S.A*)

Avila-Casado, Maria del Carmen (*University of Toronto, Toronto General Hospital UHN, Canada*)

Bae, Young Kyung (*Yeungnam University, Korea*)

Bongiovanni, Massimo (*Centre Hospitalier Universitaire Vaudois, Switzerland*)

Cho, Kyung-Ja (*University of Ulsan, Korea*)

Choi, Yeong-Jin (*The Catholic University of Korea, Korea*)

Choi, Yoo Duk (*Chonnam National University, Korea*)

Chung, Jin-Haeng (*Seoul National University, Korea*)

Gong, Gyungyub (*University of Ulsan, Korea*)

Fadda, Guido (*Catholic University of the Sacred Heart, Italy*)

Grignon, David J. (*Indiana University, U.S.A.*)

Ha, Seung Yeon (*Gachon University, Korea*)

Han, Jee Young (*Inha University, Korea*)

Jang, Se Jin (*University of Ulsan, Korea*)

Jeong, Jin Sook (*Dong-A University, Korea*)

Kang, Gyeong Hoon (*Seoul National University, Korea*)

Katoh, Ryohei (*University of Yamanashi, Japan*)

Kerr, Keith M. (*Aberdeen University Medical School, UK*)

Kim, Aeere (*Korea University, Korea*)

Kim, Jang-Hee (*Ajou University, Korea*)

Kim, Jung Ho (*Seoul National University, Korea*)

Kim, Kyoung Mee (*Sungkyunkwan University, Korea*)

Kim, Kyu Rae (*University of Ulsan, Korea*)

Kim, Se Hoon (*Yonsei University, Korea*)

Kim, Woo Ho (*Seoul National University, Korea*)

Kim, Youn Wha (*Kyung Hee University, Korea*)

Ko, Young Hye (*Sungkyunkwan University, Korea*)

Koo, Ja Seung (*Yonsei University, Korea*)

Lee, C. Soon (*University of Western Sydney, Australia*)

Lee, Hye Seung (*Seoul National University, Korea*)

Lee, Kyung Han (*Sungkyunkwan University, Korea*)

Lee, Sug Hyung (*The Catholic University of Korea, Korea*)

Lkhagvadorj, Sayamaa (*Mongolian National University of Medical Sciences, Mongolia*)

Moon, Woo Sung (*Chonbuk University, Korea*)

Ngo, Quoc Dat (*Ho Chi Minh University of Medicine and Pharmacy, VietNam*)

Park, Young Nyun (*Yonsei University, Korea*)

Ro, Jae Y. (*Cornell University, The Methodist Hospital, U.S.A.*)

Romero, Roberto (*National Institute of Child Health and Human Development, U.S.A.*)

Schmitt, Fernando (*IPATIMUP [Institute of Molecular Pathology and Immunology of the University of Porto], Portugal*)

Shahid, Pervez (*Aga Khan University, Pakistan*)

Sung, Chang Ohk (*University of Ulsan, Korea*)

Tan, Puay Hoon (*National University of Singapore, Singapore*)

Than, Nandor Gabor (*Semmelweis University, Hungary*)

Tse, Gary M. (*Prince of Wales Hospital, Hongkong*)

Vielh, Philippe (*International Academy of Cytology Gustave Roussy Cancer Campus Grand Paris, France*)

Wildman, Derek (*University of Illinois, U.S.A.*)

Yatabe, Yasushi (*Aichi Cancer Center, Japan*)

Yoon, Bo Hyun (*Seoul National University, Korea*)

Yoon, Sun Och (*Yonsei University, Korea*)

Statistics Editors

Kim, Dong Wook (*National Health Insurance Service Ilsan Hospital, Korea*)

Lee, Hye Sun (*Yonsei University, Korea*)

Manuscript Editor

Chang, Soo-Hee (*InfoLumi Co., Korea*)

Contact the Korean Society of Pathologists/the Korean Society for Cytopathology

Publishers: Jae Bok Park, MD, Hye Kyoung Yoon, MD

Editors-in-Chief: Soon Won Hong, MD, Chong Jai Kim, MD

Published by the Korean Society of Pathologists/the Korean Society for Cytopathology

Editorial Office

Room 1209 Gwanghwamun Officia, 92 Saemunan-ro, Jongno-gu, Seoul 03186, Korea

Tel: +82-2-795-3094 Fax: +82-2-790-6635 E-mail: office@jpathol.tn.org

#1508 Renaissancetower, 14 Mallijae-ro, Mapo-gu, Seoul 04195, Korea

Tel: +82-2-593-6943 Fax: +82-2-593-6944 E-mail: office@jpathol.tn.org

Printed by iMiS Company Co., Ltd. (JMC)

Jungang Bldg. 18-8 Wonhyo-ro 89-gil, Yongsan-gu, Seoul 04314, Korea

Tel: +82-2-717-5511 Fax: +82-2-717-5515 E-mail: ml@smileml.com

Manuscript Editing by InfoLumi Co.

210-202, 421 Pangyo-ro, Bundang-gu, Seongnam 13522, Korea

Tel: +82-70-8839-8800 E-mail: infolumi.chang@gmail.com

Front cover image: Immunoexpression of CD8⁺ T cell number ≥ 25 , programmed death-ligand1 $\geq 5\%$ and nuclear factor κ B on acral malignant melanoma (Figs. 1-3). p167.

© Copyright 2018 by the Korean Society of Pathologists/the Korean Society for Cytopathology

© Journal of Pathology and Translational Medicine is an Open Access journal under the terms of the Creative Commons Attribution Non-Commercial License (<http://creativecommons.org/licenses/by-nc/4.0>).

© This paper meets the requirements of KS X ISO 9706, ISO 9706-1994 and ANSI/NISO Z.39.48-1992 (Permanence of Paper).

This journal was supported by the Korean Federation of Science and Technology Societies Grant funded by the Korean Government.

CONTENTS

REVIEW

141 Let Archived Paraffin Blocks Be Utilized for Research with Waiver of Informed Consent

Yong-Jin Kim, Jeong Sik Park, Karam Ko, Chang Rok Jeong

ORIGINAL ARTICLES

148 Molecular Screening of Small Biopsy Samples Using Next-Generation Sequencing in Korean Patients with Advanced Non-small Cell Lung Cancer: Korean Lung Cancer Consortium (KLCC-13-01)

Bo Mi Ku, Mi Hwa Heo, Joo-Hang Kim, Byoung Chul Cho, Eun Kyung Cho, Young Joo Min, Ki Hyeong Lee, Jong-Mu Sun, Se-Hoon Lee, Jin Seok Ahn, Keunchil Park, Tae Jung Kim, Ho Yun Lee, Hojoong Kim, Kyung-Jong Lee, Myung-Ju Ahn

157 Utility of BRAF VE1 Immunohistochemistry as a Screening Tool for Colorectal Cancer Harboring *BRAF* V600E Mutation

Jeong-Hwa Kwon, Byung-Kwan Jeong, Yong Sik Yoon, Chang Sik Yu, Jihun Kim

164 The Major Role of NF- κ B in the Depth of Invasion on Acral Melanoma by Decreasing CD8⁺ T Cells

Hermin Aminah Usman, Bethy S. Hernowo, Maringan Diapari Lumban Tobing, Reti Hindritiani

171 Cytologic Diagnosis of Noninvasive Follicular Thyroid Neoplasm with Papillary-like Nuclear Features and Its Impact on the Risk of Malignancy in the Bethesda System for Reporting Thyroid Cytopathology: An Institutional Experience

Milim Kim, Joung Eun Kim, Hyun Jeong Kim, Yul Ri Chung, Yoonjin Kwak, So Yeon Park

CASE REPORTS

179 Duodenal Adenocarcinoma of Brunner Gland Origin: A Case Report

Ji Hye Moon, Kyoungbun Lee, Han-Kwang Yang, Woo Ho Kim

183 Erdheim-Chester Disease Involving Lymph Nodes and Liver Clinically Mimicking Lymphoma: A Case Report

Yeoun Eun Sung, Yoon Seo Lee, Jieun Lee, Kyo Young Lee

191 Post-transplant Amputation Traumatic Neuroma of the Hilum and Extrahepatic Duct in a Liver Donor

Na Rae Kim, Hyun Yee Cho, Dong Hae Chung, Keon Kuk Kim, Jae Hee Cho, Seung Joon Choi

195 Expression of CD34 and β -Catenin in Malignant Rhabdoid Tumor of the Liver Mimicking Proximal-Type Epithelioid Sarcoma

Woo Cheal Cho, Fabiola Balarezo

198 Secretory Carcinoma Arising in a Fibroadenoma: A Brief Case Report

Sharon Lim, Min Keun Shim, Eun Yoon Cho, Soo Youn Cho

202 Aberrant CD3 Expression in a Relapsed Plasma Cell Neoplasm

Jai-Hyang Go

206 Merkel Cell Carcinoma Metastatic to Pleural Fluid: A Case Report

Ye-Young Rhee, Soo Hee Kim, Eun Kyung Kim, Se Hoon Kim

Instructions for Authors for *Journal of Pathology and Translational Medicine* are available at <http://jpatholm.org/authors/authors.php>

Let Archived Paraffin Blocks Be Utilized for Research with Waiver of Informed Consent

Yong-Jin Kim · Jeong Sik Park¹
Karam Ko² · Chang Rok Jeong³

Department of Pathology, School of Medicine,
Kyungpook National University, Daegu;

¹Department of Philosophy, College of
Humanities, Kyungpook National University,
Daegu; ²Korea Study Group for Biomedical
Ethics, Seoul; ³Department of Ethics Education,
Teachers' College, Kyungpook National University,
Daegu, Korea

Received: January 5, 2018

Accepted: February 7, 2018

Corresponding Author

Chang Rok Jeong, PhD
Department of Ethics Education, Teachers' College,
Kyungpook National University, 80 Daehak-ro
Buk-gu, Daegu 41566, Korea
Tel: +82-53-950-5868
Fax: +82-53-950-5947
E-mail: canthos@hanmail.net

Advances in biomedical and genetic research have contributed to more effective public health improvement via bench-to-bed research and the emergence of personalized medicine. This has certainly showcased the importance of archived human tissues, especially paraffin-embedded blocks in pathology. Currently in Korea, undue legislative regulations of the Bioethics and Safety Act suspend and at times discourage studies from taking place. In this paper, the authors underline the value of paraffin blocks in the era of personalized and translational medicine. We discuss detailed clauses regarding the applicability of paraffin blocks from a legal perspective and compare Korea's regulations with those of other countries. The necessity for allowing waived consent and Institutional Review Board (IRB) approval will be argued throughout. The authors suggest that researchers declare the following to obtain IRB approval and waiver of informed consents: research could not be practically carried out without a waiver of consent; the proposed research presents no more than minimal risk of harm to subjects, and the waiver of consent will not adversely affect the rights and welfare of subjects; and research will not utilize a tissue block if only 1 is available for each subject, to allow future clinical use such as re-evaluation or further studies.

Key Words: Paraffin block; Bioethics and Safety Act; Pathology research; Human biospecimen; Written consent

Formalin-fixed paraffin-embedded blocks (hereinafter 'paraffin blocks') are human tissue derivatives obtained during routine diagnostic or therapeutic procedures in hospitals. Tissues procured from patients are referred to the pathology department, cut into sections, and embedded into paraffin blocks for histopathologic examination. The blocks are stored in the archives of pathology laboratories for many years to be available for possible tests and re-examinations.

Paraffin blocks also serve as legal proof of diagnostic or therapeutic procedures, such as surgery, having been carried out. Therefore, paraffin blocks are regarded as a part of the medical records for hospitals and are kept for at least 10 years in most hospitals.¹ With increasing reliance on biopsy for diagnosis, tissue samples are collected daily and produced in astronomical numbers in hospitals all over Korea. Assuming that these blocks have been retained since establishment of a hospital, millions of paraffin blocks may be archived in each hospital today.

Rapid advances in genomic and molecular research methods, such as extracting DNA from blocks and studying it in genetic

research, have highlighted the value of paraffin blocks. Linking paraffin blocks with existing clinical databases in biomedical research will not only save time for research, but is also safe and does not cause any physical or psychological harm to patients. This type of biospecimen archival research was responsible for finding the link between lung cancer and smoking, identification of *BRCA1* and *BRCA2* genes, advances in breast cancer research, and many other bench-to-bed findings. Research using such biospecimens can allow prediction of toxicity, evaluation of gene expression in normal and diseased tissue, and study of biomarkers for assessing therapeutic efficacy, and assist in clinical research to evaluate patient risk stratification, prognostication, and pharmacogenomics.² This potential will enhance the quality of medicine and hasten developments in curing disease, thereby improving the health of the general public. The enormous potential of achieving medico-scientific discoveries by attaining diverse bio-data from a clinical database without any risk to subjects makes paraffin block research invaluable.

These potentials can change and overcome current limitations

faced in hospitals between screening and treatment in diverse fields of clinical practice. They will also lead to improved personalized treatment and the development of more targeted and efficient drugs. Because hospitals have stored an immense number of biospecimens over the years, research utilizing these materials is key to improving public health and bringing medicine to a new level.

However, for such beneficial research to be launched in Korea, it must first gain consent and approval via Institutional Review Board (IRB) review, according to the current Bioethics and Safety Acts. However, the existing legislation on human biospecimens is ambiguous. Judgements rely on how a committee interprets the act; often, research is not approved and therefore discouraged.

The authors examine the current standpoint of Korea's Bioethics and Safety Acts and compare it with those of other countries that hold different perspectives on research utilizing paraffin blocks. We then suggest ethical and legal ways to utilize paraffin blocks in research.

EXEMPTION OF WRITTEN CONSENT FOR RESEARCH OF INSTITUTIONAL REVIEW BOARD

Human derivatives defined in the 'Bioethics and Safety Act' (hereafter abbreviated as the 'Bioethics Act', 2015 Chapter 1 General, Article 2) are plasma, chromosomes, DNA, RNA, proteins, and the like derived from human body constituents. According to this act, research using paraffin blocks defined as human derivatives is required to obtain the consent of the provider and approval of an institutional committee.³ Such regulation seems logically applicable when research requires collection of tissue or any other form of human derivatives directly from subjects.

Currently in Korea, however, human derivatives in paraffin blocks are not collected for research purposes, but are procured for clinical diagnosis and treatment. During the process of procurement, tissue is extracted with patient consent. In addition, tissue is a disposable human derivative in accordance with Article 2 clause 5 of the Wastes Management Act (body tissue obtained in hospital). Thus, a consent for surgery should be considered consent to "extraction" and result in a legal process for treatment of "extracted material." Consenting to extraction should be seen as abandoning the tissue once the original purpose, for example surgical operation, has been fulfilled. It is questionable whether additional consent of the material provider (patient) is needed when using material that has been abandoned or agreed

to be discarded for research. This differs from human derivatives extracted for research purposes, which require consent from participants before a study can commence. Conversely, if the patient wants to dispose of his/her surgically extracted tissue and/or did not wish for it to be used for research, use of the tissue would require additional consent. Therefore, some IRB committees assert that paraffin blocks for which consent for research with human derivatives has not been acquired cannot be used as a resource for study.

In fact, when an anonymous institutional committee inquired about the use of paraffin blocks for research, the Ministry of Health and Welfare's response was as follows.³

Question: I am wondering if a study using paraffin blocks should be deliberated in accordance with studies of human derivatives. When a paraffin block is produced for diagnostic purposes and the researchers would like to use it for further studies (including genetic tests) after diagnosis, do the researchers require approval of the plan and agreement before the research, such as research involving human subjects, or can they go ahead and proceed without the consent? In case of paraffin blocks, it is a kind of medical record and it is not produced for the purpose of research. So how should we review this research plan?⁴

Answer: Studies using paraffin blocks are also human-derived studies. Although the paraffin block after the medical diagnosis may be regarded as one of the medical records, the cost of the paraffin block production is paid by the patient and used for diagnostic purposes. Thus using the block for research purpose is an "unintended purpose use." Therefore, IRB review and consent is required in accordance with the study of the human derivatives. It is not exempted from acquiring consent, and necessary to review the research plan in accordance with Article 16 clause 3 of the Act and consider whether or not the written consent should be waived.

According to this answer, the following facts may be deduced: (1) paraffin block study is a study of human derivatives, and for the paraffin blocks initially intended for diagnostic purpose, use in research is considered an "unintended purpose use." Therefore, the IRB review and approval process is necessary in accordance with the study of human derivatives. (2) The decision of whether or not to allow waiver of consent may not be based on the fact that the material in question was "originally produced for diagnostic purpose," but should be made in accordance with Article 16 (3) of the Bioethics Act (risks and benefits in human subjects and obtaining written consent). This gives discretionary power to the IRB committee. While the answer to the question is accurate, many IRB committees still hesitate to exercise this right

to discretion and instead understand that paraffin blocks cannot be used in research.

Bioethics Act Article 16 (Consent of Human Subjects) clause 1 stipulates that in cases of research involving human subjects, researchers must obtain written consent from research subjects prior to conducting the study. However, Article 16 clause 3 states, “Notwithstanding clause 1, if the following requirements are satisfied, the written consent of the research subject may be waived with the approval of the IRB. (1) If the consent of the subject is not realistically feasible or has a serious impact on the validity of the study. (2) There is no reason that subject will refuse to give consent, and that without consent, the risk to the study.”

According to the act, research using paraffin blocks may be exempted from the consent acquisition requirement for the following reasons: (1) it is practically not feasible to obtain the consent of the person who provided the paraffin block. Studies using paraffin blocks are mostly on cancerous tissues, and patients are often deceased. In fact, accessing medical records and personal information to obtain consent may be considered a violation of the provider’s privacy. (2) There is no physical or psychological risk to the subject in research using paraffin blocks. As the research only utilizes tissues that have been already obtained and archived, the research cannot cause physical harm or pain. There is no personal contact; therefore, there is no risk of psychological harm. In addition, social anxiety due to the risk of identity exposure is also excluded if personal information is not used through anonymization. However, research that requires personal infor-

mation should require consent.

When reviewing a plan for research utilizing paraffin blocks, the ethics of consent should be taken into account as well as that the block is considered a type of medical record. In other words, it should be considered whether the block to be used in a study infringes on a patient’s right to medical treatment. There may be several blocks available, and using only 1 for research does not seem to raise any issue. However, if there is only 1 paraffin block of a patient, it may not be used for research. It may be necessary to respond to a patient request in the future or to further examine the tissue for the originally intended purpose. Because paraffin blocks are a type of medical record, these abovementioned guidelines are applicable only to blocks archived less than 10 years ago, since the legal retention period of medical records is 10 years.

In addition, studies using paraffin blocks may be exempt from IRB review under Article 36 (2) of the Bioethics Act depending on the study content. For the study of human derivatives, an IRB review waiver may be applicable in the following cases: research that does not collect or record personally identifiable information (PII); or research that uses the human body collected and stored by a biobank or that uses unidentifiable personal information unless verified through the biobank that provided the information. If these conditions are met, research using paraffin blocks is exempt from IRB review.

Table 1. Countries with bioethics legislative organizations and their views

| Country | Organization | Legislation/Publication | View on research using archived tissues |
|-------------------|--|---|---|
| Republic of Korea | National Bioethics Review Committee | Bioethics and Safety Acts (2016) | IRB review and approval: required. Consent: required, may be waived in specific cases, with discretionary power of the IRB committee. |
| United States | Department of Health and Human Services US FDA HIPAA SACHRP | Common rule Human subjects regulations Privacy Rule, Security Rule SACHRP Guideline | Consent: If personal information is secured, can be used without further consent. IRB review and approval: exempted, if personal information is secured and the tissue was not collected for research purpose. |
| Japan | Ministry of Health, Labour and Welfare | Pharmaceutical Affairs Act and the Act on the Safety of Regenerative Medicine | No specific regulations on archived tissue research. No consent needed after tissue has been acquired (diagnostic/treatment purpose). |
| Singapore | Medical Council Bioethics Advisory Committee | Human Biomedical Research Act (2015) Ethical Guidelines for Human Biomedical Research (2010) | Consent and IRB review may or may not be required for residual/archived tissue (case by case). |
| United Kingdom | The Human Tissue Authority | Human Tissue Act (2004) | Consent is not required. IRB approval and review: not required, if personal information is unidentifiable or anonymized. |
| Australia | National Health and Medical Research Council | National Statement on Ethical Conduct in Human Research (2015) Privacy Act (2001) | Consent waiver is possible. IRB approval and review: required. Residual tissues considered as abandoned. |

IRB, Institutional Review Board.

CASES IN OTHER COUNTRIES

The regulations and guidelines published by each country differ, and at times the definition of terminologies and positions on exemption of informed consent vary in a way that confuses researchers and stakeholders. The main publications and legislative acts on archived tissue are summarized in Table 1.

United States

In the United States, there are several regulatory bodies that guide and regulate research on human tissue or biodata: the “Common Rule” and Secretary’s Advisory Committee on Human Research Protection (SACHRP) in the Department of Health and Human Services (HHS), the U.S. Food and Drug Administration (FDA), and the Health Insurance Portability and Accountability Act (HIPAA). Researchers and institutions wishing to conduct research using biodata or human tissues in the United States must follow the regulations of the abovementioned bodies. These regulations allow a waiver of informed consent for research using archived tissues provided that personal information is secured.

The Common Rule states that research involving the collection or study of existing data, documents, records, pathological specimens, or diagnostic specimens may be exempt from these requirements if the information is recorded by the investigator in such a manner that subjects cannot be identified directly or through identifiers linked to the subjects (45 CFR 46.101(b)(4)). The FDA also indicates that it will refrain from enforcing regulations of informed consent in the following cases⁵: when a study uses leftover specimens; if the specimens are accompanied with only minimal clinical information (age, sex, and existing laboratory results); specimens are not individually identifiable; and the individuals caring for patients are different from and do not share information with those conducting the investigation.

The SACHRP,⁶ in the form of questions and answers, explains:

Question 1: Tissue biopsies were obtained for clinical diagnostic purposes, which have now been satisfied. The patients did not provide study specific informed consent for the research use of the tissue specimens. The hospital pathology department is willing to provide a portion of the remaining biopsy specimens to an investigator who will perform research assays. In order to allow matching with relevant clinical information, the specimens will be provided with identifiers such that the investigator can readily ascertain the identity of subjects. Is consent of the patient from whom the biopsy was taken (or waiver of consent) required for the secondary research use?

Answer: Yes. Under this scenario, informed consent of the

subjects should either be obtained or waived under 45 CFR 46.116(d) because the samples are identifiable to the recipient investigator.

Question 2: Tissue biopsies were obtained for clinical diagnostic purposes, which have now been satisfied. The hospital pathology department is willing to provide a portion of the remaining biopsy specimens to an investigator who will perform research assays. The specimens will be coded such that the investigator will not be able to readily ascertain the identity of individuals. Is consent of the patient from whom the biopsy was taken (or waiver of consent) required for the secondary research use?

Answer: No. Under this scenario, neither consent nor waiver is required, because the activity is not considered to be research involving human subjects.

From regulations on waivers of informed consent, it is clear that in the United States, if a researcher does not know and is not provided with the personal information of a given sample, and if the material cannot be linked to the subject, then consent of the sample provider is not necessary. Furthermore, study of human derivatives without PII is excluded from studies of human subjects. This is considered nonhuman subject research and does not require IRB approval and review.⁷

In addition, the American Pathological Society (APS) has stated that diagnostic tissue and research tissue are different and that residual tissues after the diagnostic purpose has been fulfilled are regarded as abandoned.⁸ Thus, the APS permits study of specimens that have already fulfilled their original purpose and are now “abandoned,” leaving the abandoned tissue free from the necessity of obtaining informed consent if it is to be used in research. Provided that personal information associated with a sample is secured, the abandoned or residual tissue can be used in research without IRB review and approval.

Japan (no specific law for archived tissue research or human tissue research)

In 2002, the Japanese Society of Pathology announced that archived tissue belongs to patients and that it is the responsibility of pathologists to respond to a patient’s claim of ownership.

“The object of the pathological examination must be preserved in a form in which the dignity and privacy of the patient is protected. This consideration is also true for medical certificates, microscopic specimens, paraffin blocks or visual images. In addition, the organ, tissue, or microscopic specimen after the end of pathologic diagnosis will belong to the patient himself. Therefore, if there is a request for ownership it is necessary to return the material.”⁹

However, in 2014, the Declaration was amended as follows. “Since the ethics of bioethics and medical ethics change according to the changes of times and society, the ethics committee of the Japanese Society of Pathologists invites external members to review them repeatedly, Considering the medical mission and the responsibility for society as pathologist, we have concluded that the 2002 decision was not necessarily appropriate.”

Subsequently, even if there is a request for the return of all or part of the materials from a patient or his/her family, the archived specimen should not be returned or transferred unless proper use or management is guaranteed. It is difficult to deny that returning a specimen may interfere with the duties of hospitals and pathologists to explain the etiology and state of illness. Also, doing so is against public morals (goodwill and social order). Considering the value of paraffin blocks in medical research, the change in the position of the Japanese Society of Pathology is highly significant.

The current Bioethics Act of South Korea requires that individual researchers cannot collect or store human derivatives. Individual researchers are only allowed to collect relevant material for research, which is subject to approval by the institutional committee. The remaining research resources, if available, may be stored in a biobank. For these regulations to be effective in reality, a tissue bank should be established in all hospitals.

However, this is not the case in reality. Funding for the establishment of a tissue bank is not yet provided to all hospitals in Korea, and subsidies are also being decreased annually. It is likely that hospitals will continue to be unable to support a facility that does not generate revenue. Considering these points, it should be possible to facilitate the exchange of research and utilization of paraffin blocks stored in hospitals.

Singapore

A Bioethics Advisory Committee report released in 2002 and updated in 2015 indicates that human tissue banks in Singapore, in the past, were mainly built as an “incidental by-product of diagnostic procedures,” indicating that samples were commonly obtained during medical treatment or diagnostic procedures.¹⁰ The report states that tissue donation should be considered an altruistic gift and the donor does not retain rights to the donated tissues or intellectual property rights.

Although every effort should be made to obtain consent for the use of leftover tissue for research, if consent cannot be obtained, then the IRB should have discretion to waive the consent requirement if the patient is not identifiable.

It is current practice to use biospecimens that remain after

clinical requirements to validate laboratory tests or undergo clinical audit without consent of the providers and without IRB approval, if specimens are irreversibly deidentified. Singapore also allows biomedical research on human tissues for 1 or more researchers, as long as they receive IRB approval. In other words, individual researchers can collect and store human derivatives, once permitted by an IRB committee.

According to the act, the IRB may exempt requirement for consent in which the research involves no more than minimal risk to the research subject or sample provider and the biospecimen or health information is individually unidentifiable (part I, part II waiver of requirement for appropriate consent for human biomedical research involving human biological material or health information).¹¹

Just as in the United States, Singapore also gives a waiver of consent when the health information is unidentifiable and if the research involves minimal risk to the sample provider.

Australia

In Australia, the National Health and Medical Research Council (NHMRC) regulates research on human tissues and approves ethical review processes established by institutional review committees. It updated and published a National Statement on Ethical Conduct in Human Research in 2015.¹²

There are 2 pathways that allow researchers to study human tissues. The full ethics application pathway involves prospective collection of biospecimens for research, whereas in the low-risk application pathway, prospective collection of biospecimens can be carried out with minimal risk to participants using stored specimens that would otherwise be discarded (e.g., after surgical operations, surplus to clinical requirements) (Chapter 3.4.11). The regulations indicate that if the specimen was obtained for clinical purposes and has been retained by an accredited clinical pathology service, it may be used for research purposes as long as the personal information of the provider is unidentifiable.

The guideline states that if a specimen is surplus to diagnostic requirements and would otherwise be destroyed, the personal information of the provider is protected, and there is no known or likely reason a participant would not have consented if they had been asked, a waiver may be considered (Chapter 2.3.10, 3.4.12). The NHMRC recognizes that it is impractical to obtain consent for biospecimens to be used in research when the material has been archived.

Korea does not have a separate pathway for archived tissue research or for low-risk research. A separate clause or ethical guideline for archived tissue will clarify possible questions and

conflicting interests from researchers. Australia recognizes the difficulty for researchers in seeking informed consent from patients regarding archived tissue and allows waiver of consent for archived tissue research.

United Kingdom

The Human Tissue Act (HTA, 2004), proposed by the Human Tissue Authority, regulates the removal, storage, and use of human tissue. The Human Tissue Authority issues good practice guidance in codes of practice. It also licenses and inspects post-mortem pathological activities and storage of human tissue in hospitals. The Act provides a number of exceptions to the general rule that appropriate consent is required to store or use human tissue for scheduled purposes.

The Act states that tissues or organs removed by surgery might be considered “abandoned” by patients and can be used in ways seen fit by an institution. Samples of tissues collected from patients or subjects are considered “gifts” or “donations,” although the research must be conducted according to ethical standards.¹³

Consent is not needed for the use of surplus or residual tissue taken from living patients that is left over after diagnostic or surgical procedures. It states that the use of residual tissue in research is exempted from consent provided that the research project has ethical approval (IRB approval) and the researcher cannot identify the tissue provider and is not likely to be able to do so in the future.

The Act also allows tissue from living or deceased subjects to be used for research without consent. Consent is not required for tissue that has been imported or comes from a body that has been imported. Consent is also not required for tissue that is or comes from the body of a person who died before the consent rules were enforced, and if at least 100 years have passed since the date of death.

In the United Kingdom, research on residual tissue is regulated in a similar manner as in the United States. Residual tissue is regarded as abandoned, thus requiring no informed consent in research as long as the confidentiality of personal information is secured and the information is not identifiable. Research on tissue with unidentifiable personal information is considered nonhuman subject research, and an IRB review and approval process is not required. However, if tissue is collected and stored for research purposes, research using these archived tissues requires IRB review and approval. In Korea, a clear distinction must be made between research using already-removed cells and tissues and research that requires an invasive method of collecting cells

and tissues from a living person. Archived tissue research is safe and has no risk of psychologically or physically harming subjects. Provided that information is secured and unidentifiable, research using paraffin blocks should have fewer restrictions than research of human subjects dose.

CONCLUSION

In the era of personalized medicine, paraffin blocks are tremendously valuable and important. They serve as materials for biomedical, pharmaceutical, and genetic research. In this paper, the authors have highlighted the value of paraffin blocks in biomedical research and what role they may play if research is allowed with a less complicated and more reasonable approval process. To validate the limitations of the current Bioethics Act in Korea, the authors have presented the views of 5 countries regarding archived tissue research.

The current Bioethics Act has severe restrictions regarding research on archived tissues, and the authors suggest that archived tissue research should have a separate clause or guideline. All 5 countries discussed here allow waiver of consent or do not require consent to utilize paraffin blocks in research. Australia requires IRB review and approval. However, in the United States, Japan, and the United Kingdom, IRB review and approval are not required because paraffin block research is considered nonhuman subject research. The authors believe that IRB review and approval should be waived or not required because paraffin tissue research does not raise health risks for tissue providers provided that personal information is anonymized and unidentifiable. This will ease the unreasonable burdens researchers face before being given the chance to conduct research and in turn facilitates biomedical research advancements in Korea.

The authors suggest that paraffin blocks can be used in research while abiding by the Bioethics Act on the use of paraffin blocks and IRB review process in the following manner:

First, researchers should be able to explain that acquiring consent is impractical. For instance, the researcher should be able to explain that a sample is stored close to or past the date of legally required storage duration or that access to personal information for contact raises ethical questions. The sample provider or family members of the provider may not want to know findings or health-related information obtained from the sample. This act not only infringes on the human rights and autonomy of the provider, but may also psychologically harm the sample providers. However, reasons such as inconvenience regarding acquiring consent for a large quantity of paraffin blocks may not

be considered viable excuses.

Second, the researcher must prove that the study is low risk and does not require consent. In other words, the research contents should be anonymized so as to not be connected with a sample provider's personal information.

Third, the paraffin blocks are to be used only if they are not the only sample of the provider, which will maintain residual tissue after the study. Because paraffin blocks serve as a type of medical record, they must be available at the provider's request to use for a certain period of time. If all 3 conditions are met, archived research using paraffin blocks should be allowed to be exempt from written consent and IRB review.

The authors hope IRB committees consider these assertions and encourage the use of paraffin blocks in research. In addition, the Korean Society of Pathology should establish more specific guidelines to safely protect the personal information of sample providers while promoting the advancement of biomedical research by allowing information-secured tissue research to be exempted from reviews and consents.

Conflicts of Interest

No potential conflict of interest relevant to this article was reported.

REFERENCES

- Ryu YJ, Kim H, Jang S. Proposal for the development of a human biological material management system for research hospitals. *J Korean Med Assoc* 2012; 55: 292-303.
- McDonald SA. Principles of research tissue banking and specimen evaluation from the pathologist's perspective. *Biopreserv Biobank* 2010; 8: 197-201.
- Lee HJ. Review and consent for the human materials research in Bioethics and Safety Act. *Kangwon Law Rev* 2015; 45: 479-516.
- Information Portal of Institutional Review Boards designated by the Ministry of Health and Welfare. 100 Questions and 100 answers. 2013 to 2014 collection of open writings 30. Sejong: Ministry of Health and Welfare, 2015.
- U.S. Food and Drug Administration. Exception from general requirements for informed consent (21 CFR 50.23(e)) [Internet]. Silver Spring: U.S. Food and Drug Administration, c2011-2017 [cited 2017 May 13]. Available from: <https://www.gpo.gov/fdsys/pkg/FR-2011-06-24/pdf/2011-15816.pdf>.
- Office for Human Research Protections. Attachment D: FAQ's terms and recommendations on informed consent and research use of biospecimens [Internet]. Rockville: Office for Human Research Protections, 2011 [cited 2017 May 8]. Available from: <https://www.hhs.gov/ohrp/sachrp-committee/recommendations/2011-october-13-letter-attachment-d/>.
- e-CFR. Code of Federal Regulations (CFR) title 45 part 46 [Internet]. St. Louis: U.S. Government Publishing Office, 2017 [cited 2017 May 9]. Available from: http://www.ecfr.gov/cgi-bin/text-idx?tpl=/ecfrbrowse/Title45/45cfr46_main_02.tpl.
- Dry S. Who owns diagnostic tissue blocks? *Lab Med* 2009; 40: 69-73.
- Tsutsumi H. Question to a doctor (quote it from "idea four communication 82nd, pp. 4-9, 2012"). A question and answer about a pathological diagnosis and management: "the use of the pathology specimen of the breast cancer" question (Idea four, Ikuko Nakazawa) [Internet]. Toyoake: Fujita Health University, 2014 [cited 2018 Jan 1]. Available from: <http://info.fujita-hu.ac.jp/pathology1/idea-four.pdf.pdf>.
- National Bioethics Advisory Committee. Human tissue for biomedical research: tumour banks [Internet]. Singapore: Academy of Medicine, 2002 [cited 2017 Jul 1]. Available from: http://ams.edu.sg/view-pdf.aspx?file=media%5C752_fi_611.pdf&ofile=HumanTissueeForBiomedicalResearchTumourBanks.pdf.
- Singapore Statutes Online. Human Biomedical Research Act 2015 (No. 29 of 2015) [Internet]. Singapore: Nanayang Technological University, 2015 [cited 2017 Jul 1]. Available from: <http://statutes.agc.gov.sg/aol/download/0/0/pdf/binaryFile/pdfFile.pdf?CompId:03a5373e-148c-464f-90b8-526704d01c11>.
- The Royal College of Pathologists of Australasia. The ethical and legal issues in relation to the use of human tissue and test results in Australia. Surry Hills: The Royal College of Pathologists of Australasia, 2014.
- The National Archives. Human Tissue Act 2004. Section 1-44 [Internet]. Norwich: Stationary Office Ltd., c2004 [cited 2017 Jul 4]. Available from: http://www.opsi.gov.uk/acts/acts2004/ukpga_20040030_en_1.

Molecular Screening of Small Biopsy Samples Using Next-Generation Sequencing in Korean Patients with Advanced Non-small Cell Lung Cancer: Korean Lung Cancer Consortium (KLCC-13-01)

Bo Mi Ku* · Mi Hwa Heo^{1*}
Joo-Hang Kim² · Byoung Chul Cho³
Eun Kyung Cho⁴ · Young Joo Min⁵
Ki Hyeong Lee⁶ · Jong-Mu Sun¹
Se-Hoon Lee¹ · Jin Seok Ahn¹
Keunchil Park¹ · Tae Jung Kim⁷
Ho Yun Lee⁷ · Hojoong Kim⁸
Kyung-Jong Lee⁸ · Myung-Ju Ahn¹

Samsung Biomedical Research Institute, Sungkyunkwan University School of Medicine, Seoul; ¹Division of Hematology-Oncology, Department of Medicine, Samsung Medical Center, Sungkyunkwan University School of Medicine, Seoul; ²CHA Bundang Medical Center, CHA University, Seongnam; ³Division of Medical Oncology, Yonsei Cancer Center, Seoul; ⁴Division of Hematology and Medical Oncology, Department of Internal Medicine, Gachon University Gil Medical Center, Incheon; ⁵Division of Oncology, Department of Hematology and Oncology, Ulsan University Hospital, Ulsan; ⁶Division of Medical Oncology, Chungbuk National University Hospital, Chungbuk National University College of Medicine, Cheongju; ⁷Department of Radiology and Center for Imaging Science, Samsung Medical Center, Sungkyunkwan University School of Medicine, Seoul; ⁸Division of Pulmonary and Critical Care Medicine, Department of Medicine, Samsung Medical Center, Sungkyunkwan University School of Medicine, Seoul, Korea

Received: December 28, 2017

Revised: February 26, 2018

Accepted: March 12, 2018

Corresponding Author

Kyung-Jong Lee, MD
Division of Pulmonary and Clinical Care Medicine,
Department of Medicine, Samsung Medical Center,
Sungkyunkwan University School of Medicine,
81 Irwon-ro, Gangnam-gu, Seoul 06351, Korea
Tel: +82-2-3410-0777
Fax: +82-2-3410-6956
E-mail: kj2011.lee@samsung.com

Myung-Ju Ahn, MD
Division of Hematology-Oncology, Department of
Medicine, Samsung Medical Center,
Sungkyunkwan University School of Medicine, 81
Irwon-ro, Gangnam-gu, Seoul 06351, Korea
Tel: +82-2-3410-3438
Fax: +82-2-3410-1754
E-mail: silk.ahn@samsung.com

*Bo Mi Ku and Mi Hwa Heo contributed equally to this work.

Background: Non-small cell lung cancer (NSCLC) is a common type of cancer with poor prognosis. As individual cancers exhibit unique mutation patterns, identifying and characterizing gene mutations in NSCLC might help predict patient outcomes and guide treatment. The aim of this study was to evaluate the clinical adequacy of molecular testing using next-generation sequencing (NGS) for small biopsy samples and characterize the mutational landscape of Korean patients with advanced NSCLC. **Methods:** DNA was extracted from small biopsy samples of 162 patients with advanced NSCLC. Targeted NGS of genomic alterations was conducted using Ion AmpliSeq Cancer Hotspot Panel v2. **Results:** The median age of patients was 64 years (range, 32 to 83 years) and the majority had stage IV NSCLC at the time of cancer diagnosis (90%). Among the 162 patients, 161 patients (99.4%) had novel or hotspot mutations (range, 1 to 21 mutated genes). Mutations were found in 41 genes. Three of the most frequently mutated genes were *TP53* (151, 93.2%), *KDR* (104, 64.2%), and epidermal growth factor receptor (*EGFR*; 69, 42.6%). We also observed coexistence of *EGFR* and other oncogene (such as *KRAS*, *PIC3CA*, *PTEN*, and *STK11*) mutations. Given that 69.6% (48/69) of *EGFR* mutant patients were treated with *EGFR* tyrosine kinase inhibitors, *EGFR* mutant status had higher prognostic ability in this study. **Conclusions:** These results suggest that targeted NGS using small biopsy samples is feasible and allows for the detection of both common and rare mutations in NSCLC.

Key Words: Carcinoma, non-small cell lung; Targeted next-generation sequencing; Small biopsy; Receptor, epidermal growth factor

The majority of patients diagnosed with non-small cell lung cancer (NSCLC) present with advanced stage disease and have extremely poor prognosis.¹ Recent advances in the understanding of lung cancer biology and improvements in technology have allowed molecular classification of NSCLC.^{2,3} Classifying NSCLC into distinct actionable subtypes with mutually exclusive driver oncogenes has led to the development of targeted therapy.³ Better survival has been observed after treatment with epidermal growth factor receptor (EGFR) or anaplastic lymphoma kinase (ALK) tyrosine kinase inhibitors (TKIs) in patients harboring the appropriate activating mutation or translocation, compared with standard chemotherapy.^{3,4}

Although several genes including *EGFR* and *ALK* have been identified as potential oncogenic drivers and targets for therapy, a large fraction of NSCLC patients do not have mutations in these commonly mutated genes. Thus, there are needs to identify additional driver oncogenes and targets for treatment. In addition, many NSCLC patients also harbor other co-existing molecular alterations that might influence the efficacy of a targeted therapy, leading to primary or secondary resistance. It is important to investigate these concurrent genetic alterations to reveal clinically significant predictive and prognostic markers. However, several challenges remain in the implementation of multiple molecular tests to find therapeutic or prognostic markers. First, most NSCLC biopsy samples are not amenable to multiple molecular tests due to the small amounts of tissues obtained by bronchoscopy or core biopsy. In addition, conventional molecular tests such as Sanger sequencing and polymerase chain reaction (PCR) are insensitive to alterations occurring at allele frequencies lower than 20%. Finally, multiple and separate tests result in higher costs and longer turn-around time. Thus, a more comprehensive, sensitive, and time/cost-effective multiplex test is necessary to optimize the application of targeted therapy.^{5,6} Consequently, incorporation of molecular screening using next-generation sequencing (NGS) in the pathologic evaluation of NSCLC is now considered the standard in clinical practice.^{7,8}

The rapid development of NGS technologies has enabled a new paradigm in precision medicine for oncology. It is now possible to identify oncogenic alterations that would have been previously undiscovered by conventional tests such as sequencing. For the routine clinical molecular diagnostic testing in NSCLC, NGS need to meet some criteria; NGS platform should be able to detect targetable driver mutations from limited amounts of input DNA from small biopsy or cytology samples, the turn-around time should be short, and the cost should be low. Unlike whole-genome sequencing or whole-exome sequencing, targeted

NGS including selected genes that show frequent alterations in cancer can reduce the amount of tissue, time, and cost required for testing.⁹⁻¹¹

To validate the accuracy and feasibility of targeted NGS, we used Ion AmpliSeq Cancer Hotspot Panel v2 to identify the variety of tumor-associated mutations in formalin-fixed paraffin-embedded (FFPE) or fresh frozen (FF) specimens from 162 advanced NSCLC patients in Korea. In this study, we analyzed multiple somatic mutations found in our advanced NSCLC cohort in order to detect known actionable mutations and discover potential therapeutic targets and prognostic biomarkers for NSCLC.

MATERIALS AND METHODS

Patients and tumor samples

We analyzed 162 FFPE or frozen tumor tissue specimens from advanced NSCLC patients between January 2014 and December 2015 at Samsung Medical Center (SMC). All samples were collected before any treatments were initiated. Procedures used for tumor tissue sampling varied, including video-assisted thoracoscopic surgery, core-needle biopsy, bronchoscopy, and endobronchial ultrasonography. Clinical data were obtained retrospectively from electronic medical records. The clinical variables assessed were sex, age at diagnosis, smoking history, tumor subtype, cancer stage, *EGFR* mutation, *ALK* rearrangement, chemotherapy regimen, TKIs, and tumor response. Separately, *EGFR* mutation status was tested by real-time PCR using the peptide nucleic acid (PNA)-clamping EGFR Mutation Detection Kit (Panagene, Inc., Daejeon, Korea). Real-time PCR was performed using a CFX96 (Bio-Rad, Hercules, CA, USA) and all reagents were included in the kit. PCR cycling and mutation detection were done as previously described.¹² *ALK* rearrangement status was tested by immunohistochemistry and confirmed by fluorescence *in situ* hybridization (FISH). All procedures involving tumor specimens were reviewed and approved by the Institutional Review Board (IRB) of SMC and all data were fully anonymized (SMC 2013-08-113-020). Written informed consent was provided by all patients.

DNA extraction

All tissue sections were reviewed by pathologists, and only those with tumor content more than 10% were included in the study. Genomic DNA was extracted from FFPE samples using the QIAamp DNA FFPE Tissue Kit (Qiagen, Hilden, Germany) or FF tumor specimens using QIAamp DNA mini kit. Purified DNA was quantitated by NanoDrop (Invitrogen Life Technolo-

gies, Carlsbad, CA, USA) and Qubit Fluorometer (Invitrogen Life Technologies).

Next-generation sequencing and data analysis

The Ion Torrent Ion AmpliSeq Cancer Hotspot Panel v2 (Life Technologies) was used. This panel detects hotspot regions, including ~2,800 COSMIC mutations of 50 oncogenes and tumor suppressor genes. A total of 162 cases of NSCLC specimens were subjected to NGS on the AmpliSeq platform. Sequencings were done according to previously described methods.¹³ Variants calls were further processed to reduce potential false-positives. Coverage (> 500×) was considered as filtering criteria and the minimal variant allele frequency was 2% for confirming variants as real. After filtering using these criteria, variants causing amino acid change and frameshift were finally used for statistical analysis.

Statistical analysis

Clinical and radiological response to treatment was assessed according to Response Evaluation Criteria In Solid Tumor ver. 1.1. Kaplan-Meier estimates were used for the analysis of all time-to-event variables. Progression-free survival (PFS) was calculated from the date of chemotherapy to the date of disease progression or death from any cause or the date of last follow-up. The overall survival (OS) was measured from the date of chemotherapy to the date of death from any cause and was censored at the date of the last follow-up visit. Variables with $p < .05$ were considered significant. All statistical analyses were performed using PASW Statistics ver. 23.0 (SPSS Inc., Chicago, IL, USA).

RESULTS

Patient characteristics

The clinical characteristics of advanced NSCLC patients included in the present study are summarized in Table 1. The median age was 64 years (range, 32 to 83 years) and gender proportions were roughly equal (male 57% vs female 43%). Seventy-nine patients (59%) were smokers or former smokers, 83 patients (51%) were never smokers. The NSCLC subtype distribution was as follows: adenocarcinoma (139/162, 85.8%), squamous cell carcinoma (17/162, 10.5%), adenosquamous cell carcinoma (1/162, 0.6%), and other (5/162, 3.1%). The majority of patients had stage IV NSCLC at the time of cancer diagnosis (145/162; 90%). In stage IV NSCLC patients, the median PFS was 6.2 months (95% CI, 4.2 to 8.1) and OS was 19.6 months (95% CI, 15.4 to 23.7). *EGFR* mutation test was done in 145 patients,

Table 1. The baseline characteristics of patients

| Characteristic | No. (%) (n=162) |
|-------------------------|-----------------|
| Age (yr) | |
| Median | 64 |
| Range | 32–83 |
| Sex | |
| Male | 92 (57) |
| Female | 70 (43) |
| Smoking history | |
| Never-smoker | 83 (51) |
| Current | 33 (20) |
| Ex-smoker | 46 (28) |
| Histology | |
| Adenocarcinoma | 139 (86) |
| Squamous cell carcinoma | 17 (10) |
| Adenosquamous | 1 (1) |
| NSCLC, other | 5 (3) |
| Clinical stage | |
| I–II | 7 (4) |
| IIIA | 5 (3) |
| IIIB | 5 (3) |
| IV | 145 (90) |
| Brain metastasis | |
| Present | 49 (30) |
| Absent | 113 (70) |
| Biopsy type | |
| VATS | 45 (28) |
| CNB_lung | 23 (14) |
| CNB_others | 22 (14) |
| Bronchoscopy | 31 (19) |
| EBUS | 41 (25) |
| First treatment | |
| Chemotherapy | 81 (50) |
| EGFR TKI | 51 (32) |
| ALK TKI | 3 (2) |
| No treatment | 27 (16) |

NSCLC, non-small cell lung carcinoma; VATS, video-assisted thoracoscopic surgery; CNB, core-needle biopsy; EBUS, endobronchial ultrasonography; EGFR, epidermal growth factor receptor; TKI, tyrosine kinase inhibitor; ALK, anaplastic lymphoma kinase.

and the mutation was detected in 64 patients (44.1%) by real-time PCR using PNA-clamping. Positive results for *ALK* rearrangement by FISH were detected in 14 patients (8.6%). In this cohort, 81 patients were treated with cytotoxic chemotherapy (81/162, 50.0%), 51 with EGFR TKIs (51/162, 31.5%), and three with ALK TKIs (3/162, 1.8%) as first-line therapy.

Molecular profiling of advanced NSCLC

We employed targeted NGS technology to evaluate somatic mutations occurring in advanced NSCLC, using the Ion Torrent Ion AmpliSeq Cancer Hotspot Panel. Among the detected mutations, only those annotated in the Catalogue of Somatic Muta-

tions in Cancer (COSMIC) database were considered. Mutations were found in 41 genes and commonly detected in the following genes: *TP53* (151, 93.2%), *KDR* (104, 64.2%), *EGFR* (69, 42.6%), *APC* (51, 31.5%), *RB1* (30, 18.5%), *SMAD4* (28, 17.3%), *MET* (22, 13.6%), *STK11* (20, 12.3%), *RET* (18, 11.1%), *ALK* (17, 10.5%), and *KRAS* (13, 8.0%), as shown in Fig. 1. Only one patient had no mutation while 161 (99.4%) patients possessed more than one mutation (range, 1 to 21; median, 4). The vast majority of identified mutations were single nucleotide variant (SNV) followed by deletion (Del) and insertion (Ins). In accordance with the frequency described in previous studies,^{1,3} *EGFR* mutations were found in 42.6% patients and most of them (54/69, 78.3%) were typical mutations (30 Del exon 19 and 24 L858R). One of these was a triple *EGFR* mutant (L858R/G873R/Q787L) and ten were double *EGFR* mutant (3 Del exon 19/G873R, 2 Del exon 19/A750P, 1 Del exon 19/S752Y, 1 Del exon 19/K754N, 2 L858R/G873R, 1 L858R/T790M). Besides *TP53* and *EGFR*, the most frequently mutated gene was *KDR*, and *KDR* mutations appeared in codon 472 (103 Q472H) and codon 875 (1 T875A). One patient with *KDR* Q472H had concurrent *KDR* S1148C. *MET* mutations were found in codon 375 (17 N375S) and codon 179 (5 A179T). Although one *MET* R970C in exon 14 was simultaneously found with N375S, this has not been reported as cause of *MET* exon 14 skipping.¹⁴ *STK11* mutations were found in

codon 354 (19 F354L) and codon 176 (1 D176G). Two samples detecting *STK11* F354L had other *STK11* mutation in codon 281 (P281L). Seventeen *ALK* mutations were all in codon 1184 (G1184E). In concordance with the known frequency of *KRAS* mutations in Asian population (5%–10%),¹⁵ they were found in 8% of this cohort. Most *KRAS* mutations appeared in codon 12 (1 G12A, 4 G12C, 3 G12D, 1 G12R, and 2 G12V) with two mutations in codon 50 (T50P). *PIK3CA* mutations (E81K, R401Q, E542G, E545A, E545K, Q546K, and H1047R) were detected in seven samples and one patient had double *PIK3CA* mutants (E542G/E545A). *PTEN* mutations (K66E, R130X, Q171X, and P246L) were identified in four patients.

We also observed co-occurrence of some of the most frequently mutated and clinically significant genes. Five patients simultaneously had mutations in both *EGFR* and *KRAS*. *EGFR* mutations also harbored *PIK3CA* and *PTEN* mutations, which were detected in three and two patients, respectively. In addition, although *STK11* mutations were most commonly seen in association with *KRAS* mutations, we found seven cases with co-occurrence of *EGFR* and *STK11* mutations in this study.

Comparison of mutational profiles obtained with the AmpliSeq assay

Based on mutation results considering the location of mutation sites, *EGFR* mutations were consistently detected by tar-



Fig. 1. Heatmap of mutations found in 162 non-small cell lung cancer samples. In the upper panel, the first row indicates sex, the second row smoking status, and the third row histology. A histogram shows the percentage of mutations in each gene (left). The horizontal axis presents the complete dataset of patients and the vertical axis illustrates mutated genes (right).

geted NGS using AmpliSeq Cancer Panel and conventional PNA-clamping PCR (42.6% vs 44.1%). In 145 patients tested for *EGFR* mutation, the comparison results of *EGFR* mutations detected by targeted NGS and conventional PNA-clamping PCR are summarized in Table 2. When comparing mutation detection of *EGFR* in FFPE and FF samples, a high concordance rate (92.4%) was seen between NGS and PNA-clamping PCR. However, targeted NGS method identified additional *EGFR* mutations in 14 concordant cases and seven discordant cases that were not identified by PNA-clamping PCR. The most frequently found additional *EGFR* mutation was G873R which was found in 12 patients. We observed three discordant cases that showed positive results (all Del exon 19) in PNA-clamping, but negative in NGS. Considering the high sensitivity of NGS, these results may be due to tumor heterogeneity.

Although most of the patients had a single biopsy, four patients

had repeated biopsies and had double tumors tested. Except for one consistent case, the other three cases showed slightly different mutation profiles (Table 3). These differences may be due to tumor heterogeneity or tumor evolution.

Impact of mutation status on survival

We evaluated the relationships between *EGFR* somatic mutations and survival. Activating *EGFR* mutations have been reported as prognostic factors in other studies.^{16,17} In this study cohort, 69.6% (48/69) of patients with *EGFR* mutations were treated with EGFR TKIs. The presence of *EGFR* mutations were definitive predictive markers of both PFS (hazard ratio [HR], 2.59; 95% confidence interval [CI], 1.75 to 3.85) (Fig. 2A) and OS (HR, 2.00; 95% CI, 1.30 to 3.09) (Fig. 2B). Median PFSs were 3.8 months for *EGFR* wild-type group and 14.6 months for *EGFR* mutant group. The median OS for *EGFR*

Table 2. Comparison of *EGFR* mutations detected by targeted NGS and PNA-clamping PCR

| Sample type | No. of cases compared | Concordant (NGS/PNA) | | Discordant (NGS/PNA) | | | Concordance (%) |
|-------------|-----------------------|----------------------|-----|----------------------|-----|-----|-----------------|
| | | -/- | +/+ | -/+ | +/- | +/+ | |
| FFPE | 131 | 69 | 53 | 2 | 6 | 1 | 93.1 |
| FF | 14 | 5 | 7 | 1 | 1 | 0 | 85.7 |
| Total | 145 | 74 | 60 | 3 | 7 | 1 | 92.4 |

EGFR, epidermal growth factor receptor; NGS, next-generation sequencing; PNA, peptide nucleic acid; PCR, polymerase chain reaction; FFPE, formalin-fixed paraffin-embedded; FF, fresh frozen.

Table 3. Mutations identified in four patients with repeat biopsy samples

| Patient No. | Mutations identified in first sample | Mutations identified in second sample |
|-------------|---|---|
| 1 | <i>KDR</i> Q472H, <i>APC</i> A1582P, <i>MET</i> N375S, <i>TP53</i> R248W, <i>TP53</i> P72R | <i>KDR</i> Q472H, <i>APC</i> A1582P, <i>TP53</i> R248W, <i>TP53</i> P72R |
| 2 | <i>ERBB4</i> T926M, <i>KIT</i> M541L, <i>TP53</i> H179R, <i>TP53</i> P72R | <i>ERBB4</i> T926M, <i>KIT</i> M541L, <i>FLT</i> F590L, <i>TP53</i> H179R, <i>TP53</i> P72R |
| 3 | <i>PIK3CA</i> E542K, <i>PTPN11</i> G503V, <i>TP53</i> E285K, <i>TP53</i> P72R, <i>TP53</i> P72A, <i>SRC</i> Q529X | <i>KIT</i> M541L, <i>KDR</i> Q472H, <i>TP53</i> P72R |
| 4 | <i>CTNNB1</i> D32A, <i>KDR</i> Q472H, <i>EGFR</i> ex19 del, <i>EGFR</i> A750P, <i>CDKN2A</i> H66R, <i>TP53</i> P72R | <i>CTNNB1</i> D32A, <i>KDR</i> Q472H, <i>EGFR</i> ex19 del, <i>EGFR</i> A750P, <i>CDKN2A</i> H66R, <i>TP53</i> P72R |

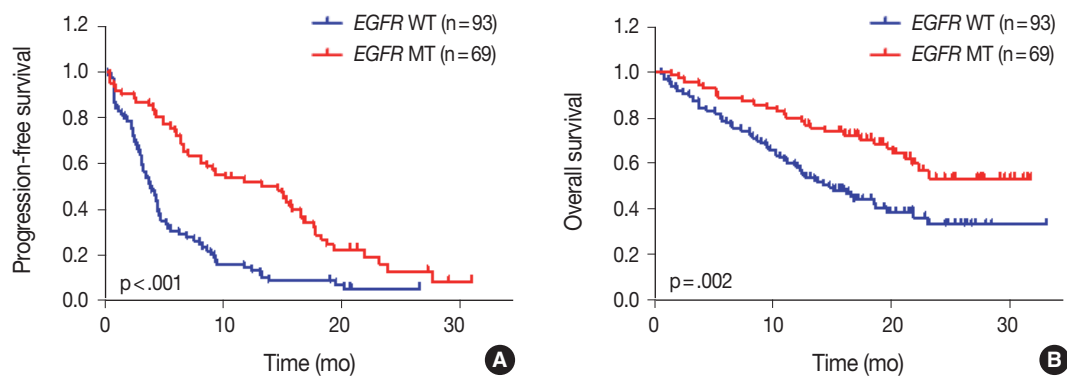


Fig. 2. Impact of epidermal growth factor receptor (*EGFR*) mutational status on survival. (A) Progression-free survival of patients with *EGFR* mutant (MT) compared with *EGFR* wild-type (WT) patients. (B) Overall survival of all patients according to *EGFR* status. p-values were obtained using the log-rank test.

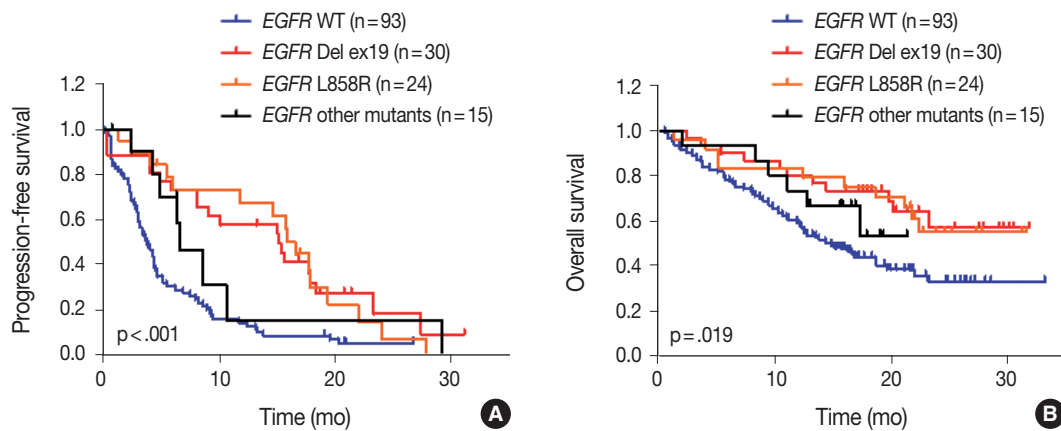


Fig. 3. Impact of different types of epidermal growth factor receptor (*EGFR*) mutations on survival. Progression-free survival (A) and overall survival (B) of patients with different types of *EGFR* mutations compared with *EGFR* wild type (WT) patients. *p*-values were obtained using the log-rank (Mantel-Cox) test.

wild-type group was 14.8 months, but the median OS for *EGFR* mutant group was not reached. When PFS was analyzed after grouping the patients according to the three types of *EGFR* mutations (Del ex19, L858R, and others), the median PFSs were different between activating mutations (15.1 months for Del ex19 and 17.7 months for L858R) and others (6.6 months) (Fig. 3A). However, the median OS was not reached in the three types of *EGFR* mutations (Fig. 3B).

DISCUSSION

Currently, molecular testing for *EGFR* mutations and *ALK* rearrangements is essential for targeted therapy in patients with NSCLC. However, the heterogeneous nature of NSCLC can lead to inaccurate molecular classification and therapeutic resistance. Other genetic alterations that have been found and have potential therapeutics include *ROS1*, *RET*, and *NTRX* gene rearrangement, *MET* exon 14 skipping, and *MET* amplification.^{4,18,19} However, there are no standard molecular diagnostic tests for these genetic alterations. In addition, an important limitation in current routine diagnosis is that the quantity of DNA extracted from small biopsy samples (FFPE or FF) is not adequate for multiple molecular tests in most cases. To cope with this limitation, comprehensive multiplex testing using NGS is necessary to improve the efficacy of targeted therapy for NSCLC patients. With advances in NGS technology, several target regions of interest can be sequenced concurrently and thereby improve the chances of identifying rare mutations. In this study, 162 Korean advanced NSCLC samples were assessed for mutations in oncogenes and tumor suppressor genes using an NGS platform (AmpliSeq Cancer Hotspot Panel). This targeted sequencing

method shows high accuracy and requires only small quantities of sample (10 ng DNA), enabling researchers to sequence challenging small biopsy samples such as FFPE. Genetic alterations were confirmed in 99.4% of samples and 14 additional *EGFR* mutations (L707E, G719A, G719C, L747S, A750P, S752Y, K754N, S768I, V769L, V774M, T783A, S784P, Q787L, and G873R) were identified that were not detected with PNA-clamping PCR. In addition, we found some of the most frequently altered and clinically significant genes such as *KRAS*, *MET*, *STK11*, *PIK3CA*, and *PTEN* mutations. Moreover, the higher sensitivity of NGS platform should increase the identification of concomitant mutations. These results suggest the feasibility and usefulness of targeted sequencing to identify low frequency mutations and detect additional mutations that are helpful to understand the clinical outcomes of the patients in each group.

For patients with *EGFR*-mutant NSCLC, *EGFR* TKIs are found to increase response rates and survival time.^{16,17} In concordance with these data, *EGFR* mutations were associated with significant improvements of PFS and OS compared to *EGFR* wild-type patients, because most patients were treated with *EGFR* TKIs. Despite these benefits of *EGFR* TKIs, not all patients respond to treatment and most *EGFR*-mutant NSCLC patients develop acquired resistance.

Tumor suppressor *TP53* mutations are frequently detected in most human cancers. *TP53* was also the most commonly altered gene in this study, and this result is consistent with those of previous studies.^{20,21} *TP53* was concurrently mutated with many other genes such as *EGFR* and *KRAS* in this study, perhaps due to the high frequency of *TP53* mutations found in our samples. Whereas the frequency of *TP53* mutation is well known, therapeutic options based on this alteration are scarce and controversial

in patients with lung cancer. A previous study on advanced NSCLC found an association between *TP53* mutation and shorter median OS, but another study, on the other hand, reported no association between *TP53* mutation and survival.^{22,23}

Our data also identified *KDR* Q472H polymorphism in 103 patients (31 homozygotes and 72 heterozygotes). *KDR* Q472H has been reported to increase tumor microvasculature and shown to mediate vascular endothelial growth factor receptor 2 phosphorylation in NSCLC.²⁴ Furthermore, *KDR* Q472H had a higher proliferative and invasive capacity in melanoma.²⁵ Although we did not find a significant correlation between *KDR* Q472H and survival in EGFR TKI- or chemotherapy-treated NSCLC patients, the prognostic value of *KDR* Q472H should be different after treatment with vascular endothelial growth factor pathway inhibitors.

Although *KRAS* mutations are the most common oncogenic driver, there are some ethnic differences. The frequency of *KRAS* mutations in Asian is 5%–15%. In addition, *KRAS* mutations usually occur in *EGFR* wild-type tumors.^{18,26} In this study, we detected 13 *KRAS* mutations (8%) and five concurrent *KRAS/EGFR* mutations (3.0%) via NGS. In these five patients, three patients, who were clinically confirmed to have *EGFR* L858R mutations, received EGFR TKI (gefitinib) treatment with partial response or progression of the disease. Other two patients were treated with chemotherapy and showed 0.8 and 9.3 months of PFS. Although the prognostic effect of *KRAS* mutations was not clear due to small sample size, these results suggest that *KRAS* mutation test using NGS platform may help determine the appropriate therapy for NSCLC patients.

Recent studies have demonstrated that mutations in EGFR-downstream genes such as *PIK3CA*, *PTEN*, and *STK11* are associated with *de novo* resistance to EGFR TKI.²⁷ Furthermore, *PIK3CA* and *PTEN* mutations may result in resistance to EGFR TKI.⁴ In this study, we found *PIK3CA* and *PTEN* mutations in seven (4.3%) and four (2.5%) patients, respectively. Concurrent *EGFR/PIK3CA* mutations were detected in three patients. All of them received EGFR TKI (2 gefitinib and 1 erlotinib) treatment and showed partial response with different range of PFS (6.6–21.3 months). Concurrent *EGFR/PTEN* mutations were found in two patients and one received EGFR TKI (afatinib) treatment with partial response (PFS, 8.1 months). However, neither *PIK3CA* nor *PTEN* mutation status alone had significant effects on PFS and OS in the *EGFR*-mutant group. In *STK11*, we identified mutations in 20 patients (19 F354L and 1 D176G). *STK11* encodes the serine/threonine protein kinase and is part of the STK11/AMPK/mammalian target of rapamycin

signaling pathway. *STK11* mutations were commonly found, and inactivation of *STK11* is known to promote tumorigenesis and is associated with worse survival outcome.^{20,28} The overall rate of *STK11* mutations (12.3%) was slightly lower than that indicated by The Cancer Genome Atlas (17%).¹⁸ This discrepancy can be explained by the origin of the population; *STK11* mutations have been reported to be associated with European ancestry.^{19,21} *STK11* mutations often coexist with *KRAS* mutations and have confounding prognostic significance.^{29,30} However, in this study, we found only one concurrent *KRAS/STK11* (G12A/D176G) mutation. This patient received chemotherapy (AP: doxorubicin, cisplatin) and showed partial response with 4.4 months of PFS. A recent study reported that pathogenic *STK11* F354L mutations had been recurrently identified in three EGFR TKI non-responders, while these mutations had not been found in EGFR TKI responders.²⁰ In our study, seven *STK11* F354L mutations were recurrently found in EGFR TKI-treated patients. Among them, six (treated with gefitinib and erlotinib) showed partial response (PFS, 4.1 to 17.8 months) and one (treated with afatinib) showed stable disease (PFS, 19.3 months). This discrepancy may be due to the small sample size of *STK11* mutant patients. Thus, more research is required to identify the clinical implications of *STK11* mutations.

Our study has a few limitations. Our analysis relied on targeted sequencing to investigate genetic alterations and thus the genes selected in this study may only explain a portion of the total genetic alterations. The NGS platform used in this study (AmpliSeq Cancer Hotspot Panel) detected only SNVs, and thus it was impossible to detect copy number variations (CNVs) and translocations. Furthermore, other novel genetic or epigenetic alterations may have been missed. Most tumor samples were acquired from small biopsy samples, and thus there were not enough tissue available for more comprehensive analysis. Therefore, there is a need for new NGS platforms to simultaneously detect SNVs, CNVs, and translocations, even with small amounts of tissue samples. In addition, functional effects of the detected mutations were not evaluated *in vitro*.

Our results demonstrate that targeted sequencing using NGS is feasible for mutation profiling of small biopsy samples in NSCLC. We also demonstrated previously unappreciated mutations, enabling further refinements of subclassification for the prediction of therapeutic effects. In conclusion, we suggest that more comprehensive genomic characterizations of NSCLC with small biopsy samples would reveal coexisting alterations that might influence the efficacy of therapy.

Conflicts of Interest

No potential conflict of interest relevant to this article was reported.

Acknowledgments

This research was supported by a grant of the Korea Health Technology R&D Project through the Korea Health Industry Development Institute (KHIDI), funded by the Ministry of Health & Welfare, Republic of Korea (grant number: HI16C1984).

REFERENCES

- Jung KW, Won YJ, Oh CM, *et al.* Prediction of cancer incidence and mortality in Korea, 2016. *Cancer Res Treat* 2016; 48: 451-7.
- Chen Z, Fillmore CM, Hammerman PS, Kim CF, Wong KK. Non-small-cell lung cancers: a heterogeneous set of diseases. *Nat Rev Cancer* 2014; 14: 535-46.
- Richer AL, Friel JM, Carson VM, Inge LJ, Whitsett TG. Genomic profiling toward precision medicine in non-small cell lung cancer: getting beyond EGFR. *Pharmgenomics Pers Med* 2015; 8: 63-79.
- Camidge DR, Pao W, Sequist LV. Acquired resistance to TKIs in solid tumours: learning from lung cancer. *Nat Rev Clin Oncol* 2014; 11: 473-81.
- Han JY, Kim SH, Lee YS, *et al.* Comparison of targeted next-generation sequencing with conventional sequencing for predicting the responsiveness to epidermal growth factor receptor-tyrosine kinase inhibitor (EGFR-TKI) therapy in never-smokers with lung adenocarcinoma. *Lung Cancer* 2014; 85: 161-7.
- Rathi V, Wright G, Constantin D, *et al.* Clinical validation of the 50 gene AmpliSeq Cancer Panel V2 for use on a next generation sequencing platform using formalin fixed, paraffin embedded and fine needle aspiration tumour specimens. *Pathology* 2017; 49: 75-82.
- Kris MG, Johnson BE, Berry LD, *et al.* Using multiplexed assays of oncogenic drivers in lung cancers to select targeted drugs. *JAMA* 2014; 311: 1998-2006.
- Ballester LY, Luthra R, Kanagal-Shamanna R, Singh RR. Advances in clinical next-generation sequencing: target enrichment and sequencing technologies. *Expert Rev Mol Diagn* 2016; 16: 357-72.
- Padmanabhan V, Steinmetz HB, Rizzo EJ, *et al.* Improving adequacy of small biopsy and fine-needle aspiration specimens for molecular testing by next-generation sequencing in patients with lung cancer: a quality improvement study at Dartmouth-Hitchcock Medical Center. *Arch Pathol Lab Med* 2017; 141: 402-9.
- Zheng G, Tsai H, Tseng LH, *et al.* Test feasibility of next-generation sequencing assays in clinical mutation detection of small biopsy and fine needle aspiration specimens. *Am J Clin Pathol* 2016; 145: 696-702.
- Kim ST, Lee J, Hong M, *et al.* The NEXT-1 (Next generation pERsonalized tX with mulTi-omics and preclinical model) trial: prospective molecular screening trial of metastatic solid cancer patients, a feasibility analysis. *Oncotarget* 2015; 6: 33358-68.
- Kim HJ, Lee KY, Kim YC, *et al.* Detection and comparison of peptide nucleic acid-mediated real-time polymerase chain reaction clamping and direct gene sequencing for epidermal growth factor receptor mutations in patients with non-small cell lung cancer. *Lung Cancer* 2012; 75: 321-5.
- Ku BM, Jung HA, Sun JM, *et al.* High-throughput profiling identifies clinically actionable mutations in salivary duct carcinoma. *J Transl Med* 2014; 12: 299.
- Lee GD, Lee SE, Oh DY, *et al.* MET exon 14 skipping mutations in lung adenocarcinoma: clinicopathologic implications and prognostic values. *J Thorac Oncol* 2017; 12: 1233-46.
- Karachaliou N, Mayo C, Costa C, *et al.* KRAS mutations in lung cancer. *Clin Lung Cancer* 2013; 14: 205-14.
- Rosell R, Carcereny E, Gervais R, *et al.* Erlotinib versus standard chemotherapy as first-line treatment for European patients with advanced EGFR mutation-positive non-small-cell lung cancer (EURTAC): a multicentre, open-label, randomised phase 3 trial. *Lancet Oncol* 2012; 13: 239-46.
- Kuan FC, Kuo LT, Chen MC, *et al.* Overall survival benefits of first-line EGFR tyrosine kinase inhibitors in EGFR-mutated non-small-cell lung cancers: a systematic review and meta-analysis. *Br J Cancer* 2015; 113: 1519-28.
- Cancer Genome Atlas Research Network. Comprehensive molecular profiling of lung adenocarcinoma. *Nature* 2014; 511: 543-50.
- Dearden S, Stevens J, Wu YL, Blowers D. Mutation incidence and coincidence in non small-cell lung cancer: meta-analyses by ethnicity and histology (mutMap). *Ann Oncol* 2013; 24: 2371-6.
- Lim SM, Kim HR, Cho EK, *et al.* Targeted sequencing identifies genetic alterations that confer primary resistance to EGFR tyrosine kinase inhibitor (Korean Lung Cancer Consortium). *Oncotarget* 2016; 7: 36311-20.
- Mäki-Nevala S, Sarhadi VK, Rönty M, *et al.* Hot spot mutations in Finnish non-small cell lung cancers. *Lung Cancer* 2016; 99: 102-10.
- Murakami I, Hiyama K, Ishioka S, Yamakido M, Kasagi F, Yokosaki Y. p53 gene mutations are associated with shortened survival in patients with advanced non-small cell lung cancer: an analysis of medically managed patients. *Clin Cancer Res* 2000; 6: 526-30.
- Lim EH, Zhang SL, Li JL, *et al.* Using whole genome amplification (WGA) of low-volume biopsies to assess the prognostic role of

- EGFR*, *KRAS*, *p53*, and *CMET* mutations in advanced-stage non-small cell lung cancer (NSCLC). *J Thorac Oncol* 2009; 4: 12-21.
24. Glubb DM, Cerri E, Giese A, *et al.* Novel functional germline variants in the VEGF receptor 2 gene and their effect on gene expression and microvessel density in lung cancer. *Clin Cancer Res* 2011; 17: 5257-67.
 25. Silva IP, Salhi A, Giles KM, *et al.* Identification of a novel pathogenic germline KDR variant in melanoma. *Clin Cancer Res* 2016; 22: 2377-85.
 26. Roberts PJ, Stinchcombe TE. *KRAS* mutation: should we test for it, and does it matter? *J Clin Oncol* 2013; 31: 1112-21.
 27. Kim HR, Cho BC, Shim HS, *et al.* Prediction for response duration to epidermal growth factor receptor-tyrosine kinase inhibitors in *EGFR* mutated never smoker lung adenocarcinoma. *Lung Cancer* 2014; 83: 374-82.
 28. Pécuchet N, Laurent-Puig P, Mansuet-Lupo A, *et al.* Different prognostic impact of *STK11* mutations in non-squamous non-small-cell lung cancer. *Oncotarget* 2017; 8: 23831-40.
 29. Gleeson FC, Kipp BR, Levy MJ, *et al.* Somatic *STK11* and concomitant *STK11/KRAS* mutational frequency in stage IV lung adenocarcinoma adrenal metastases. *J Thorac Oncol* 2015; 10: 531-4.
 30. Imielinski M, Berger AH, Hammerman PS, *et al.* Mapping the hallmarks of lung adenocarcinoma with massively parallel sequencing. *Cell* 2012; 150: 1107-20.

Utility of BRAF VE1 Immunohistochemistry as a Screening Tool for Colorectal Cancer Harboring *BRAF* V600E Mutation

Jeong-Hwa Kwon
Byung-Kwan Jeong · Yong Sik Yoon¹
Chang Sik Yu¹ · Jihun Kim

Departments of Pathology and ¹Surgery, Asan Medical Center, University of Ulsan College of Medicine, Seoul, Korea

Received: January 25, 2018

Revised: March 16, 2018

Accepted: March 27, 2018

Corresponding Author

Jihun Kim, MD, PhD

Department of Pathology, Asan Medical Center,
University of Ulsan College of Medicine, 88
Olympic-ro 43-gil, Songpa-gu, Seoul 05505, Korea
Tel: +82-2-3010-4556
Fax: +82-2-472-7898
E-mail: jihunkim@amc.seoul.kr

Background: *BRAF* mutation has been recognized as an important biomarker of colorectal cancer (CRC) for targeted therapy and prognosis prediction. However, sequencing for every CRC case is not cost-effective. An antibody specific for *BRAF* V600E mutant protein has been introduced, and we thus examined the utility of BRAF VE1 immunohistochemistry for evaluating *BRAF* mutations in CRC. **Methods:** Fifty-one *BRAF*-mutated CRCs and 100 age and sex-matched *BRAF* wild-type CRCs between 2005 and 2015 were selected from the archives of Asan Medical Center. Tissue microarrays were constructed and stained with BRAF VE1 antibody. **Results:** Forty-nine of the 51 *BRAF*-mutant CRCs (96.1%) showed more than moderate cytoplasmic staining, except for two weakly stained cases. Six of 100 *BRAF* wild-type cases also stained positive with BRAF VE1 antibody; four stained weakly and two stained moderately. Normal colonic crypts showed nonspecific weak staining, and a few CRC cases exhibited moderate nuclear reactivity (3 *BRAF*-mutant and 10 *BRAF* wild-type cases). *BRAF*-mutated CRC patients had higher pathologic stages and worse survival than *BRAF* wild-type patients. **Conclusions:** BRAF VE1 immunohistochemistry showed high sensitivity and specificity, but occasional nonspecific staining in tumor cell nuclei and normal colonic crypts may limit their routine clinical use. Thus, BRAF VE1 immunohistochemistry may be a useful screening tool for *BRAF* V600E mutation in CRCs, provided that additional sequencing studies can be done to confirm the mutation in BRAF VE1 antibody-positive cases.

Key Words: Colorectal neoplasms; *BRAF* mutation; Immunohistochemistry; DNA sequencing

Colorectal cancer (CRC) is one of most common forms of malignancy worldwide and deadliest cancer-related diseases.¹ It has been described to result from sequential activation of oncogenes and concomitant inactivation of tumor suppressor genes.¹ Among these various oncogenic events, approximately 10%–15% of CRC patients are characterized by a mutation in v-Raf murine sarcoma viral oncogene homolog B (*BRAF*).^{1,2} *BRAF* oncogene encoding BRAF protein, which is localized in the downstream of *RAS*, leads to the stimulation of mitogen-activated protein kinase pathway. It contains a typical hot spot oncogenic mutation, typically V600E (change from valine to glutamic acid at codon 600), which accounts for up to 80% of all *BRAF* mutations.³ *BRAF* mutation has also been reported to be an independent predictor of poor prognosis in CRC.^{1,4} Typically, *BRAF* mutations in CRC can be detected by Sanger sequencing or allele-specific polymerase chain reaction (PCR), but these methods are time-consuming and costly. Recently, immunohistochemistry (IHC) using an antibody specific for *BRAF* V600E mutant protein (BRAF VE1 antibody) has been proposed as a useful diag-

nostic tool for *BRAF* V600E mutation detection in CRC,^{5,6} but its clinical utility is controversial. For instance, the staining quality of BRAF VE1 antibody in CRC has been reported to be inferior to that in melanoma or thyroid cancer.^{7,8} Thus, it is unclear whether BRAF VE1 antibody can be used in the clinic to detect *BRAF* V600E mutation in CRC in place of sequencing analyses. In this study, we evaluated the usefulness of BRAF VE1 IHC for detecting *BRAF* V600E mutations in CRC and analyzed the clinicopathologic characteristics of *BRAF*-mutant CRCs compared to those in *BRAF* wild-type controls.

MATERIALS AND METHODS

Patients and samples

The study group consisted of 51 surgically resected primary or metastatic CRC cases harboring *BRAF* V600E mutation (colonoscopic biopsy [n = 17], primary tumor resection [n = 31], and metastasectomy [n = 3]) and 100 age and sex-matched *BRAF* wild-type CRCs (colonoscopic biopsy [n = 14], primary

tumor resection [n = 81], and metastasectomy [n = 5]). They were selected from the surgical pathology files between 2005 and 2015 at the Department of Pathology, Asan Medical Center, University of Ulsan College of Medicine, Seoul, Korea. The *BRAF* V600E mutation status was confirmed by Sanger sequencing (n = 75), quantitative allele-specific PCR (n = 16), and mass spectrometry-based genotyping (n = 60). All cases were *KRAS* wild-type. Histopathological features of the 151 CRCs were reviewed by two pathologists (J.H.K. and J.K.) and clinical information including age, gender, tumor location, histology, lymphovascular invasion, perineural invasion, serosal involvement, nodal status, and follow-up results was obtained from the medical records. This study was approved by the Institutional Review Board (IRB) (2015-1393) of Asan Medical Center, and patient informed consent was waived by the IRB.

Tissue microarray construction and IHC

Tissue microarrays (TMAs) were constructed from 34 surgically resected *BRAF*-mutated samples and 86 *BRAF* wild-type samples.

The TMA was constructed using a hollow needle to remove a tissue core (0.2 cm in diameter) from tumors on paraffin-embedded tissue blocks. These cores were then inserted into recipient blocks. Sections of the TMA blocks were cut using a microtome, mounted on a microscope slide, and then stained. TMA and biopsy samples were subjected to IHC analysis using anti-*BRAF* antibody (mouse monoclonal, clone VE1, catalog number: 790-4855, Ventana Medical Systems, Tucson, AZ, USA) and a BenchMark XT automatic immunostaining device (Ventana Medical Systems) with an OptiView DAB IHC Detection Kit (Ventana Medical Systems) according to the manufacturer's instructions with slight modifications: we diluted primary antibody with recommended dilution buffer to 1:4 and increased primary antibody incubation time from 16 to 32 minutes, in order to prevent nonspecific background signals.

IHC staining results were graded using a 4-tier grading system according to the staining intensity as follows: 0 (no staining), 1+ (faint), 2+ (moderate), and 3+ (strong) (Fig. 1A–C). Only cytoplasmic staining was considered positive. As a positive control, we selected a case of papillary thyroid carcinoma harboring

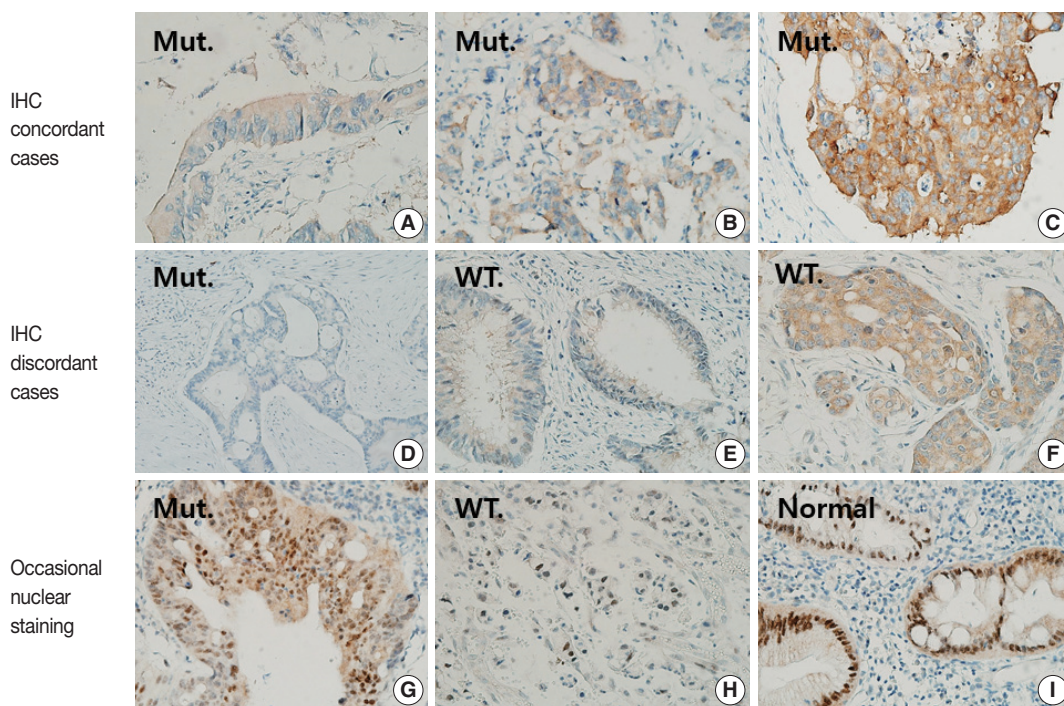


Fig. 1. Various staining patterns for BRAF VE1 immunohistochemistry (IHC). (A–C) BRAF VE1 is stained in cytoplasm with variable intensities in *BRAF*-mutated colorectal cancers (CRCs). 1+, faint (A); 2+, moderate (B); and 3+, strong (C). (D–F) Representative figures for cases with discrepancies between BRAF VE1 IHC and BRAF sequencing results. Negative staining in a *BRAF*-mutated CRC (D); 1+, faint cytoplasmic staining in a *BRAF* wild-type CRC (E); and 2+, moderate cytoplasmic staining in a *BRAF* wild-type CRC (F). (G–I) Representative figures for cases showing nuclear BRAF VE1 staining. (G) A *BRAF*-mutated CRC showing nuclear staining as well as moderate cytoplasmic staining. (H) A *BRAF* wild-type CRC showing only nuclear staining. (I) Non-neoplastic colonic crypts showing strong nuclear and faint cytoplasmic staining. Mut., *BRAF*-mutated CRCs; WT, *BRAF* wild-type CRCs.

BRAF V600E mutation and strong BRAF VE1 staining. As a negative control, we used normal tonsil tissue stained in the same manner with and without primary antibody. When the results of BRAF VE1 IHC differed from those of *BRAF* sequencing, we repeated BRAF VE1 IHC using whole tumor sections that were cut from the same paraffin block from which DNA had been extracted for *BRAF* sequencing.

Determination of *BRAF* mutation status

BRAF V600E mutation status was confirmed by Sanger sequencing (n = 75), quantitative allele-specific PCR (n = 16), or mass spectrometry-based genotyping (n = 60) as described previously.⁹⁻¹¹ All tumor tissue sections were macrodissected to increase tumor purity. When tumor purity in the macrodissected area was low (< 40%) and Sanger sequencing did not detect *BRAF* mutations, the *BRAF* mutation status was confirmed by a more sensitive method such as quantitative allele-specific PCR or mass spectrometric genotyping.

Statistical analysis

To compare clinicopathologic variables, statistical analyses were performed using SPSS ver. 20.0 statistical software (IBM Corp., Armonk, NY, USA) and differences between the two groups were compared by either chi-square test or Fisher's exact test. The Kaplan-Meier method with log-rank test and multivariate Cox proportional hazards regression models were applied for survival analyses. Two-sided p-values of < .05 were considered statistically significant.

RESULTS

Diagnostic performance of BRAF VE1 IHC

Forty-nine of 51 CRCs (96.1%) harboring *BRAF* V600E mutation showed cytoplasmic staining for BRAF VE1 antibody with variable intensities (Table 1, Fig. 1A–D): 3+ in 23 cases (45.1%), 2+ in 24 cases (47.1%), and 1+ in two cases (3.9%). In two *BRAF*-mutant cases (3.9%), no signal was detected by BRAF

VE1 IHC. In 100 *BRAF* wild-type controls, 94 (94%) cases showed no staining, while six cases (6%) showed cytoplasmic staining with moderate (2 cases, 2%) or weak (4 cases, 4%) intensities (Table 1, Fig. 1E, F). Thus, the sensitivity, specificity, positive predictive value, and negative predictive value of BRAF VE1 IHC were 96.1%, 94%, 89.1%, and 97.9%, respectively. The cutoff for a positive staining was set to 1+ or bigger score because the area under curve was maximal at this cutoff in receiver operating characteristic (ROC) curve analysis (Supplementary Fig. S1). *BRAF* V600E mutant tumors with negative BRAF VE1 staining or *BRAF* wild-type tumors with positive BRAF VE1 staining did not exhibit any distinct clinicopathologic features (Supplementary Tables S1, S2).

Analysis of cases with discrepant results between *BRAF* mutation status and BRAF VE1 IHC results

For cases with discrepant results between *BRAF* sequencing and BRAF VE1 IHC, we repeated BRAF VE1 IHC on the same paraffin block from which DNA had been extracted for sequencing analyses. However, BRAF VE1 IHC on the whole tumor section showed the same results as those on TMA. As for *BRAF*-mutant cases that showed negative BRAF VE1 IHC results, IHC was repeated using matched biopsy tissues to exclude the possibility of false negative results due to poor fixation. However, the matched biopsy tissues showed the same results. Conversely, for *BRAF* wild-type cases that showed positive IHC results, we first investigated whether the discrepancies were due to false negative sequencing results associated with low tumor purity. All *BRAF* wild-type cases with positive immunostaining were examined for tumor purity on hematoxylin and eosin-stained slides; in most cases, tumor purity was more than 30%, and *BRAF* wild-type status of those cases were confirmed by allele-specific PCR study. One *BRAF* wild-type CRC with BRAF IHC staining intensity of 2+ had tumor purity of about 5%, but repeated allele-specific PCR study failed to reveal *BRAF* V600E mutation.

Table 1. Correlation of gene mutation of *BRAF* V600E and immunohistochemical results in colorectal cancer

| <i>BRAF</i> sequencing | BRAF VE1 immunostaining | | | | Total |
|------------------------|-------------------------|------------------------|-----------|----------------------|-------|
| | 1+ | 2+ | 3+ | Negative | |
| V600E mutation | 2 (3.9) | 24 (47.1) ^a | 23 (45.1) | 2 (3.9) | 51 |
| Wild-type | 4 (4) | 2 (2) | 0 | 94 ^b (94) | 100 |
| Total | 6 | 26 | 23 | 96 | 151 |

Values are presented as number (%).

^aThree *BRAF* mutated colorectal cancers (5.9%) showed both nuclear and cytoplasmic staining; ^bOne *BRAF* wild-type colorectal cancer (1%) showed only nuclear staining.

Atypical patterns of BRAF VE1 IHC and nonspecific staining in normal colonic mucosa

Three *BRAF* V600E mutated cases (5.9%) showed moderate nuclear staining together with moderate cytoplasmic staining, and one *BRAF* V600E wild type case showed only moderate nuclear staining (Fig. 1G, H, Supplementary Table S3). In addition, normal colonic mucosa was also stained, especially along the crypt surface (Fig. 1I).

Clinicopathologic characteristics of *BRAF* mutant CRC

BRAF V600E mutated CRC cases showed significantly worse overall and progression-free survival (Fig. 2). Patients with *BRAF* V600E mutant CRC more frequently showed right-sided location, lymphovascular invasion, larger tumor size, and higher TNM stage at diagnosis than did patients with *BRAF* wild-type CRC. Particularly, *BRAF* V600E mutant CRCs showed more frequent serosal penetration and peritoneal seeding (Table 2). Because the intensities of BRAF VE1 immunostaining varied within the *BRAF* V600E mutant CRC group, we speculated that *BRAF* mutant CRCs with higher mutant BRAF protein expression might show worse prognosis if mutant BRAF protein actually plays a role in the aggressive biologic behavior. Indeed, *BRAF* mutant CRC cases with higher mutant BRAF protein expression tended to show shorter overall and progression-free survival than those with lower mutant BRAF protein expression, although the differences were not statistically significant (Table 3, Fig. 3).

DISCUSSION

In the present study, we showed that the diagnostic perfor-

mance of BRAF VE1 antibody was relatively good (sensitivity, specificity, and positive predictive values of 96.1%, 94%, and 89.1%, respectively). However, several *BRAF* V600E mutant CRCs showed no or weak BRAF VE1 staining ($n = 4$) or *BRAF* wild-type CRCs showed unequivocal cytoplasmic BRAF VE1 staining ($n = 6$). In addition, four CRC cases showed nonspecific nuclear BRAF VE1 staining as did normal colonic mucosa. Thus, the usefulness of BRAF VE1 IHC may be limited; it may be difficult to use BRAF VE1 IHC as a routine clinical test, although it may be useful as a screening tool when used in conjunction with subsequent confirmatory sequencing.

BRAF-mutant CRCs, which were all microsatellite stable, were in advanced stages at diagnosis ($p < .001$) and showed worse overall and recurrence-free survival than *BRAF* wild-type CRCs. These results are consistent with those of most previous studies.¹²⁻¹⁴ Moreover, *BRAF*-mutant CRCs were associated with the right colon, larger primary tumor size, and presence of lymphovascular invasion, all of which are consistent with the results of most previous studies.²

Recently, BRAF VE1 antibody has been used as a biomarker of CRC in IHC studies of BRAF. The clinical usefulness of BRAF VE1 antibody in colon cancer is controversial, but most studies showed that BRAF VE1 IHC has an excellent sensitivity.^{5,6} Interpretation of BRAF VE1 IHC may be difficult due to technical problems such as poor fixation or staining failure.^{15,16} Thus, we compared BRAF VE1 IHC and fixation quality between surgically resected tissues and matched colonoscopic biopsy tissues of two *BRAF* mutant CRC cases that showed negative staining results. There was no difference between the biopsied tissue and surgically resected tissue.

For *BRAF* wild-type CRCs showing positive immunostaining

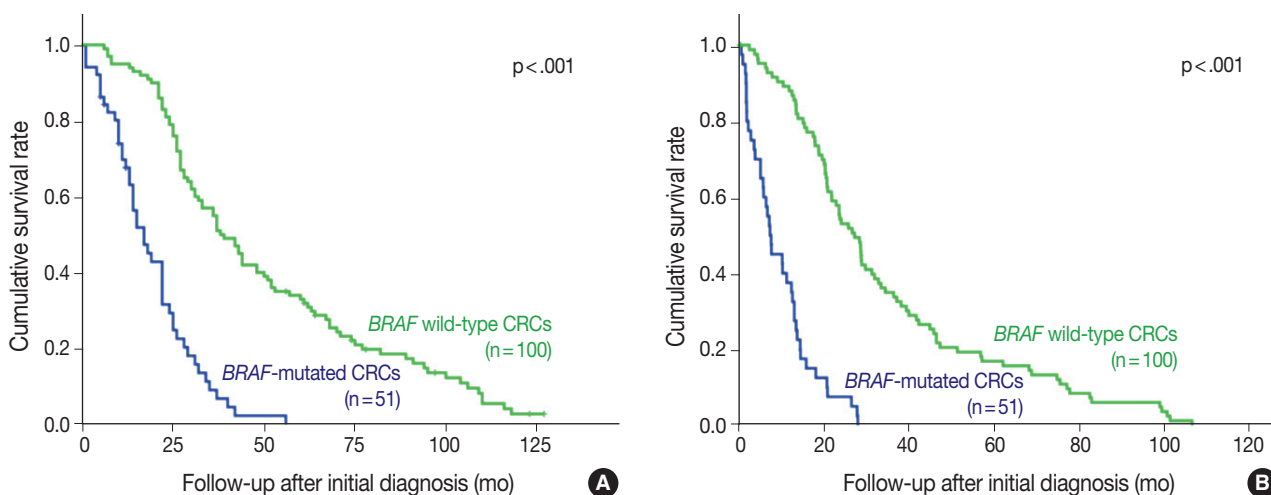


Fig. 2. *BRAF*-mutated colorectal cancer (CRC) patients have shorter overall (A) and progression-free survival (B) periods ($p < .001$).

Table 2. Clinicopathological features and prognosis of *BRAF* wild-type colorectal cancers

| Clinicopathologic characteristic | <i>BRAF</i> mutant (n=51) | <i>BRAF</i> wild-type (n=100) | p-value |
|--|---------------------------|-------------------------------|---------|
| Age (yr) | 57 (36–77) | 56 (36–76) | .419 |
| Sex | | | .189 |
| Male | 27 (52.9) | 64 (64.0) | |
| Female | 24 (47.1) | 36 (36.0) | |
| Location | | | <.001 |
| Left side colon | 20 (39.2) | 91 (91.0) | |
| Right side colon | 31 (60.8) | 9 (9.0) | |
| Tumor size (greatest dimension size, cm) | 5.8 (2–18) | 4.5 (0.9–11.2) | .002 |
| T stage | | | <.001 |
| 1–3 | 22 (43.1) | 77 (77.0) | |
| 4a | 12 (23.5) | 5 (5.0) | |
| 4b | 4 (7.8) | 0 | |
| TX | 13 (25.5) | 18 (18.0) | |
| N stage | | | .001 |
| N0 | 2 (3.9) | 19 (19.0) | |
| N1 | 9 (17.6) | 34 (34.0) | |
| N2 | 26 (49.0) | 29 (29.0) | |
| NX | 13 (25.5) | 18 (18.0) | |
| Distant metastasis | | | <.001 |
| No | 0 | 1 (1.0) | |
| Unifocal | 2 (3.9) | 26 (26.0) | |
| Multifocal | 49 (96.1) | 73 (73.0) | |
| Lymphovascular invasion | 31 (60.8) | 35 (35.0) | <.001 |
| Perineural invasion | 23 (45.1) | 33 (33.0) | .065 |
| Resection margin involve | 7 (18.4) | 3 (3.5) | .005 |
| Immunostaining results of BRAF VE1 | | | <.001 |
| Negative | 2 (3.9) | 94 (94.0) | |
| 1+ | 2 (3.9) | 4 (4.0) | |
| 2+ | 24 (47.1) | 2 (2.0) | |
| 3+ | 23 (45.1) | 0 | |
| Peritoneal seeding | 31 (60.8) | 13 (13.0) | <.001 |

Values are presented as median (range) or number (%).

Crosstab analysis for categorical and ordinal variables used chi-square test and for numerical variables used Student t test.

Table 3. Prognostic factors for *BRAF*-mutated colorectal cancer

| | Univariate HR (95% CI) | p-value | Multivariate HR (95% CI) | p-value |
|----------------------------|------------------------|---------|--------------------------|---------|
| Strong BRAF intensity (3+) | 1.84 (0.99–3.42) | .054 | 3.36 (1.29–8.75) | .013 |
| Sex male | 0.98 (0.70–1.39) | .919 | 2.67 (0.99–7.18) | .052 |
| Location | | | | |
| Left side colon | Reference | | Reference | |
| Right side colon | 1.01 (0.55–1.84) | .977 | 1.65 (0.67–4.09) | .279 |
| Involved resection margin | 1.43 (0.69–2.94) | .337 | 4.27 (1.20–15.19) | .025 |
| Perineural invasion | 1.58 (1.06–2.37) | .025 | 0.32 (0.10–0.97) | .044 |
| Lymphovascular invasion | 2.14 (1.45–3.18) | <.001 | 10.05 (2.13–47.43) | .004 |
| Lymph node metastasis | | .380 | | .107 |
| N0 | Reference | | Reference | |
| N1 | 4.27 (0.51–36.08) | .182 | 0.11 (0.01–1.98) | .133 |
| N2 | 4.22 (0.55–32.35) | .166 | 0.29 (0.02–4.01) | .289 |
| T category | | .001 | | .023 |
| 1–3 | Reference | | Reference | |
| 4a | 3.13 (1.71–5.71) | <.001 | 4.89 (1.46–16.40) | .010 |
| 4b | 2.36 (0.73–7.59) | .150 | 0.77 (0.19–3.19) | .720 |
| Peritoneal seeding | 1.53 (0.83–2.87) | .188 | 1.31 (0.56–3.03) | .533 |

HR, hazard ratio; CI, confidence interval.

Univariate and multivariate Cox-regression analyses were used to calculate hazard ratio of clinicopathologic factors on overall survival. Multivariate Cox-regression analysis used the Enter method.

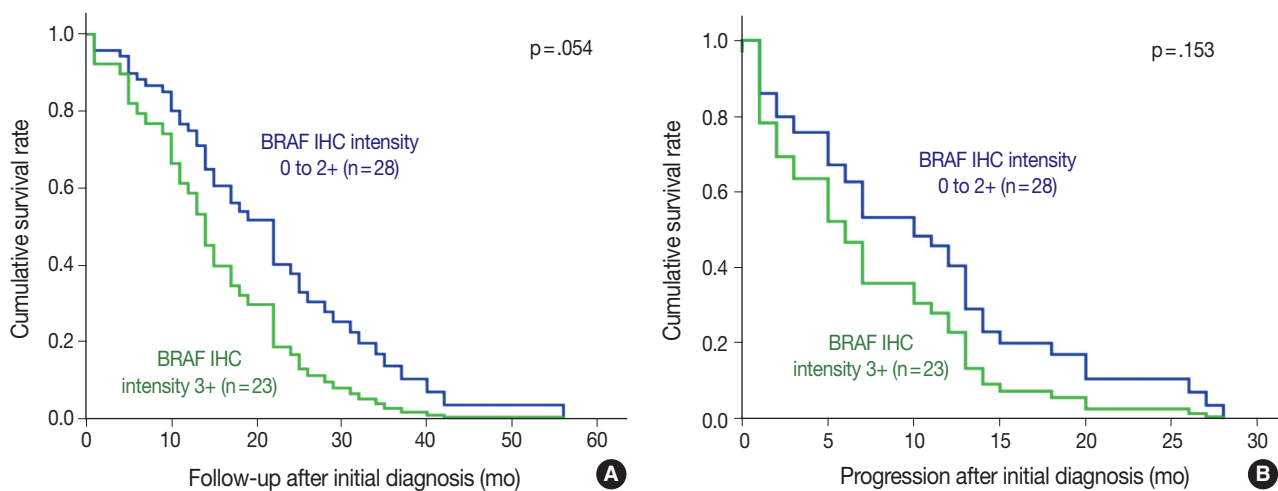


Fig. 3. *BRAF*-mutated colorectal cancer patients with high immunohistochemistry (IHC) intensity generally showed shorter overall (A) and progression-free survival (B) than patients with low IHC intensity ($p > .05$).

results, the discrepancies might have resulted from false-negative sequencing results if the tumor purity is very low. For example, tumors with signet rings or tumors with high mucin content have low tumor purity.¹⁷ Therefore, we examined the tumor purity of all *BRAF* wild-type CRCs that stained positive in IHC. In most cases, false-negative sequencing results were excluded by repeating *BRAF* mutation analyses using more sensitive methods, but in one *BRAF* wild-type CRC with a tumor purity of approximately 5% and *BRAF* VE1 2+, we could not conduct more sensitive mutation analysis because tissue material was unavailable. Therefore, in this case, the possibility of a false-negative sequencing result could not be excluded.

Interestingly, CRC cases with more intense *BRAF* VE1 immunostaining had a tendency to the shorter overall and progression-free survival. Although this result is difficult to interpret, the expression of *BRAF* V600E mutant protein may play a biological role in tumor aggressiveness rather than being a simple surrogate marker for prognosis. However, our study has a few limitations. Since we performed *BRAF* VE1 IHC in CRCs with known *BRAF* mutational status in a retrospective manner, the strength of evidence may be limited compared to that of a prospective design. In addition, a relatively small number of *BRAF* V600E mutant CRCs may limit the statistical power. Finally, the evaluation of prognostic value of *BRAF* mutations might be limited because the study population had a selection bias; it had not been selected in a consecutive manner.

Based on our results, the diagnostic performance of *BRAF* VE1 IHC showed relatively good but sometimes ambiguous staining, which may limit its routine clinical use; thus, *BRAF* VE1 IHC cannot replace *BRAF* sequencing studies. Despite these

limitations, *BRAF* VE1 IHC may be carefully used as a screening tool for *BRAF* V600E mutation detection in a research basis, as *BRAF* VE1 IHC is more cost-effective and less time-consuming than *BRAF* sequencing studies.

Electronic Supplementary Material

Supplementary materials are available at Journal of Pathology and Translational Medicine (<http://jpatholm.org>).

Conflicts of Interest

No potential conflict of interest relevant to this article was reported.

REFERENCES

- Barras D. *BRAF* mutation in colorectal cancer: an update. *Biomark Cancer* 2015; 7(Suppl 1): 9-12.
- Boulagnon C, Dudez O, Beaudoux O, et al. *BRAF*V600E gene mutation in colonic adenocarcinomas: immunohistochemical detection using tissue microarray and clinicopathologic characteristics: an 86 case series. *Appl Immunohistochem Mol Morphol* 2016; 24: 88-96.
- Ritterhouse LL, Barletta JA. *BRAF* V600E mutation-specific antibody: a review. *Semin Diagn Pathol* 2015; 32: 400-8.
- Safae Ardekani G, Jafarnejad SM, Tan L, Saeedi A, Li G. The prognostic value of *BRAF* mutation in colorectal cancer and melanoma: a systematic review and meta-analysis. *PLoS One* 2012; 7: e47054.
- Bledsoe JR, Kamionek M, Mino-Kenudson M. *BRAF* V600E immunohistochemistry is reliable in primary and metastatic colorectal carcinoma regardless of treatment status and shows high intratumoral homogeneity. *Am J Surg Pathol* 2014; 38: 1418-28.

6. Mesteri I, Bayer G, Meyer J, *et al.* Improved molecular classification of serrated lesions of the colon by immunohistochemical detection of *BRAF* V600E. *Mod Pathol* 2014; 27: 135-44.
7. Loes IM, Immervoll H, Angelsen JH, *et al.* Performance comparison of three *BRAF* V600E detection methods in malignant melanoma and colorectal cancer specimens. *Tumour Biol* 2015; 36: 1003-13.
8. Schafroth C, Galvan JA, Centeno I, *et al.* VE1 immunohistochemistry predicts *BRAF* V600E mutation status and clinical outcome in colorectal cancer. *Oncotarget* 2015; 6: 41453-63.
9. Gonzalez de Castro D, Angulo B, Gomez B, *et al.* A comparison of three methods for detecting *KRAS* mutations in formalin-fixed colorectal cancer specimens. *Br J Cancer* 2012; 107: 345-51.
10. Lang AH, Drexel H, Geller-Rhomberg S, *et al.* Optimized allele-specific real-time PCR assays for the detection of common mutations in *KRAS* and *BRAF*. *J Mol Diagn* 2011; 13: 23-8.
11. Shin SJ, Chun SM, Kim TI, *et al.* Feasibility of multiplexed gene mutation detection in plasma samples of colorectal cancer patients by mass spectrometric genotyping. *PLoS One* 2017; 12: e0176340.
12. Zlobec I, Bihl MP, Schwarb H, Terracciano L, Lugli A. Clinicopathological and protein characterization of *BRAF*- and *K-RAS*-mutated colorectal cancer and implications for prognosis. *Int J Cancer* 2010; 127: 367-80.
13. Lochhead P, Kuchiba A, Imamura Y, *et al.* Microsatellite instability and *BRAF* mutation testing in colorectal cancer prognostication. *J Natl Cancer Inst* 2013; 105: 1151-6.
14. Ogino S, Noshio K, Kirkner GJ, *et al.* CpG island methylator phenotype, microsatellite instability, *BRAF* mutation and clinical outcome in colon cancer. *Gut* 2009; 58: 90-6.
15. Adackapara CA, Sholl LM, Barletta JA, Hornick JL. Immunohistochemistry using the *BRAF* V600E mutation-specific monoclonal antibody VE1 is not a useful surrogate for genotyping in colorectal adenocarcinoma. *Histopathology* 2013; 63: 187-93.
16. Qiu T, Lu H, Guo L, *et al.* Detection of *BRAF* mutation in Chinese tumor patients using a highly sensitive antibody immunohistochemistry assay. *Sci Rep* 2015; 5: 9211.
17. Ogino S, Brahmandam M, Cantor M, *et al.* Distinct molecular features of colorectal carcinoma with signet ring cell component and colorectal carcinoma with mucinous component. *Mod Pathol* 2006; 19: 59-68.

The Major Role of NF- κ B in the Depth of Invasion on Acral Melanoma by Decreasing CD8⁺ T Cells

Hermin Aminah Usman
Bethy S. Hernowo
Maringan Diapari Lumban Tobing¹
Reti Hindritiani²

Departments of Anatomical Pathology,
¹Obstetrics and Gynecology and
²Dermatovenerology, Faculty of Medicine,
Universitas Padjadjaran/Hasan Sadikin General
Hospital, Bandung, Indonesia

Received: December 19, 2017
Revised: March 28, 2018
Accepted: April 4, 2018

Corresponding Author
Hermin Aminah Usman, MD
Department of Anatomy Pathology, Faculty of
Medicine, Universitas Padjadjaran, Jl. Eyckman No
38, Bandung, Indonesia
Tel: +62-222551126
Fax: +62-222031447
E-mail: hermin@unpad.ac.id

Background: The tumor microenvironment including immune surveillance affects malignant melanoma (MM) behavior. Nuclear factor κ B (NF- κ B) stimulates the transcription of various genes in the nucleus and plays a role in the inflammatory process and in tumorigenesis. CD8⁺ T cells have cytotoxic properties important in the elimination of tumors. However, inhibitory receptors on the cell surface will bind to programmed death-ligand 1 (PD-L1), causing CD8⁺ T cells to lose their ability to initiate an immune response. This study analyzed the association of NF- κ B and PD-L1 expression levels and CD8⁺ T-cell counts with depth of invasion of acral MM, which may be a predictor of aggressiveness related to an increased risk of metastasis. **Methods:** A retrospective cross-sectional study was conducted in the Department of Anatomical Pathology, Faculty of Medicine, Universitas Padjadjaran/Hasan Sadikin Hospital using 96 cases of acral melanoma. Immunohistochemical staining was performed on paraffin blocks using anti-NF- κ B, -PD-L1, and -CD8 antibodies and invasion depth was measured using dotSlide-imaging software. **Results:** The study showed significant associations between the individual expression of NF- κ B and PD-L1 and CD8⁺ T-cell number, with MM invasion depth. NF- κ B was found to be a confounding variable of CD8⁺ T-cell number ($p < .05$), but not for PD-L1 expression ($p = .154$). Through multivariate analysis it was found that NF- κ B had the greatest association with the depth of invasion ($p < .001$), whereas PD-L1 was unrelated to the depth of invasion because it depends on the number of CD8⁺ T cells ($p = .870$). **Conclusions:** NF- κ B plays a major role in acral MM invasion, by decreasing the number of CD8⁺ T cells in acral MM.

Key Words: Acral; CD8⁺ T cells; Invasion; Melanoma; NF- κ B; PD-L1

The main factor associated with metastasis in malignant melanoma (MM) is the ability of tumor cells to invade the surrounding tissue and reach lymphovascular vessels. Nuclear factor κ B (NF- κ B) is a protein complex which functions as a transcription factor to stimulates transcription of various genes. NF- κ B translocates to the nucleus and acts as a transcription factor in the nucleus, leading to increases in the expressions of genes that play roles in proliferation, invasion, anti-apoptosis, and survival of tumor cells.¹ Several studies have demonstrated the role of NF- κ B in thyroid carcinoma with a *BRAFV600E* gene mutation that causes increased invasion and metastasis² and, in ovarian malignancy NF- κ B leads to progression and metastasis.³

MM behavior is influenced by various oncogenes and the tumor microenvironment, namely immune surveillance, characterized by inflammatory cell infiltration.⁴⁻⁷ Inflammatory reactions generally have two roles in carcinogenesis. In the acute phase, activation of NF- κ B is part of the body's immune defense system involved in the process of tumor cell elimination. On the other

hand, however, NF- κ B consecutively functions in a pro-tumorigenic manner.^{8,9} The protective role of NF- κ B as a tumor cell eliminator changes under circumstances of chronic inflammation, resulting in an "immune escape" leading to a stronger pro-tumorigenic role. However, the immune response which act as a defense against tumor cell invasion and progression is primarily carried out by CD8⁺ T cells.¹⁰⁻¹³ T cells expresses the inhibitory receptor programmed death 1 (PD-1) on their cell surface and one of its ligand is programmed death-ligand 1 (PD-L1).¹⁴ The appearance of T cells as tumor-infiltrating lymphocytes (TILs) in the tumor and surrounding the tumor stimulates the expression of PD-L1 in tumor cells in an attempt to avoid the cytotoxic cell execution process.¹⁴ The aim of this research was to analyze the role of NF- κ B and its interaction with CD8 with respect to immune surveillance and PD-L1 on acral MM.

MATERIALS AND METHODS

Paraffin blocks from patients who had undergone excisional and surgical biopsies and had been diagnosed histopathologically as having acral MM between 1 January 2011 and 31 December 2016 were used in this study. Ethical clearance was approved by the Health Research Ethics Committee of the Faculty of Medicine Universitas Padjadjaran with a waiver of informed consent (1155/UN6.C1.3.2/KEPK/PN/2016).

Acral melanoma was defined as a melanoma located on the non-hair bearing skin of the palms and soles or under the nails, which has histopathological features of both acral lentiginous melanoma and subtypes such as superficial spreading melanoma and nodular melanoma. Clinicopathological parameters included in the analysis were: age, sex, Clark level, ulceration, and degree of lymphocytic infiltration. TILs were defined as lymphocytes infiltrating and disrupting tumor nests and/or in direct contact with tumor cells as observed by hematoxylin and eosin staining. The cases were classified into four grades (0–3) according to TIL density (mild, moderate, or marked) and distribution (focal, multifocal, or diffuse across the entire extent of the tumor). The invasion depth was measured from the epidermal surface to the deepest part of the invasion in the dermis using Olympus BX-51/22 dotSlide digital virtual microscope (Olympus, Center Valley, PA, USA).

Immunohistochemical examination

Immunohistochemical staining on the samples was performed manually using a labeled streptavidin biotin immunoperoxidase complex method, using the Starr Trek Universal HRP Detection system (Biocare Medical, Concord, CA, USA). Samples were sectioned to 4-μm thicknesses, deparaffinized using xylene and rehydrated using an alcohol solution. Antigen retrieval used a decloak-ing tool for 45–60 minutes at a temperature of 98°C. The primary antibodies were NF-κB, CD8 (clone SP16), and PD-L1/CD274 (clone SP142) purchased from Spring Bioscience (Pleasanton, CA, USA). Immunoexpression of NF-κB in nuclei was assessed using semi-quantitative scores based on the intensity and distribution of the positive cells. Intensity scores were negative (0), weak (1), moderate (2), and strong (3), and the percentage of positive cells were grades as follows: 0, 0%; 1, < 25%; 2, 26%–50%; 3, 51%–75%; and 4, 76%–100%. The final score was calculated using Histoscore, namely the intensity × distribution with scores of 0–6 regarded as negative, scores of 8–12 were stated as positive (Fig. 1).¹⁵ PD-L1 staining in membranes and in the cytoplasm was assessed on a semi-quantitative scale:

positive when stained area was ≥5% and negative when < 5% (Fig. 2).¹⁶ The number of CD8⁺ T cells was assessed by counting the number lymphocytes stained brown on the tumor cell membrane by an anti-CD8 antibody. Results were divided into < 25 and ≥25 lymphocytes (Fig. 3).

Statistical analysis

Statistical analysis used the non-parametric Mann-Whitney test. A $p \leq .05$ was considered significant. The data obtained were recorded on a special form and then processed using SPSS program ver. 22.0 for Windows (IBM Corp., Armonk, NY, USA).

RESULTS

In this study, 135 total samples were available but only 96 were eligible for inclusion in the study.

Table 1 shows that the mean age of acral MM patients was 61.73 years old. Males and females accounted for 52.1% and

Table 1. Clinicopathological characteristics of acral melanoma patients

| Variable | No. (%) (n=96) |
|--------------------------|-----------------|
| Age | |
| Mean ± SD | 61.730 ± 12.330 |
| Sex | |
| Male | 50 (52.1) |
| Female | 46 (47.9) |
| Depth of invasion (mm) | |
| Mean ± SD | 8.074 ± 6.902 |
| Clark Level | |
| I | 0 |
| II–III | 28 (29.2) |
| IV–V | 68 (70.8) |
| Ulceration | |
| No | 36 (37.5) |
| Yes | 60 (62.5) |
| TILs | |
| Grade 0–I | 49 (51.0) |
| Grade II–III | 47 (49.0) |
| NF-κB | |
| Negative | 44 (45.8) |
| Positive | 52 (54.2) |
| CD8 ⁺ T cells | |
| < 25 | 62 (64.6) |
| ≥ 25 | 34 (35.4) |
| PD-L1 | |
| < 5% | 68 (70.8) |
| ≥ 5% | 28 (29.2) |

SD, standard deviation; TIL, tumor-infiltrating lymphocyte; NF-κB, nuclear factor κB; PD-L1, programmed death-ligand 1.

47.9% of patients, respectively, and the mean of depth of invasion was 8.074 mm. There were no samples that has a Clark level I and samples with a Clark level (II–V) and TILs grade (0–IV) were divide into two groups as shown below.

Table 2 shows that the Clark level and ulceration have statistically significant associations with the depth of invasion of acral melanoma ($p < .001$). The association of pathological characteristics (NF- κ B expression, CD8⁺ T-cell number, and PD-L1 expression) with the depth of invasion of acral melanoma was also statistically significant.

NF- κ B expression had a positive association with the depth of invasion ($p < .001$). When cells were positive for NF- κ B expression, the invasion of tumor cells in acral melanoma was deeper.

Table 2 demonstrates that when the invasion of tumor cells in acral melanoma was deeper, fewer CD8⁺ T cells were observed (< 25). Thus, the association was negative and statistically significant statistic ($p < .001$). The association between PD-L1 expression and the depth of invasion was also a negative association. When the depth of invasion was deeper, the percentage of cells expressing PD-L1 was $< 5\%$ and was a statistically significant result ($p = .001$).

The data in Table 2 demonstrate that all pathological charac-

Table 2. Association of clinicopathological characteristics and depth of invasion on acral melanoma

| Variable | Depth of invasion (mm) | p-value |
|--------------------------|------------------------|---------|
| Age | 8.074 ± 6.902 | .109 |
| Sex | | .086 |
| Male | 8.770 ± 7.235 | |
| Female | 7.319 ± 6.515 | |
| Clark level | | < .001 |
| II–III | 3.969 ± 3.023 | |
| IV–V | 9.765 ± 7.343 | |
| Ulceration | | < .001 |
| No | 5.353 ± 4.896 | |
| Yes | 9.707 ± 7.433 | |
| TILs | | .206 |
| Grade 0–I | 8.465 ± 6.263 | |
| Grade II–III | 7.668 ± 7.558 | |
| NF- κ B | | < .001 |
| Negative | 4.755 ± 3.075 | |
| Positive | 10.883 ± 7.951 | |
| CD8 ⁺ T cells | | < .001 |
| < 25 | 9.708 ± 6.970 | |
| ≥ 25 | 5.096 ± 5.760 | |
| PD-L1 | | < .001 |
| < 5% | 9.002 ± 7.034 | |
| ≥ 5% | 5.821 ± 6.115 | |

Values are presented as mean ± standard deviation.

TIL, tumor-infiltrating lymphocyte; NF- κ B, nuclear factor κ B; PD-L1, programmed death-ligand 1.

teristics examined (NF- κ B, PD-L1, and CD8⁺ T-cell number) had individual association with the depth of invasion. The data show a positive association between NF- κ B expression and the depth of invasion, while PD-L1 expression and CD8⁺ T-cell number had negative associations in acral melanoma.

The data in Table 3 demonstrate that the association of NF- κ B expression with PD-L1 expression and CD8⁺ T-cell number has different statistical significance. The statistical test for CD8⁺ T-cell number was significant ($p = .001$) while PD-L1 was not significant ($p = .154$). This proves that NF- κ B is a confounding variable for CD8⁺ T-cell numbers but not for PD-L1 expression.

Data on the association of PD-L1 with CD8⁺ T cells is shown in the Table 4. The number of CD8⁺ T cells affects the level of PD-L1 expression; this result was statistically significant ($p < .001$).

The multivariate analysis results presented in Table 5 show that the most influential factor on the invasion depth in acral MM is NF- κ B ($p < .001$). No significant results were found in the analysis of Clark level ($p = .185$), ulceration ($p = .156$), TILs ($p = .935$), CD8⁺ T-cell number ($p = .870$) or PD-L1 ($p = .495$).

DISCUSSION

NF- κ B immunoexpression is strongly associated with the depth of invasion in acral MM. An association between immunopositivity for NF- κ B and the in depth of invasion was found, as shown in Table 2. The NF- κ B pathway is important for tumor

Table 3. Association of NF- κ B with PD-L1 and CD8⁺ T cells in acral melanoma

| Variable | NF- κ B | | p-value |
|--------------------------|-----------------|-----------------|---------|
| | Negative (n=44) | Positive (n=52) | |
| PD-L1 | | | .154 |
| < 5% | 28 (63.6) | 40 (76.9) | |
| ≥ 5% | 16 (36.4) | 12 (23.1) | |
| CD8 ⁺ T cells | | | .001 |
| < 25 | 21 (47.7) | 41 (78.8) | |
| ≥ 25 | 23 (52.3) | 11 (21.2) | |

Values are presented as number (%).

NF- κ B, nuclear factor κ B; PD-L1, programmed death-ligand 1.

Table 4. Association of PD-L1 expression with CD8⁺ T cells number in acral melanoma

| PD-L1 | CD8 ⁺ T cells | | p-value |
|-------|--------------------------|-------------|---------|
| | < 25 (n=62) | ≥ 25 (n=34) | |
| < 5% | 60 (96.8) | 8 (23.5) | < .001 |
| ≥ 5% | 2 (3.2) | 26 (76.5) | |

Values are presented as number (%).

PD-L1, programmed death-ligand 1.

Table 5. Multivariate analysis of variables related to depth of invasion based on binary double linear regression analysis

| Variable | Unstandardized coefficients | | Standardized coefficients | p-value |
|--------------|-----------------------------|----------------|---------------------------|---------|
| | B | Standard error | Beta | |
| Clark level | 2,505.896 | 1,876.505 | 0.166 | .185 |
| Ulceration | 2,285.568 | 1,595.783 | 0.161 | .156 |
| TILs | -107.175 | 1,313.089 | -0.008 | .935 |
| NF-κB | 5,166.865 | 1,353.669 | 0.375 | <.001 |
| CD8+ T cells | 416.860 | 2,538.846 | 0.029 | .870 |
| PD-L1 | -1,541.337 | 2,248.71 | -0.102 | .495 |

Variables involved are significantly bivariably with $p < .25$.

TIL, tumor-infiltrating lymphocyte; NF-κB, nuclear factor κB; PD-L1, programmed death-ligand 1.

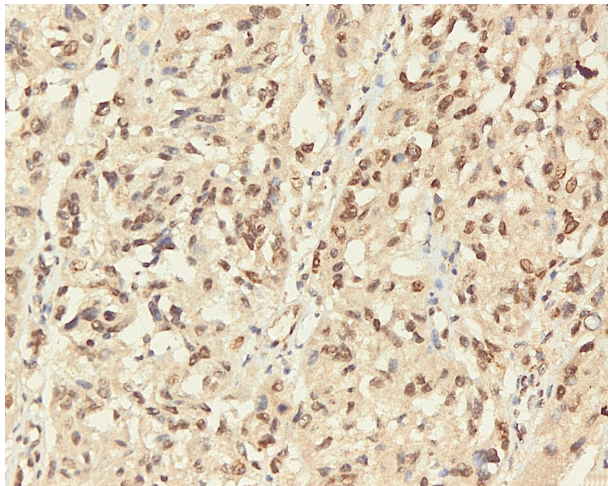


Fig. 1. Positive immunorexpression of nuclear factor κB on acral malignant melanoma.

cell survival, as NF-κB serves as a transcription factor to regulate the expression of anti-apoptotic, pro-proliferative, and pro-metastatic genes. The NF-κB pathway is activated through IκB kinase (IKK). IKK stimulates phosphorylation and degradation of the IκB inhibitor (IκB) through the proteasome, causing translocation of NF-κB into the cell nucleus. One of the genes upregulated by NF-κB in the nucleus is Snail, an inducer of metastasis through the epithelial mesenchymal transition (EMT) process of initiating tumor invasion.¹⁷ Snail is a transcription factor in the zinc-finger protein family that plays a role in metastasis and in the anti-apoptotic processes. Snail stimulates the metastasis through repression of E-cadherin, an adhesion molecule in cells. Loss of cell adhesion resulting from decreased E-cadherin will lead to the EMT process. Snail also affects EMT through down-regulation of claudin and occludin. Claudin and occludin maintain cell polarity. When claudin is down-regulated, cell polarity is lost, which increases the potential for EMT and invasion. In addition, Snail may induce matrix metalloproteinase (MMP) to increase tumor cell invasion capabilities.^{17,18} Another possible explanation

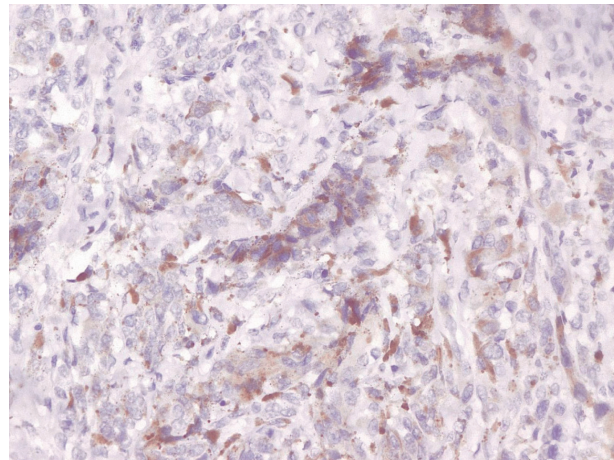


Fig. 2. Immunorexpression of progammed death-ligand1 $\geq 5\%$ on acral malignant melanoma.

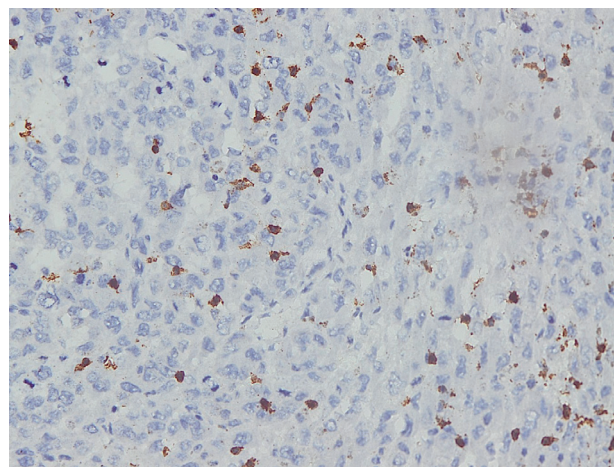


Fig. 3. CD8+ T cell number ≥ 25 by immunohistochemistry on acral malignant melanoma.

for the association of NF-κB with the invasion depth of acral MM is that NF-κB translocation to the cell nucleus also directly stimulates the expression of MMPs, especially MMP-9. Overexpression of MMP-9 increases the ability of cells to degrade extracellular matrix, making it easier for cells to invade.¹⁹ Song *et al.*¹⁵

reported a similar event where EMT process was stimulated through the NF- κ B activation pathway in hepatic carcinoma.

According to Table 2, the depth of invasion of acral MM is also associated with the number of CD8⁺ T cells: that is low CD8⁺ T-cell counts (< 25) more commonly found at invasion depths of > 4 mm (mean, 9.078 mm). This is in accordance with the research conducted by Castaneda *et al.*¹⁶ In that study, it was stated that TILs in acral MM were fewer in number compared to in other MM types and this corresponded to the depth of invasion, progression rate and survival rate.

In this study, NF- κ B was a confounding variable for the emergence of CD8⁺ T cells, as is supported by the data presented in Table 3. Thus, the association can be explained through various other data as described below.

NF- κ B is associated with various inflammatory factors including tumor necrosis factor α (TNF- α), interleukin 1, interleukin 6, reactive oxygen species, and cyclooxygenase 2 (COX-2). The imbalance of these inflammatory factors can lead to various conditions such as DNA damage, suppressor genes inactivity, increased invasion and metastatic capability of cancer cells, immune escapes, or other tumorigenic mechanisms.²⁰

In some studies, the increased activity of NF- κ B stimulates expression of COX-2 inflammatory factor.^{20,21} COX-2, also known as prostaglandin endoperoxidase 2 (PTGS2), is an enzyme that converts arachidonic acid metabolism into prostaglandins, especially prostaglandin E2 (PGE2), which is a main mediator of the inflammatory and angiogenic processes. COX-2 functions by inhibiting apoptosis and immune surveillance, promoting angiogenesis and improving cancer cell invasion and metastasis as well as influencing cell differentiation.^{20,21} COX-2 can also suppress antigen presentation and immune activation in cancer. COX-2 suppresses interferon-gamma secretion from T cells and induces immunosuppressive factor of regulatory T cells, which in turn plays a role in causing tumor resistance to immunotherapy.²²

Cancer immunology is a dynamic process involving the immune system and tumor cells consisting of three phases: elimination, equilibrium, and escape. During the elimination phase, the immune system successfully eliminates tumor cells through the immune surveillance network. Equilibrium is a latent period of the immune system after elimination phase failure causes tumor cells to become less-immunogenic. The escape phase is when tumor cells become less immunogenic, resulting in a tumor mass that is clinically detectable as a result of immune evasion.²² The study by Jang²² showed a strong association between COX-2 expression and the number of regulatory T cells. Reg T cells induce apoptosis in CD8⁺ T cells via perforin, FasL, and granzyme B,

resulting in an inverse relationship between the number of Reg T cells and CD8⁺ T cells.²² In addition, other studies have described that CD8⁺ T cells will decrease in number as a result of PGE2 expressed from COX-2. This happens because PGE2 removes CD127 on the surface of CD8⁺ T cells so as to decrease the function of CD8⁺ T cells in immune surveillance and decrease their proliferative ability.²³ Thus, based on this explanation and data from the results of this study (Tables 2, 3), the decreased number of CD8⁺ T cells may be affected by NF- κ B via COX2 and Reg T cells and this corresponds to the depth of invasion in acral MM.

In this study, we found an association between PD-L1 immunoeexpression and the depth of invasion. Specifically, as shown in Table 2, expression of PD-L1 in < 5% of cells was found at invasion depths of > 4 mm (mean, 9.002 mm). PD-L1 expression in various types of malignancies including MM correlates with different prognostic outcomes. The results of this study were consistent with studies of squamous carcinoma,²⁴ melanocytic lesions²⁵ and hepatic carcinoma.²⁶ In these prior studies, it was stated that low PD-L1 expression was associated with larger tumor size, increased depth of invasion, disease progression and lower survival rates. However, results of this study differed from other studies of desmoplastic melanoma,²⁷ breast carcinoma,²⁸ gastric carcinoma,²⁹ renal carcinoma,³⁰ and glioma.³¹ In these studies, although stated that there is an association of PD-L1 expression with disease progressivity and a worse prognosis, the association was negative such that the higher the PD-L1 expression the worse the prognosis. In renal carcinoma, PD-L1 expression has been reported to induce EMT by up-regulating the sterol regulatory element-binding protein 1 (SREBP-1c) gene.³⁰ In glioma studies, PD-L1 expression has been reported to stimulate tumor cell proliferation and induce vascular endothelial growth factor expression causing angiogenesis and tumor progression.³¹ However, in this study low PD-L1 expression was actually associated with the depth of invasion.

T cells have inhibitory receptors called PD-1 on their surfaces which are bound by PD-L1 as their ligand. The PD-1/PD-L1 bonding axis inhibits proliferation, inhibit anti-apoptotic, decreases T-cell survival and suppresses signaling by gamma interferon, interleukin 2 and TNF- α against T cells.¹² PD-L1 is expressed by tumor cells. The presence of a bond between PD-1 and PD-L1 results in a decrease in anti-tumor activity from effector T cells.³²

PD-L1 expression is consistent with the number of CD8⁺ T cells in the adjacent tumor and is associated with disease progression.^{27,28,30,31} The association between PD-L1 expression and the number of CD8⁺ T cells was demonstrated in this study, based on the data in Table 4. Specifically, when PD-L1 was expressed

at < 5%, the number of CD8⁺ T cells counted was < 25. Based on the data in Table 2, there is a proven association between PD-L1 expression and invasion depth in acral melanoma. However, the data in Table 3 suggests that NF- κ B is apparently not a confounding variable for the emergence of PD-L1 expression. Thus, we concluded that the emergence of PD-L1 expression in acral MM depends on the presence of CD8⁺ T cells (Table 4). Multivariate analysis data (Table 5) revealed that NF- κ B has a major role in invasion of acral malignant melanoma. Its expression affects the depth of invasion while decreasing the number of CD8⁺ cells at the same time.

Our data demonstrates that the depth of invasion of acral melanoma is affected by NF- κ B, PD-L1 and the number of CD8⁺ T cells. We conclude that NF- κ B is the major factor associated with the depth of invasion and is negatively associated with the number of CD8⁺ T cells in acral melanoma. Thus, positive NF- κ B immunorexpression can be a predictive factor of acral melanoma aggressiveness related to an increasing risk of metastasis. Further studies on the microenvironment of tumors emphasizing various inflammatory factors and immune response are needed to find an appropriate, inexpensive, easily available targeted therapy for MM cases.

Conflicts of Interest

No potential conflict of interest relevant to this article was reported.

REFERENCES

- Oeckinghaus A, Ghosh S. The NF- κ B family of transcription factors and its regulation. *Cold Spring Harb Perspect Biol* 2009; 1: a000034.
- Bommarito A, Richiusa P, Carissimi E, *et al.* BRAFV600E mutation, TIMP-1 upregulation, and NF- κ B activation: closing the loop on the papillary thyroid cancer trilogy. *Endocr Relat Cancer* 2011; 18: 669-85.
- Yang G, Xiao X, Rosen DG, *et al.* The biphasic role of NF- κ B in progression and chemoresistance of ovarian cancer. *Clin Cancer Res* 2011; 17: 2181-94.
- Mao Y, Qu Q, Zhang Y, Liu J, Chen X, Shen K. The value of tumor infiltrating lymphocytes (TILs) for predicting response to neoadjuvant chemotherapy in breast cancer: a systematic review and meta-analysis. *PLoS One* 2014; 9: e115103.
- Bogunovic D, O'Neill DW, Belitskaya-Levy I, *et al.* Immune profile and mitotic index of metastatic melanoma lesions enhance clinical staging in predicting patient survival. *Proc Natl Acad Sci U S A* 2009; 106: 20429-34.
- Kluger HM, Zito CR, Barr ML, *et al.* Characterization of PD-L1 expression and associated T-cell infiltrates in metastatic melanoma samples from variable anatomic sites. *Clin Cancer Res* 2015; 21: 3052-60.
- Thomas NE, Busam KJ, From L, *et al.* Tumor-infiltrating lymphocyte grade in primary melanomas is independently associated with melanoma-specific survival in the population-based genes, environment and melanoma study. *J Clin Oncol* 2013; 31: 4252-9.
- DiDonato JA, Mercurio F, Karin M. NF- κ B and the link between inflammation and cancer. *Immunol Rev* 2012; 246: 379-400.
- Ben-Neriah Y, Karin M. Inflammation meets cancer, with NF- κ B as the matchmaker. *Nat Immunol* 2011; 12: 715-23.
- Kakavand H, Wilmott JS, Menzies AM, *et al.* PD-L1 expression and tumor-infiltrating lymphocytes define different subsets of MAPK inhibitor-treated melanoma patients. *Clin Cancer Res* 2015; 21: 3140-8.
- Tjin EP, Krebbers G, Meijlink KJ, *et al.* Immune-escape markers in relation to clinical outcome of advanced melanoma patients following immunotherapy. *Cancer Immunol Res* 2014; 2: 538-46.
- Dolan DE, Gupta S. PD-1 pathway inhibitors: changing the landscape of cancer immunotherapy. *Cancer Control* 2014; 21: 231-7.
- Ott PA, Hodi FS, Robert C. CTLA-4 and PD-1/PD-L1 blockade: new immunotherapeutic modalities with durable clinical benefit in melanoma patients. *Clin Cancer Res* 2013; 19: 5300-9.
- Momtaz P, Postow MA. Immunologic checkpoints in cancer therapy: focus on the programmed death-1 (PD-1) receptor pathway. *Pharmacogenomics Pers Med* 2014; 7: 357-65.
- Song FN, Duan M, Liu LZ, *et al.* RANKL promotes migration and invasion of hepatocellular carcinoma cells via NF- κ B-mediated epithelial-mesenchymal transition. *PLoS One* 2014; 9: e108507.
- Castaneda CA, Torres-Cabala C, Castillo M, *et al.* Tumor infiltrating lymphocytes in acral lentiginous melanoma: a study of a large cohort of cases from Latin America. *Clin Transl Oncol* 2017; 19: 1478-88.
- Lin K, Baritaki S, Militello L, Malaponte G, Bevelacqua Y, Bonavida B. The role of B-RAF mutations in melanoma and the induction of EMT via dysregulation of the NF- κ B/Snail/RKIP/PTEN Circuit. *Genes Cancer* 2010; 1: 409-20.
- Wu Y, Zhou BP. TNF- α /NF- κ B/Snail pathway in cancer cell migration and invasion. *Br J Cancer* 2010; 102: 639-44.
- Guarneri C, Bevelacqua V, Polesel J, *et al.* NF- κ B inhibition is associated with OPN/MMP9 downregulation in cutaneous melanoma. *Oncol Rep* 2017; 37: 737-46.
- Dai J, Wang H, Dong Y, Zhang Y, Wang J. Bile acids affect the growth of human cholangiocarcinoma via NF- κ B pathway. *Cancer*

- Invest 2013; 31: 111-20.
21. Nguyen LK, Cavadas MA, Kholodenko BN, Frank TD, Cheong A. Species differential regulation of COX2 can be described by an NFκB-dependent logic AND gate. *Cell Mol Life Sci* 2015; 72: 2431-43.
 22. Jang TJ. Progressive increase of regulatory T cells and decrease of CD8+ T cells and CD8+ T cells/regulatory T cells ratio during colorectal cancer development. *Korean J Pathol* 2013; 47: 443-51.
 23. Chou JP, Ramirez CM, Ryba DM, Koduri MP, Effros RB. Prostaglandin E2 promotes features of replicative senescence in chronically activated human CD8+ T cells. *PLoS One* 2014; 9: e99432.
 24. Oliveira-Costa JP, de Carvalho AF, da Silveira da GG, *et al.* Gene expression patterns through oral squamous cell carcinoma development: PD-L1 expression in primary tumor and circulating tumor cells. *Oncotarget* 2015; 6: 20902-20.
 25. Taube JM, Anders RA, Young GD, *et al.* Colocalization of inflammatory response with B7-h1 expression in human melanocytic lesions supports an adaptive resistance mechanism of immune escape. *Sci Transl Med* 2012; 4: 127ra37.
 26. Sideras K, Biermann K, Verheij J, *et al.* PD-L1, Galectin-9 and CD8+ tumor-infiltrating lymphocytes are associated with survival in hepatocellular carcinoma. *Oncoimmunology* 2017; 6: e1273309.
 27. Frydenlund N, Leone D, Yang S, *et al.* Tumoral PD-L1 expression in desmoplastic melanoma is associated with depth of invasion, tumor-infiltrating CD8 cytotoxic lymphocytes and the mixed cytomorphological variant. *Mod Pathol* 2017; 30: 357-69.
 28. Soliman H, Khalil F, Antonia S. PD-L1 expression is increased in a subset of basal type breast cancer cells. *PLoS One* 2014; 9: e88557.
 29. Qing Y, Li Q, Ren T, *et al.* Upregulation of PD-L1 and APE1 is associated with tumorigenesis and poor prognosis of gastric cancer. *Drug Des Devel Ther* 2015; 9: 901-9.
 30. Wang Y, Wang H, Zhao Q, Xia Y, Hu X, Guo J. PD-L1 induces epithelial-to-mesenchymal transition via activating SREBP-1c in renal cell carcinoma. *Med Oncol* 2015; 32: 212.
 31. Xue S, Hu M, Li P, *et al.* Relationship between expression of PD-L1 and tumor angiogenesis, proliferation, and invasion in glioma. *Oncotarget* 2017; 8: 49702-12.
 32. Hersey P, Gallagher S. A focus on PD-L1 in human melanoma. *Clin Cancer Res* 2013; 19: 514-6.

Cytologic Diagnosis of Noninvasive Follicular Thyroid Neoplasm with Papillary-like Nuclear Features and Its Impact on the Risk of Malignancy in the Bethesda System for Reporting Thyroid Cytopathology: An Institutional Experience

Milim Kim^{1,2*} · Joung Eun Kim^{3*}
Hyun Jeong Kim¹ · Yul Ri Chung^{1,2}
Yoonjin Kwak² · So Yeon Park^{1,2}

¹Department of Pathology, Seoul National University Bundang Hospital, Seongnam;

²Department of Pathology, Seoul National University College of Medicine, Seoul;

³Seoul National University College of Medicine, Seoul, Korea

Received: March 14, 2018

Accepted: April 3, 2018

Corresponding Author

So Yeon Park, MD, PhD

Department of Pathology, Seoul National University Bundang Hospital, 82 Gumi-ro 173beon-gil,

Bundang-gu, Seongnam 13620, Korea

Tel: +82-31-787-7712

Fax: +82-31-787-4012

E-mail: syprd@snu.ac.kr

*Milim Kim and Joung Eun Kim contributed equally to this work.

Background: This study was performed to analyze cytologic diagnosis of noninvasive follicular thyroid neoplasm with papillary-like nuclear features (NIFTP) and its impact on the risk of malignancy (ROM) in the Bethesda System for Reporting Thyroid Cytopathology (TBSRTC). **Methods:** Five thousand five hundred and forty-nine cases of thyroid fine-needle aspiration cytology (FNAC) diagnosed between 2012 and 2014 were included in this study. Diagnostic categories based on TBSRTC were compared with final surgical diagnoses, and the ROM in each category was calculated both when NIFTP was included in malignant lesions and when excluded from malignant lesions. **Results:** Of the 5,549 thyroid FNAC cases, 1,891 cases underwent surgical resection. In final diagnosis, 1,700 cases were revealed as papillary thyroid carcinoma (PTC), and 25 cases were reclassified as NIFTP. The cytologic diagnoses of NIFTP were non-diagnostic in one, benign in five, atypia of undetermined significance (AUS) in 14, follicular neoplasm in two, and suspicious for malignancy in three cases. Collectively, NIFTP/encapsulated follicular variant of PTC (EFVPTC) were more frequently classified as benign, AUS, or follicular neoplasm and less frequently categorized as malignant compared to conventional PTCs. Exclusion of NIFTP from malignant diagnoses resulted in a slight decrease in malignancy rates in non-diagnostic, benign, AUS, follicular neoplasm, and suspicious for malignancy categories without any statistical significance. **Conclusions:** The decrease in the ROM was not significant when NIFTP was excluded from malignant lesions. In thyroid FNACs, NIFTP/EFVPTCs were mostly classified into indeterminate categories. Therefore, it might be feasible to separate NIFTP/EFVPTC from conventional PTC on FNAC to guide clinicians to conservative management for patients with NIFTP/EFVPTC.

Key Words: Thyroid; Fine-needle aspiration cytology; Encapsulated follicular variant of papillary thyroid carcinoma; Noninvasive follicular thyroid neoplasm with papillary-like nuclear features; Risk of malignancy; Bethesda system

Fine-needle aspiration cytology (FNAC) with ultrasonography is the most commonly used method for preoperative testing of thyroid nodules. FNAC is a diagnostic test for the majority of benign nodules, most papillary thyroid carcinomas (PTCs), and other carcinomas, while it is considered a screening test for follicular-patterned lesions.¹ Most thyroid FNAC specimens are currently classified according to the Bethesda System for Reporting Thyroid Cytopathology (TBSRTC). This scheme consists of six major diagnostic categories: non-diagnostic/unsatisfactory, benign, atypia of undetermined significance/follicular lesion of undetermined significance (AUS/FLUS), follicular neoplasm/suspicious for a follicular neoplasm, suspicious for malignancy, and malignant.² Each diagnostic category possesses a different

risk of malignancy (ROM) and thus, offers a guide to optimal clinical management.^{2,3}

Recently, a new diagnostic term “noninvasive follicular thyroid neoplasm with papillary-like nuclear features (NIFTP)” was introduced for thyroid neoplasms previously classified as noninvasive encapsulated follicular variant of PTC (noninvasive EFVPTC) noting its indolent clinical behavior.⁴ The principal intent was to avoid overtreatment for patients with these tumors. Several outcomes are expected from revision of the nomenclature. In addition to alleviating the psychological impact of cancer diagnosis, it would also reduce complications of total thyroidectomy, risk of secondary tumors following radioactive iodine therapy, and the overall cost of health care.^{5,6} Since NIFTP denotes an indolent

behavior, one may regard surgical resection as unnecessary. However, surgical resection is essential for diagnosis of NIFTP. Moreover, it is important to note that the advent of the term NIFTP is not a discovery but rather an introduction of a new terminology for the clarification of a borderline concept from the former dichotomous era.

The introduction of the nomenclature NIFTP and its exclusion from malignant diagnoses raised some issues in thyroid FNAC. Retrospective analyses have demonstrated that it has affected the ROM in each of the TBSRTC diagnostic categories accordingly.^{1,7-10} Some studies, in particular, have shown that, if NIFTP were no longer termed carcinoma, there would be a marked decrease in the ROM for the indeterminate categories of TBSRTC such as AUS/FLUS, follicular neoplasm/suspicious for a follicular neoplasm, and suspicious for malignancy.^{1,8,11}

Western series have reported that NIFTP comprise 7%–28% of all PTCs.^{8,11-14} However, a recent report from Asian countries showed a very low incidence of NIFTP, comprising 0% to 4.7% of PTCs.^{15,16} Alteration in the risk of malignancies after the introduction of NIFTP is closely related to its incidence,⁹ and thus, the impact of NIFTP diagnoses on the ROM in diagnostic categories of TBSRTC would be low in Asian countries. Thus, we aimed to analyze cytologic diagnosis of NIFTP and its impact on the ROM in each diagnostic category of TBSRTC.

MATERIALS AND METHODS

Case selection

We retrospectively reviewed a total of 5,624 thyroid FNAC specimens from 5,127 patients, diagnosed at Seoul National University Bundang Hospital from January 2012 to December 2014. Of the 5,624 FNACs, 1,784 (31.7%) were consult cases from outside hospitals. Of the 5,127 patients, 174 patients had multiple thyroid nodules for which FNAC was performed separately and each counted as an individual case in this study. In the 71 patients who had repeated FNACs for the same nodule, the diagnostic category with the highest ROM was selected. Finally, 5,549 thyroid FNACs were included in this study. All thyroid FNAC slides were prepared with conventional smear with Papanicolaou staining and were diagnosed according to the diagnostic categories of TBSRTC.² In our institution, category III (AUS) is subcategorized into four subgroups: (1) AUS-NA, AUS having focal nuclear atypia (NA) suggestive of papillary carcinoma, but not diagnostic for category V (suspicious for malignancy); (2) AUS-MF, AUS showing a predominant population of microfollicles (MFs), but not sufficient for diagnosis of

category IV (follicular neoplasm); (3) AUS-HC, AUS showing predominance of Hurthle cells (HC); and (4) AUS-others, AUS not otherwise specified. This study was approved by the Institutional Review Board (IRB) of Seoul National University Bundang Hospital (IRB No. B-1803-456-102), and the requirement for informed consent was waived.

Pathologic review of surgical resection specimens

Of the 5,549 thyroid FNACs, cases with subsequent surgical resection were extracted from the electronic medical records. Histologic diagnoses for surgical resection specimens were reviewed and matched with the results of FNACs for the corresponding nodules. For PTC, we re-evaluated histologic variants such as conventional type, encapsulated follicular variant, infiltrative follicular variant, tall cell variant and etc. We carefully reviewed all the slides of EFVPTC and identified NIFTP according to the recently proposed diagnostic criteria.⁴ For a histological diagnosis of NIFTP, a thyroid tumor had to fulfill the following criteria: (1) encapsulation or clear demarcation, (2) follicular growth pattern, (3) nuclear features of PTC (nuclear score 2–3), (4) no capsular or vascular invasion, and (5) no aggressive histology (no tumor necrosis, no high mitotic activity). Regarding the follicular growth pattern, specific conditions were set as follows: (1) < 1% papillae, (2) no psammoma bodies, and (3) < 30% solid/trabecular/insular pattern. The ROM in each category of TBSRTC was calculated using cases with subsequent surgical resection or all FNAC cases.

Statistical analyses

Statistical analyses were performed using SPSS statistics ver. 22.0 (IBM Corp., Armonk, NY, USA). The Pearson chi-square test or Fisher exact test was used to compare the frequencies of categorical variables between two groups. A p-value of less than .05 was considered statistically significant. All p-values reported were two-sided.

RESULTS

Diagnostic categories of TBSRTC

Diagnostic categories of the 5,549 thyroid FNACs and their frequencies are as follows (Table 1): 727 cases (13.1%) of category I (non-diagnostic), 2,125 cases (38.3%) of category II (benign), 882 cases (15.9%) of category III (AUS), 44 cases (0.8%) of category IV (follicular neoplasm), 499 cases (9.0%) of category V (suspicious for malignancy), and 1,272 cases (22.9%) of category VI (malignant). The 882 cases of AUS were composed of 542

AUS-NA (61.4%), 132 AUS-MF (15.0%), 73 AUS-HC (8.3%), and 135 AUS-others (15.3%).

Comparison of diagnostic categories of TBSRTC with final surgical diagnoses

Of the 5,549 thyroid FNAC cases, 1,891 cases underwent surgical resection. Final surgical diagnoses are presented in Table 2. In surgical resection specimens, 1,700 cases were revealed as PTC including 1,445 conventional PTCs, 70 EFVPTCs, 62 infiltrative follicular variant of PTC (infiltrative FVPTCs), 106 tall cell variants, and 17 other rare variants (Table 3). Of the 70 EFVPTCs in surgical resection specimens, 25 cases were finally reclassified as NIFTP after reviewing of the slides. The cytologic diagnoses of NIFTP were non-diagnostic in one (4.0%), benign in five (20.0%), AUS in 14 (56.0%) (Fig. 1), follicular neoplasm

in two (8.0%), and suspicious for malignancy in three (12.0%). Of the 14 cases with AUS diagnoses, nine showed NA and five revealed MF pattern. The non-diagnostic case was diagnosed as follicular neoplasm in a repeated core needle biopsy. Diagnostic categories of FNAC for invasive EFVPTC were as follows: non-diagnostic in four (8.8%), benign in four (8.8%), AUS in 17 (37.8%), follicular neoplasm in two (8.3%), suspicious for malignancy in 10 (8.3%), and malignant in eight (17.8%) (Fig. 2). When comparing the cytologic diagnoses of NIFTP and EFVPTC with capsular or vascular invasion, malignant cytologic diagnoses were found in invasive EFVPTC only with a statistical difference ($p = .044$). However, there were no statistically significant differences in the frequencies of other diagnostic categories.

Comparison of diagnostic categories of TBSRTC between conventional PTC, NIFTP/EFVPTC, and infiltrative FVPTC

When comparing diagnostic categories between conventional PTC and NIFTP/EFVPTCs (Table 4), 924 of 1,445 conventional PTCs (63.9%) were diagnosed as category VI, whereas eight of the 70 NIFTP/EFVPTCs (11.4%) were diagnosed as malignancy ($p < .001$). Four NIFTP/EFVPTCs (5.7%) and none of the conventional PTCs were categorized as follicular neoplasm on FNAC ($p < .001$). While 144 conventional PTCs (10.0%) were classified as AUS, 31 NIFTP/EFVPTCs (44.3%) were classified as AUS ($p < .001$). In particular, only three of 1,445 conventional PTCs (0.2%) were classified as AUS-MF, whereas 10 of 70 NIFTP/EFVPTCs (14.3%) revealed AUS-MF pattern ($p < .001$). Six conventional PTCs (0.4%) and nine NIFTP/EFVPTCs (12.9%) were classified as benign on FNAC ($p <$

Table 1. Distribution of diagnostic categories of TBSRTC

| FNAC diagnostic category | No. (%) |
|--|--------------|
| I. Non-diagnostic | 727 (13.1) |
| II. Benign | 2,125 (38.3) |
| III. Atypia of undetermined significance (AUS) | 882 (15.9) |
| IIIA. AUS-NA | 542 (61.4) |
| IIIB. AUS-MF | 132 (15.0) |
| IIIC. AUS-HC | 73 (8.3) |
| IIID. AUS-others | 135 (15.3) |
| IV. Follicular neoplasm | 44 (0.8) |
| V. Suspicious for malignancy | 499 (9.0) |
| VI. Malignant | 1272 (22.9) |
| Total | 5,549 (100) |

TBSRTC, the Bethesda System for Reporting Thyroid Cytopathology; FNAC, fine-needle aspiration cytology; NA, nuclear atypia; MF, microfollicles; HC, Hurthle cells.

Table 2. Diagnoses of thyroid FNACs compared to final diagnoses of surgical specimens

| FNAC diagnostic category | No. of surgical specimens | Final diagnosis | | | | Other ^a |
|---------------------------|---------------------------|---------------------|--------------------|----------------------|---------------------|--------------------|
| | | Nodular hyperplasia | Follicular adenoma | Follicular carcinoma | Papillary carcinoma | |
| Non-diagnostic | 73 | 14 (19.2) | 11 (15.1) | 1 (1.4) | 47 (64.4) | 0 |
| Benign | 54 | 28 (51.9) | 6 (11.1) | 2 (3.7) | 16 (29.6) | 2 (3.7) |
| AUS | 306 | 34 (11.1) | 40 (13.1) | 15 (4.9) | 211 (68.9) | 6 (2.0) |
| AUS-NA | 215 | 12 (5.6) | 12 (5.6) | 4 (1.9) | 185 (86.0) | 2 (0.9) |
| AUS-MF | 53 | 8 (15.1) | 17 (32.1) | 11 (20.7) | 17 (32.1) | 0 |
| AUS-HC | 17 | 7 (41.2) | 9 (52.9) | 0 | 0 | 1 (5.9) |
| AUS-others | 21 | 7 (33.3) | 2 (9.5) | 0 | 9 (42.9) | 3 (14.3) |
| Follicular neoplasm | 27 | 7 (25.9) | 10 (37.0) | 5 (18.5) | 5 (18.5) | 0 |
| Suspicious for malignancy | 393 | 2 (0.5) | 1 (0.3) | 2 (0.5) | 387 (98.5) | 1 (0.3) |
| Malignant | 1,038 | 0 | 0 | 1 (0.1) | 1,034 (99.6) | 3 (0.3) |
| Total | 1,891 | 85 (4.5) | 68 (3.6) | 26 (1.4) | 1,700 (89.9) | 12 (0.6) |

Values are presented as number (%).

FNAC, fine needle aspiration cytology; AUS, atypia of undetermined significance; NA, nuclear atypia; MF, microfollicles; HC, Hurthle cells.

^aOther includes two cases of parathyroid adenoma in benign; two medullary carcinomas, one poorly differentiated carcinoma, two anaplastic carcinomas, and one lymphoma in AUS; one medullary carcinoma in suspicious for malignancy; one medullary carcinoma, one anaplastic carcinoma, and one thymic carcinoma in malignant category.

Table 3. Diagnostic categories of thyroid FNAC according to variant of PTC

| FNAC diagnostic category | Variants of PTC in final diagnosis | | | | | |
|---------------------------|------------------------------------|----------------|--|---------------------------------|-------------------|---------------------|
| | Conventional | NIFTP | Invasive encapsulated follicular variant | Infiltrative follicular variant | Tall cell variant | Other rare variants |
| Non-diagnostic | 32 (2.2) | 1 (4.0) | 4 (8.8) | 5 (7.7) | 3 (2.8) | 2 (11.8) |
| Benign | 6 (0.4) | 5 (20.0) | 4 (8.8) | 1 (1.6) | 0 | 0 |
| AUS | 144 (10.0) | 14 (56.0) | 17 (37.8) | 25 (40.3) | 8 (7.5) | 3 (17.6) |
| AUS-NA | 135 (9.3) | 9 (36.0) | 11 (24.4) | 21 (33.9) | 7 (6.6) | 2 (11.8) |
| AUS-MF | 3 (0.2) | 5 (20.0) | 5 (11.1) | 4 (6.4) | 0 | 0 |
| AUS-HC | 0 | 0 | 0 | 0 | 0 | 0 |
| AUS-others | 6 (0.4) | 0 | 1 (2.2) | 0 | 1 (0.9) | 1 (5.9) |
| Follicular neoplasm | 0 | 2 (8.0) | 2 (8.3) | 1 (1.6) | 0 | 0 |
| Suspicious for malignancy | 339 (23.5) | 3 (12.0) | 10 (4.4) | 14 (22.6) | 20 (18.9) | 1 (5.9) |
| Malignant | 924 (63.9) | 0 ^a | 8 (17.8) ^a | 16 (25.8) | 75 (70.8) | 11 (64.7) |
| Total No. | 1,445 | 25 | 45 | 62 | 106 | 17 |

Values are presented as number (%).

FNAC, fine needle aspiration cytology; PTC, papillary thyroid carcinoma; NIFTP, noninvasive follicular thyroid neoplasm with papillary-like nuclear features; AUS, atypia of undetermined significance; NA, nuclear atypia; MF, microfollicles; HC, Hurthle cells.

^ap = .044, Fisher exact test.

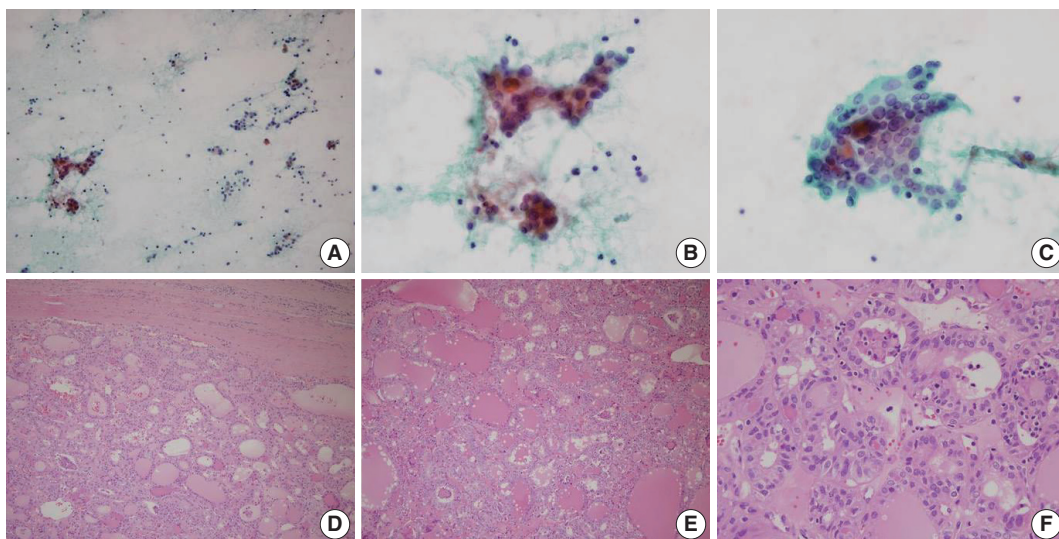


Fig. 1. A representative case of noninvasive follicular thyroid neoplasm with papillary-like nuclear features diagnosed as atypia of undetermined significance in fine-needle aspiration cytology. (A) Low power examination of cytology smear reveals small clusters and scattered single cells with low cellularity. (B) Small cell clusters showing nuclear enlargement and overlapping. (C) A cell cluster with microfollicles. Tumor cell nuclei show nuclear clearing, nuclear elongation and peripherally located micronucleoli. (D) In final histology, the tumor has a thick fibrous capsule with smooth border and shows a follicular growth pattern. (E) Follicles have densely eosinophilic colloid with peripheral scalloping and multinucleated giant cells. (F) Tumor cells show papillary thyroid carcinoma-like nuclear features.

.001). Collectively, NIFTP/EFVPTCs were more frequently classified as benign, AUS, or follicular neoplasm diagnostic categories and less frequently diagnosed as malignant compared with conventional PTCs. Similarly, infiltrative FVPTC was more frequently diagnosed as AUS ($p < .001$) and follicular neoplasm ($p = .041$) and less frequently diagnosed as malignant ($p < .001$), compared with conventional PTCs (Table 4). When comparing cytologic diagnoses between infiltrative FVPTCs and NIFTP/EFVPTCs (Table 4), infiltrative FVPTCs were less

frequently classified as benign and more frequently diagnosed as malignant, compared with NIFTP/EFVPTCs ($p = .019$ and $p = .033$, respectively).

Impact of NIFTP on ROM in each diagnostic category of TBSRTC

When NIFTPs were regarded as malignant tumors, the ROM in each diagnostic category of FNAC was as follows in histology-proven cases: non-diagnostic, 65.8%; benign, 33.3%; AUS,

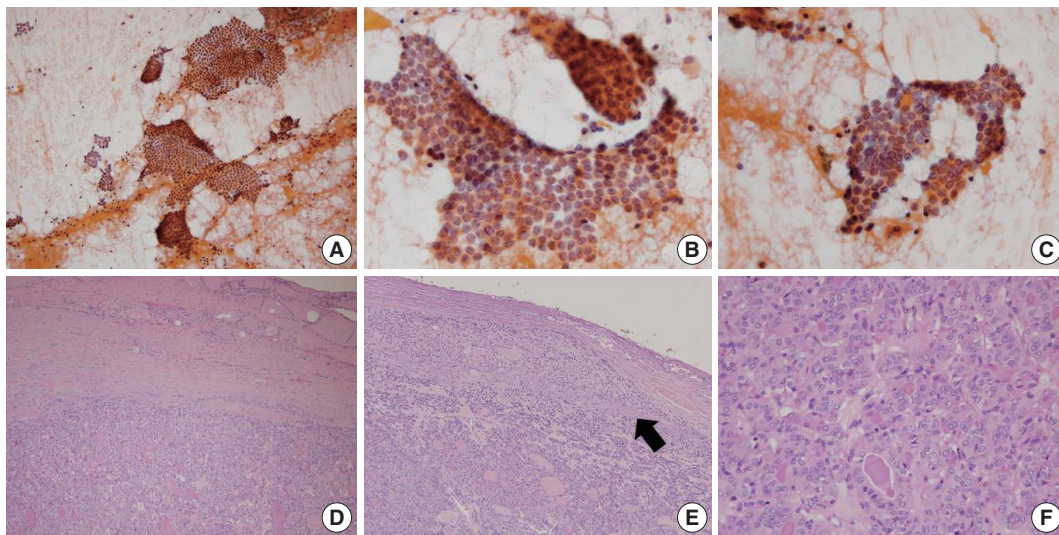


Fig. 2. A representative example of encapsulated follicular variant of papillary thyroid carcinoma with invasion classified as papillary carcinoma in fine-needle aspiration cytology. (A) Low power examination reveals large tissue fragments and small clusters in cytologic smear. (B, C) Monolayered sheets or syncytial clusters showing nuclear elongation, overlapping, loss of polarity and grooves. (D) In the final histology of surgical excision specimen, the tumor has a thick fibrous capsule with irregular border. (E) A focus of capsular invasion (arrow) is evident. (F) Tumor cells are arranged in microfollicular or trabecular pattern, showing typical papillary thyroid carcinoma-like nuclear features.

Table 4. Comparison of diagnostic categories between conventional PTC, NIFTP/EFVPTC, and infiltrative FVPTC

| FNAC diagnostic category | Conventional PTC | NIFTP/EFVPTC | Infiltrative FVPTC | p-value ^a | p-value ^b | p-value ^c |
|---------------------------|------------------|--------------|--------------------|----------------------|----------------------|----------------------|
| Non-diagnostic | 32 (2.2) | 5 (7.1) | 5 (7.7) | .025 | 1.000 | .016 |
| Benign | 6 (0.4) | 9 (12.9) | 1 (1.6) | <.001 | .019 | .259 |
| AUS | 144 (10.0) | 31 (44.3) | 25 (40.3) | <.001 | .646 | <.001 |
| AUS-NA | 135 (9.3) | 20 (28.6) | 21(33.9) | <.001 | .511 | <.001 |
| AUS-MF | 3 (0.2) | 10 (14.3) | 4 (6.4) | <.001 | .167 | <.001 |
| AUS-HC | 0 (0) | 0 (0) | 0 (0) | 1.000 | 1.000 | 1.000 |
| AUS-others | 6 (0.4) | 1 (1.4) | 0 (0) | .282 | 1.000 | 1.000 |
| Follicular neoplasm | 0 (0) | 4 (5.7) | 1 (1.6) | <.001 | .370 | .041 |
| Suspicious for malignancy | 339 (23.5) | 13 (18.6) | 14 (22.6) | .344 | .569 | .873 |
| Malignant | 924 (63.9) | 8 (11.4) | 16 (25.8) | <.001 | .033 | <.001 |

Values are presented as number (%).

PTC, papillary thyroid carcinoma; NIFTP, noninvasive follicular thyroid neoplasm with papillary-like nuclear features; EFVPTC, encapsulated follicular variant of papillary thyroid carcinoma; FVPTC, follicular variant of papillary thyroid carcinoma; FNAC, fine-needle aspiration cytology; AUS, atypia of undetermined significance; NA, nuclear atypia; MF, microfollicles; HC, Hurthle cells.

^aConventional PTC vs. NIFTP/EFVPTC; ^bNIFTP/EFVPTC vs. infiltrative FVPTC; ^cConventional PTC vs. infiltrative FVPTC.

75.8%; follicular neoplasm, 37.0%; suspicious for malignancy, 99.2%; malignant, 100% (Table 5). Next, we assessed the impact of NIFTP on the ROM in each diagnostic category. When excluding NIFTP from malignant diagnoses, an absolute decrease ranged from 0% to 9.2% and a relative decrease ranged from 0% to 27.6%. The ROM seemed to change largely in benign (33.3% to 24.1%) and AUS-MF categories (52.8% to 43.3%), but there were no statistical differences in ROMs in all diagnostic categories whether NIFTP was included in malignancy diagnoses or not.

When the ROMs were calculated in total FNAC cases, the ROM including NIFTP in each diagnostic category was as follows:

non-diagnostic, 6.6%; benign, 0.8%; AUS, 26.3%; follicular neoplasm, 22.7%; suspicious for malignancy, 78.2%; malignant, 81.6% (Table 6). Exclusion of NIFTP from malignant diagnoses resulted in an absolute decrease of 0% to 4.5% and a relative decrease of 0% to 25.0% without any statistical difference.

DISCUSSION

Introduction of NIFTP has created some challenges for thyroid FNAC: among them, its impact on the ROM in the diagnostic categories of TBSRTC and the resulting need for modification

Table 5. Impact of NIFTP on the risk of malignancy in FNAC diagnostic categories in histology-proven cases

| FNAC diagnostic category | No. | No. of malignancy including NIFTP (%) | No. of malignancy excluding NIFTP (%) | Absolute decrease in ROM (%) | Relative decrease in ROM (%) |
|---------------------------|-------|---------------------------------------|---------------------------------------|------------------------------|------------------------------|
| Non-diagnostic | 73 | 48 (65.8) | 47 (64.4) | 1.4 | 2.1 |
| Benign | 54 | 18 (33.3) | 13 (24.1) | 9.2 | 27.6 |
| AUS | 306 | 232 (75.8) | 218 (71.2) | 4.6 | 6.1 |
| AUS-NA | 215 | 191 (88.8) | 182 (84.7) | 4.1 | 4.6 |
| AUS-MF | 53 | 28 (52.8) | 23 (43.3) | 9.5 | 18.0 |
| AUS-HC | 17 | 1 (5.9) | 1 (5.9) | 0 | 0 |
| AUS-others | 21 | 12 (44.4) | 12 (44.4) | 0 | 0 |
| Follicular neoplasm | 27 | 10 (37.0) | 8 (29.6) | 7.4 | 20.0 |
| Suspicious for malignancy | 393 | 390 (99.2) | 387 (98.5) | 0.7 | 0.7 |
| Malignant | 1,038 | 1,038 (100) | 1,038 (100) | 0 | 0 |
| Total | 1,891 | 1,736 (91.8) | 1,711 (90.5) | 1.3 | 1.4 |

NIFTP, noninvasive follicular thyroid neoplasm with papillary-like nuclear features; FNAC, fine needle aspiration cytology; ROM, risk of malignancy; AUS, atypia of undetermined significance; NA, nuclear atypia; MF, microfollicles; HC, Hurthle cells.

Table 6. Impact of NIFTP on the risk of malignancy in FNAC diagnostic categories in total cases

| FNAC diagnostic category | No. | No. of malignancy including NIFTP (%) | No. of malignancy excluding NIFTP (%) | Absolute decrease in ROM (%) | Relative decrease in ROM (%) |
|---------------------------|-------|---------------------------------------|---------------------------------------|------------------------------|------------------------------|
| Non-diagnostic | 727 | 48 (6.6) | 47 (6.5) | 0.1 | 1.5 |
| Benign | 2,125 | 18 (0.8) | 13 (0.6) | 0.2 | 25.0 |
| AUS | 882 | 232 (26.3) | 218 (24.7) | 1.6 | 6.1 |
| AUS-NA | 542 | 191 (35.2) | 182 (33.6) | 1.6 | 4.5 |
| AUS-MF | 132 | 28 (21.2) | 23 (17.4) | 3.8 | 17.9 |
| AUS-HC | 73 | 1 (1.4) | 1 (1.4) | 0 | 0 |
| AUS-others | 135 | 12 (8.9) | 12 (8.9) | 0 | 0 |
| Follicular neoplasm | 44 | 10 (22.7) | 8 (18.2) | 4.5 | 19.8 |
| Suspicious for malignancy | 499 | 390 (78.2) | 387 (77.6) | 0.6 | 0.8 |
| Malignant | 1,272 | 1,038 (81.6) | 1,038 (81.6) | 0 | 0 |
| Total | 5,549 | 1,736 (31.3) | 1,711 (30.8) | 0.5 | 1.6 |

NIFTP, noninvasive follicular thyroid neoplasm with papillary-like nuclear features; FNAC, fine needle aspiration cytology; ROM, risk of malignancy; AUS, atypia of undetermined significance; NA, nuclear atypia; MF, microfollicles; HC, Hurthle cells.

of clinical management guidelines may be critical. Previous studies from Western countries have revealed decreases in the ROM across all TBSRTC categories, and significant reductions in the ROM were detected in the three indeterminate TBSRTC categories upon reclassification of noninvasive EFVPTC as NIFTP.^{8,9,11} However, in this study, introduction of the term NIFTP resulted in an insignificant decrease in the ROM in the diagnostic categories of non-diagnostic, benign, AUS, follicular neoplasm, and suspicious for malignancy.

The decrease in the risk of malignancies in each diagnostic category after the introduction of NIFTP will vary according to the institutional frequency and preceding FNAC diagnoses of NIFTP.^{9,17} While NIFTP comprises 7%–28% of PTCs in previous studies from Western countries,^{8,11–14} its proportion is quite low in Asian countries, ranging from 0% to 4.7% of PTCs.^{15,16} In this study, NIFTP represented 1.5% of all PTCs. Thus, exclusion of NIFTP from malignant diagnoses and the resultant decrease in

the ROM in diagnostic categories of TBSRTC was not significant. The incidence of NIFTP may be directly linked to the incidence of EFVPTC. In this study, EFVPTC comprised 4.1% of all PTCs and it was reported to account for 0.7% to 5.5% of PTCs in Asian countries.^{15,16} However, EFVPTC represented about 24% of all PTC cases in Western countries with its incidence increasing.^{4,18}

Previous studies have shown that NIFTP is usually diagnosed into indeterminate categories, that is, AUS/FLUS, follicular neoplasm/suspicious for a follicular neoplasm, and suspicious for malignancy. Comparative studies on cytomorphologic features of NIFTP and conventional PTC revealed that cytologic features of PTC such as nuclear pseudoinclusions, crowding, irregularities, and clearing are less frequent in NIFTP compared to conventional PTC.^{19,20} Especially, among the various nuclear features of PTC, nuclear pseudoinclusions are known to be almost absent in NIFTP.^{20,21} Moreover, by definition, NIFTP should not have

papillae and psammomatous calcification which can be found in cytologic smear of conventional PTC. Thus, the borderline nuclear features, lack of papillae and predominance of MFs in NIFTP lead to cytologic diagnoses of indeterminate categories, and rarely to malignant category. Accordingly, it is reasonable that changes in ROM are significant in indeterminate categories but insignificant in malignant category after the introduction of NIFTP. Similar to the previous studies,^{11,13,19} our study showed that NIFTP was most frequently diagnosed as AUS. Five cases were even diagnosed as benign; however, this can be explained by the frequent focal PTC-like nuclear changes in NIFTP.

In this study, FNAC diagnoses of NIFTP and EFVPTC with invasion did not show a significant difference in other diagnostic categories except for malignant category. As the distinction between invasive EFVPTC and NIFTP is basically based on the demonstration of capsular and/or vascular invasion, their cytologic features can be overlapping. However, 17.8% of invasive EFVPTC but none of the NIFTP was categorized as malignant in FNAC. It is thought that NIFTP progresses to invasive EFVPTC and thus, invasive EFVPTC may show more typical nuclear features of PTC compared to NIFTP. Recently, Chandler *et al.*²¹ reported that predominantly MF pattern, absence of pseudoinclusions, and less frequent nuclear elongation and grooves are more likely to be associated with NIFTP in comparison with invasive EFVPTC. However, other previous studies did not demonstrate differences in FNAC diagnostic categories between them.^{15,22} Maletta *et al.*²² reported that EFVPTC with invasion were typically diagnosed as follicular neoplasm or suspicious for malignancy and nuclear features including size, contour irregularities, and chromatin clearing did not differ between NIFTP and invasive EFVPTC.

There are a few limitations in this study. As a tertiary medical center, malignant cytologic diagnoses comprised as much as 22.9% of all FNAC diagnoses in our institution. That is, our study population had selection bias, and thus, the incidence of NIFTP in this study may not reflect its normal distribution. Moreover, we reviewed only EFVPTC cases to find NIFTP. Some cases which were previously diagnosed as follicular adenoma or even nodular hyperplasia may have incomplete PTC-like nuclei and may have been missed. For these reasons, there is a possibility that NIFTP was underestimated in this study.

To conclude, in this study, the decrease in the ROM was not significant when NIFTP was excluded from malignant lesions due to the low frequency of NIFTP. NIFTP/EFVPTCs were more frequently classified as benign, AUS, or follicular neoplasm categories and less frequently diagnosed as malignant, when

compared with conventional PTCs. Though there are no drastic changes in the 2017 revision of TBSRTC, it emphasizes that malignant diagnoses should be limited to cases with classic features of PTC including true papillae, psammoma bodies, and nuclear pseudoinclusions to avoid false-positives due to NIFTP.³ It appears that in thyroid FNACs, NIFTP/EFVPTCs are mostly classified into indeterminate diagnostic categories. Therefore, it might be feasible to separate NIFTP/EFVPTC from conventional PTC on FNAC to guide clinicians to conservative management for patients with NIFTP/EFVPTC.

Conflicts of Interest

No potential conflict of interest relevant to this article was reported.

REFERENCES

- Baloch ZW, Seethala RR, Faquin WC, *et al.* Noninvasive follicular thyroid neoplasm with papillary-like nuclear features (NIFTP): a changing paradigm in thyroid surgical pathology and implications for thyroid cytopathology. *Cancer Cytopathol* 2016; 124: 616-20.
- Cibas ES, Ali SZ. The Bethesda System for Reporting Thyroid Cytopathology. *Thyroid* 2009; 19: 1159-65.
- Cibas ES, Ali SZ. The 2017 Bethesda System for Reporting Thyroid Cytopathology. *Thyroid* 2017; 27: 1341-6.
- Nikiforov YE, Seethala RR, Tallini G, *et al.* Nomenclature revision for encapsulated follicular variant of papillary thyroid carcinoma: a paradigm shift to reduce overtreatment of indolent tumors. *JAMA Oncol* 2016; 2: 1023-9.
- Hauch A, Al-Qurayshi Z, Randolph G, Kandil E. Total thyroidectomy is associated with increased risk of complications for low- and high-volume surgeons. *Ann Surg Oncol* 2014; 21: 3844-52.
- Iyer NG, Morris LG, Tuttle RM, Shaha AR, Ganly I. Rising incidence of second cancers in patients with low-risk (T1N0) thyroid cancer who receive radioactive iodine therapy. *Cancer* 2011; 117: 4439-46.
- Ohuri NP, Wolfe J, Carty SE, *et al.* The influence of the noninvasive follicular thyroid neoplasm with papillary-like nuclear features (NIFTP) resection diagnosis on the false-positive thyroid cytology rate relates to quality assurance thresholds and the application of NIFTP criteria. *Cancer Cytopathol* 2017; 125: 692-700.
- Strickland KC, Howitt BE, Marqusee E, *et al.* The impact of noninvasive follicular variant of papillary thyroid carcinoma on rates of malignancy for fine-needle aspiration diagnostic categories. *Thyroid* 2015; 25: 987-92.

9. Zhou H, Baloch ZW, Nayar R, *et al.* Noninvasive follicular thyroid neoplasm with papillary-like nuclear features (NIFTP): Implications for the risk of malignancy (ROM) in the Bethesda System for Reporting Thyroid Cytopathology (TBSRTC). *Cancer Cytopathol* 2018; 126: 20-6.
10. Kiernan CM, Weiss VL, Mehrad M, Ely K, Baregamian N, Solórzano CC. New terminology-noninvasive follicular neoplasm with papillary-like nuclear features (NIFTP) and its effect on the rate of malignancy at a single institution. *Surgery* 2018; 163: 55-9.
11. Faquin WC, Wong LQ, Afrogheh AH, *et al.* Impact of reclassifying noninvasive follicular variant of papillary thyroid carcinoma on the risk of malignancy in The Bethesda System for Reporting Thyroid Cytopathology. *Cancer Cytopathol* 2016; 124: 181-7.
12. Li W, Sciallis A, Lew M, Pang J, Jing X. Implementing noninvasive follicular thyroid neoplasm with papillary-like nuclear features may potentially impact the risk of malignancy for thyroid nodules categorized as AUS/FLUS and FN/SFN. *Diagn Cytopathol* 2018; 46: 148-53.
13. Mainthia R, Wachtel H, Chen Y, *et al.* Evaluating the projected surgical impact of reclassifying noninvasive encapsulated follicular variant of papillary thyroid cancer as noninvasive follicular thyroid neoplasm with papillary-like nuclear features. *Surgery* 2018; 163: 60-5.
14. Singh R, Avila J, Jo K, *et al.* Patients with non-invasive follicular thyroid neoplasm with papillary-like nuclear features are unlikely to have malignant preoperative cytology. *Ann Surg Oncol* 2017; 24: 3300-5.
15. Hirokawa M, Higuchi M, Suzuki A, Hayashi T, Kuma S, Miyauchi A. Noninvasive follicular thyroid neoplasm with papillary-like nuclear features: a single-institutional experience in Japan. *Endocr J* 2017; 64: 1149-55.
16. Bychkov A, Hirokawa M, Jung CK, *et al.* Low rate of noninvasive follicular thyroid neoplasm with papillary-like nuclear features in Asian practice. *Thyroid* 2017; 27: 983-4.
17. Hung YP, Barletta JA. A user's guide to non-invasive follicular thyroid neoplasm with papillary-like nuclear features (NIFTP). *Histopathology* 2018; 72: 53-69.
18. Jung CK, Little MP, Lubin JH, *et al.* The increase in thyroid cancer incidence during the last four decades is accompanied by a high frequency of *BRAF* mutations and a sharp increase in *RAS* mutations. *J Clin Endocrinol Metab* 2014; 99: E276-85.
19. Brandler TC, Zhou F, Liu CZ, *et al.* Can noninvasive follicular thyroid neoplasm with papillary-like nuclear features be distinguished from classic papillary thyroid carcinoma and follicular adenomas by fine-needle aspiration? *Cancer Cytopathol* 2017; 125: 378-88.
20. Strickland KC, Vivero M, Jo VY, *et al.* Preoperative cytologic diagnosis of noninvasive follicular thyroid neoplasm with papillary-like nuclear features: a prospective analysis. *Thyroid* 2016; 26: 1466-71.
21. Chandler JB, Colunga M, Prasad ML, *et al.* Identification of distinct cytomorphologic features in the diagnosis of NIFTP at the time of preoperative FNA: implications for patient management. *Cancer Cytopathol* 2017; 125: 865-75.
22. Maletta F, Massa F, Torregrossa L, *et al.* Cytological features of "noninvasive follicular thyroid neoplasm with papillary-like nuclear features" and their correlation with tumor histology. *Hum Pathol* 2016; 54: 134-42.

Duodenal Adenocarcinoma of Brunner Gland Origin: A Case Report

Ji Hye Moon¹ · Kyoungbun Lee¹
Han-Kwang Yang^{2,3} · Woo Ho Kim^{1,3}

Departments of ¹Pathology and ²Surgery,
³Cancer Research Institute, Seoul National
University College of Medicine, Seoul, Korea

Received: August 14, 2017
Revised: September 26, 2017
Accepted: October 9, 2017

Corresponding Author

Woo Ho Kim, MD, PhD
Department of Pathology, Seoul National University
College of Medicine, 103 Daehak-ro, Jongno-gu,
Seoul 03080, Korea
Tel: +82-2-740-8269
Fax: +82-2-765-5600
E-mail: woohokim@snu.ac.kr

We report a case of adenocarcinoma originating from the duodenal Brunner glands in a 47-year-old female patient. The lesion was 0.8 cm in extent and located at the posterior wall of the first part of the duodenum. Histologically, the tumor showed transition from non-neoplastic Brunner glands through dysplastic epithelium into adenocarcinoma. The carcinoma cells were strongly positive for MUC6 protein, which is an epithelial marker for the Brunner glands. Tumor protein p53 was overexpressed in the carcinoma cells, but not in the non-neoplastic or dysplastic epithelium. Dystrophic calcification was predominant. This is the first case report of duodenal adenocarcinoma of Brunner gland origin in Korea.

Key Words: Brunner glands; Adenocarcinoma; Duodenum

Proliferative Brunner gland lesions in the duodenum are commonly found as submucosal masses upon endoscopy,¹ and most of the lesions are hyperplasia. Rarely found are adenomas or hamartomas. Adenocarcinoma arising from Brunner glands is very rare. Primary duodenal adenocarcinoma accounts for 0.3% of carcinomas of the gastrointestinal tract and among them, adenocarcinoma arising from Brunner glands constitutes only a minority.² Here, we present a case of adenocarcinoma arising from Brunner glands through dysplasia.

CASE REPORT

A 47-year-old female patient visited hospital for a national health screening program. Esophagogastroduodenoscopy revealed a 0.8-cm-sized depressed lesion at the posterior wall of the first part of the duodenum (Fig. 1A, B). Histologic analysis of the biopsy specimen revealed atypical glands forming cell clusters beneath the intact mucosal layer. The atypical clusters were arranged in tubular structures of columnar epithelium consisting of mucin-producing cells. Dystrophic calcification was scattered within the lesion, and foreign body reaction with giant cell formation was noted around the calcified materials (Fig. 1C, D). Immunohistochemistry (IHC) for CD56, chromogranin A and

synaptophysin showed negative results, excluding the possibility of a neuroendocrine tumor, which is prevalent in this region. The histologic diagnosis was well-differentiated adenocarcinoma, and the patient underwent routine preoperative work-up. Physical examination, blood tests and abdominal computed tomography (CT) scan showed no abnormal findings. A minute duodenal lesion with submucosal invasion was suspected on endoscopic ultrasonography. Since the calcification was minute, it was not recognized by simple X-ray or by CT scan even upon retrospective review.

Endoscopic resection was not an option because it is usually difficult to remove a lesion by endoscopy at the posterior wall of the duodenum. The possibility of submucosal invasion was also considered; hence, the patient received distal gastrectomy. Since the lesion was located in the duodenal bulb, the duodenal stump was made near the pancreas and the distal resection margin was close to the lesion. D1+ lymph node dissection was performed.

On gross examination, the specimen consisted of 2.7 cm long duodenum and 6.5 cm long stomach. On duodenal mucosa, a 0.8 × 0.8-cm-sized superficial depressed lesion was found (Fig. 2A). The lesion was located at the posterior wall of the duodenum, 1.9 cm distal to the pyloric ring and 0.3 cm proximal to the

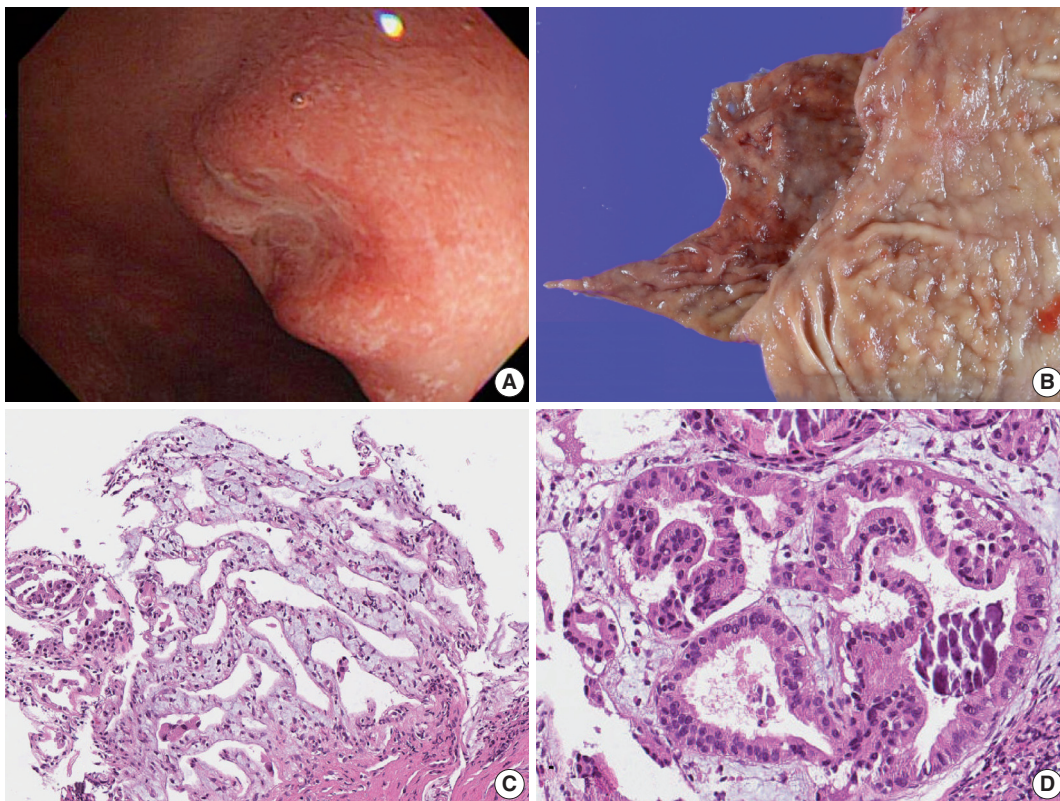


Fig. 1. Gross and microscopic images of Brunner gland adenocarcinoma. (A) Endoscopy of the duodenal carcinoma showing a 0.8-cm lesion with central depression in the posterior wall of the first segment of duodenum. (B) Gross view. (C) Microscopic image of the endoscopic biopsy showing well-differentiated adenocarcinoma consisting of branching glands. (D) High-power view demonstrates psammoma-like structures of dystrophic calcification.

distal resection margin. Pathologic examination revealed well-differentiated adenocarcinoma involving mucosal and submucosal layers. Around the carcinoma, dysplastic Brunner gland epithelium was noted. (Fig. 2B)

IHC was done for further evaluation. Gastric foveolar type mucin (MUC5AC) was focally positive and Brunner gland type mucin (MUC6) was diffusely positive (Fig. 2C). Carcinoembryonic antigen (CEA) was negative and p53 was positive in an increasing order of intensity from normal to adenoma-adenocarcinoma spectrum (Fig. 2D–F). A microsatellite instability (MSI) test was performed to investigate the involvement of mismatch repair failure during carcinogenesis. None of the five markers, which include BAT25, BAT26, D2S123, D5S346, and D17S250, showed instability.

This study was approved by the Institutional Review Board of Seoul National University Hospital (IRB No. H-1706-098-860) and performed in accordance with the principles of the Declaration of Helsinki. Patient informed consent was waived.

DISCUSSION

Adenocarcinoma from Brunner gland origin is extremely rare, and this is the first case report in Korea. Among the 108 duodenal carcinomas collected from 22 institutes in South Korea, none was suspected to arise from Brunner glands.³ Our case presents a unique Brunner gland lesion showing dysplasia and transformation into adenocarcinoma, suggesting the cell of origin to be Brunner glands. Strong positivity for the IHC of MUC6 in the dysplastic and carcinomatous epithelia also supports this speculation.

Additional ancillary tests were performed to evaluate the tumor characteristics. IHC for CEA was negative, but p53 protein was overexpressed in the tumor cells. Interestingly, p53 protein was completely negative in non-neoplastic Brunner glands and focally positive in dysplastic epithelium. The MSI test using five markers revealed the tumor to be microsatellite stable.

Since adenocarcinomas arising from Brunner glands are exceedingly rare, reported IHC results are diverse, though quite few, and there is no consensus as yet. Since 1994, 25 cases have been

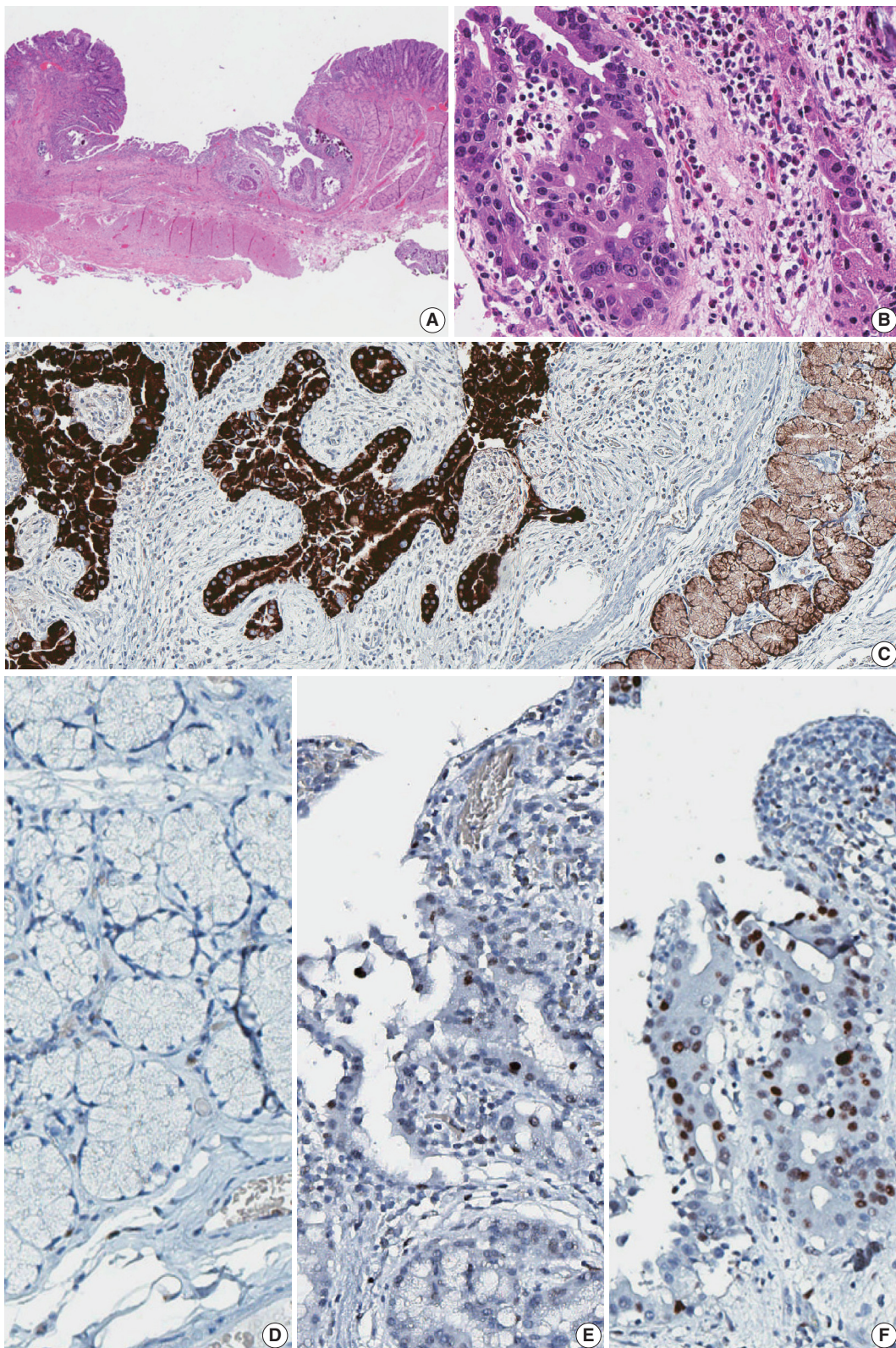


Fig. 2. Histology and immunohistochemistry of the lesion. (A) Low power view of resected duodenal segment. (B) Higher power view of adenocarcinoma. (C) MUC6 stain showed diffuse positivity in adenocarcinoma as well as adjacent Brunner glands. (D) Negative p53 staining in normal Brunner glands. (E) Focal positive p53 staining in dysplasia. (F) Strong p53 staining in adenocarcinoma.

reported in Japan.^{2,4-7} Some of them, including a recent case reported by Iwamuro *et al.* (2017),⁷ were consistent with our case; positive for MUC6 in the carcinoma component of the tumor. However, Kamei *et al.* (2013)² reported negative staining of MUC6 and MUC5AC in the tumor cells. Another report also demonstrated loss of MUC5AC and MUC6 in the Brunner glands showing epithelial atypia.⁸ The pathogenesis is unknown, but this discordance may be due to tumor cell heterogeneity, implying that some of the tumor cells may have lost their nature during progression.

There is no exclusive marker for the Brunner glands, and for this reason, the diagnosis of adenocarcinoma arising from Brunner glands depends on its distinct histology. The tumor can be treated by surgical resection, or a minimally invasive technique, such as endoscopic submucosal dissection, can be attempted if the tumor size is small and its depth shallow. Although located in the submucosal layer, its behavior is predicted to be the same as adenocarcinomas of mucosal origin, but more cases must be reported to build consensus on the prognosis and determine the standard treatment.

Here, we report a rare case of adenocarcinoma arising from Brunner glands of the duodenum. Despite the rarity of the tumor, the diagnosis was possible due to its histologic and immunohistochemical similarity with non-neoplastic Brunner glands and pre-neoplastic lesions.

Conflicts of Interest

No potential conflict of interest relevant to this article was reported.

REFERENCES

1. Fenoglio-Preiser CM, Noffsinger AE, Stemmermann GN, Lantz PE, Isaacson PG. *Gastrointestinal pathology: an atlas and text*. Philadelphia: Lippincott Williams & Wilkins, 2008; 471.
2. Kamei K, Yasuda T, Nakai T, Takeyama Y. A case of adenocarcinoma of the duodenum arising from Brunner's gland. *Case Rep Gastroenterol* 2013; 7: 433-7.
3. Chang HK, Yu E, Kim J, *et al.* Adenocarcinoma of the small intestine: a multi-institutional study of 197 surgically resected cases. *Hum Pathol* 2010; 41: 1087-96.
4. Koizumi M, Sata N, Yoshizawa K, Kurihara K, Yasuda Y. Carcinoma arising from Brunner's gland in the duodenum after 17 years of observation: a case report and literature review. *Case Rep Gastroenterol* 2007; 1: 103-9.
5. Ohta Y, Saitoh K, Akai T, Uesato M, Ochiai T, Matsubara H. Early primary duodenal carcinoma arising from Brunner's glands synchronously occurring with sigmoid colon carcinoma: report of a case. *Surg Today* 2008; 38: 756-60.
6. Kitagori K, Miyamoto S, Sakurai T. Image of the month: adenocarcinoma derived from Brunner's gland. *Clin Gastroenterol Hepatol* 2010; 8: A26.
7. Iwamuro M, Kobayashi S, Ohara N, Kawano S, Kawahara Y, Okada H. Adenocarcinoma in situ arising from Brunner's gland treated by endoscopic mucosal resection. *Case Rep Gastrointest Med* 2017; 2017: 7916976.
8. Kim K, Jang SJ, Song HJ, Yu E. Clinicopathologic characteristics and mucin expression in Brunner's gland proliferating lesions. *Dig Dis Sci* 2013; 58: 194-201.

Erdheim-Chester Disease Involving Lymph Nodes and Liver Clinically Mimicking Lymphoma: A Case Report

Yeoun Eun Sung^{1*} · Yoon Seo Lee^{2*}
Jieun Lee^{2,3} · Kyo Young Lee¹

¹Department of Pathology, ²Division of Medical Oncology, Department of Internal Medicine, Seoul St. Mary's Hospital, College of Medicine, The Catholic University of Korea, Seoul; ³Cancer Research Institute, The Catholic University of Korea, Seoul, Korea

Received: June 25, 2017
Revised: September 29, 2017
Accepted: October 16, 2017

Corresponding Author

Kyo Young Lee, MD
Department of Hospital Pathology, Seoul St. Mary's Hospital, College of Medicine, The Catholic University of Korea, 222 Banpo-daero, Seocho-gu, Seoul 06591, Korea
Tel: +82-2-2258-1618
Fax: +82-2-2258-1627
E-mail: leekyo@ catholic.ac.kr

*Yeoun Eun Sung and Yoon Seo Lee contributed equally to this work.

Erdheim-Chester disease (ECD) is a rare non-Langerhans cell histiocytosis and multisystem disease. First described in 1930, there are no more than 750 cases reported. The etiology remains unknown, but a majority of cases of ECD and Langerhans cell histiocytosis were found to have clonal mutations involving genes of the mitogen-activated protein kinase pathway. We recently encountered a 53-year-old male patient with extensive ECD involving the systemic lymph nodes, pleura, liver, and long bones clinically mimicking malignant lymphoma. Biopsies were performed at multiple sites, including a pleural mass, an external iliac lymph node, bone marrow, and the liver. Based on histopathological and immunohistochemical findings of positivity for CD68 and negativity for CD1a and S-100, the patient was diagnosed with ECD. Interferon- α was administered as the first-line treatment, but the patient rapidly progressed to hepatic failure after 2 months of treatment. We report this rare case of ECD clinically mimicking malignant lymphoma and diagnosed by careful pathological review.

Key Words: Erdheim-Chester disease; Lymph nodes; Vertebrae; Pleura; Liver

Erdheim-Chester disease (ECD) is a rare non-Langerhans cell histiocytosis (LCH) of unknown etiology. It was first described in 1930 by the pathologist William Chester in the laboratory of Jakob Erdheim in Vienna, and over 500 cases have been reported in the published literature.^{1,2} ECD is usually diagnosed between 40 and 70 years of age, and it has a slight male predominance.³ In Korea, the first ECD case was reported in 1999, and fewer than 20 cases have since been reported.² ECD is a multisystem disease involving the long bones, cardiovascular organs, lungs, central nervous system, retroperitoneum, and skin.³⁻⁵ The clinical presentation of this disease can vary strikingly but most commonly involves the skeletal system with bone pain (90%). There is usually symmetrical cortical osteosclerosis of the long bones and neurological involvement (50%) manifested as diabetes insipidus, cerebellar ataxia, and panhypopituitarism.¹ Other manifestations include cardiovascular involvement with pericardial pain or cardiac failure, as well as renal involvement and

constitutional symptoms such as fever, fatigue, or weight loss.¹ Involvement of the lymph nodes or liver is rarely reported.^{6,7} We report a rare case of ECD involving multiple systemic lymph nodes, pleura, liver, and the axial and appendicular skeleton.

CASE REPORT

A 53-year-old man was referred to the department of oncology for evaluation of rapid weight loss with inguinal lymphadenopathy. He experienced 20 kg of weight loss over 3 months, febrile sensation, night sweats, and general weakness. The patient had recently been diagnosed with diabetes mellitus, but had no other relevant medical history. Initial white blood cell (WBC) count was 4,790 cells/mm³ (neutrophil count 82%, lymphocyte count 5%), hemoglobin was 9.9 g/dL (normal range, 13.0 to 18.0 g/dL), and platelet count was 369,000/mm³ (normal range, 150,000 to 450,000/mm³). Erythrocyte sedimentation rate and

C-reactive protein were 76 mm/hr (normal range, 0 to 15 mm/hr) and 7.59 mg/dL (normal range, 0.01 to 0.47 mg/dL), respectively. Other laboratory findings including urinalysis were non-specific.

Abdominal computed tomography (CT) showed multiple enlarged lymph nodes involving the left para-aortic and aortocaval lymph nodes and common, external, and internal iliac lymph nodes (Fig. 1A–C). Splenomegaly and hepatomegaly were also suspected (Fig. 1B, D). Chest CT showed supraclavicular and mediastinal lymph node enlargement with an enhanced soft tissue mass involving the pleura (Fig. 1E, F). Positron emission tomography–computed tomography (PET-CT) was highly suggestive of malignant lymphoma involving systemic lymph nodes, consistent with CT images (Fig. 1G). PET-CT also indicated extensive involvement of the axial and appendicular skeleton including the skull, almost all vertebrae, both scapulae, pelvic bones, rib cage, sternum, and both femurs (Fig. 1H). The right pleura and spleen were also suspicious for lymphoma involvement. On bone scan, a mild and patchy activity increase was noted in the proximal shafts of both femurs and the left humerus. Subtle inhomogeneous activity was noted in the axial skeleton, although no significant activity was present. Based on imaging, malignant lymphoma with extensive systemic involvement was suspected. Additional laboratory studies showed β 2-microglobulin of 4.115 μ g/mL (normal range, 0.60 to 2.36 μ g/mL), ferritin of 2,094 ng/mL (normal range, 30 to 400 ng/mL), and lactate dehydrogenase of 612 U/L (normal range, 250 to 450 U/L). Serum protein electrophoresis showed nonspecific findings.

For pathological confirmation, initial excisional biopsy of the right pleural mass was performed via video-assisted thoracosurgery. In the surgical field, multiple pleural nodules were attached to the parietal pleura with focal involvement of the pericardium (Fig. 1I, J).

Histopathological examination of the pleural biopsy revealed a proliferating lesion of spindle to oval-shaped cells with a fibrous background (Fig. 2A, B). Some cells showed vacuolated or focal clear cytoplasm. Otherwise, they had abundant eosinophilic, fine granular cytoplasm (Fig. 2C, D), suggestive of histiocytes. In some areas, tumor cells showed a marked spindle shape with randomly arranged fascicles (Fig. 2E, F). Some lymphocytes and a few eosinophils infiltrated the tumor cells and fibrous background. Nuclei were mostly round to oval with fine chromatin and a noticeable nucleolus, showing an overall bland appearance. A few cells with hyperchromatic and pleomorphic nuclei were noted, and mitosis was rare (< 1/10 high power field) (Fig. 2D). At the boundary of the mass, tumor cells focally infiltrated the

surrounding adipose tissue.

With only these hematoxylin and eosin stain findings, the initial histopathological impression was spindle cell tumor, with a differential diagnosis of histiocytic neoplasm, dendritic cell sarcoma, sarcomatoid mesothelioma, and rare types of malignant lymphoma such as lymphocyte-depleted Hodgkin lymphoma. For further evaluation, immunohistochemical studies followed, including CD21, CD23, calretinin, epithelial membrane antigen (EMA), CD56a, CD45RB, CD30, CD15, Ki-67, and CD68 (Fig. 3A).

Dendritic cell sarcoma and sarcomatoid mesothelioma were excluded by negative findings for CD21, CD23, calretinin, and EMA along with low Ki-67 index (5%). Rare types of malignant lymphoma, such as lymphocyte-depleted Hodgkin lymphoma, were unlikely because of absence of reactivity for CD30, CD15, and CD45RB along with negative Epstein-Barr virus encoded RNA *in situ* hybridization (EBER-ISH). In addition, focal atypical lymphoid cells and some atypical Reed-Sternberg-like cells (RS-like cells) raised the possibility of peripheral T-cell lymphoma with RS-like cells; however, reactive T lymphocyte patterns of CD3, CD4, CD8, CD2, CD5, and CD7, as well as negative reactivity for EBER-ISH were found. T-cell receptor (TCR) gene rearrangement studies with polyclonal T-cell receptor δ (TCRD), γ (TCRG), and β (TCRB) results ruled out the possibility of malignant lymphoma. Instead, the tumor cells were uniformly positive for CD68, which is highly suggestive of a histiocytic lesion. Additional immunohistochemical studies of S-100 and CD1a were negative (Fig. 3B, C).

Rapid growth of the external iliac lymph node was detected on physical examination, and follow-up abdominal CT scan revealed the rapid size increase of multiple lymph nodes. Needle biopsy of an external iliac lymph node was performed. In addition, bone marrow biopsy was performed to exclude any other malignancy that might cause extensive skeletal fluorodeoxyglucose (FDG) uptake (Fig. 1G, H). Both biopsies (Fig. 2G, H) revealed tumor cells similar to those shown on previous pleural biopsy, expressing the same immunoprofile of CD68 (+), S-100 (–), and CD1a (–). Along with fibrosis, tumor cells replaced the normal lymph node structure and bone marrow space (Fig. 3E, F).

Radiological and histopathological results suggested a proliferating histiocytic lesion extensively involving bones, replacing bone marrow space, forming a pleural mass, and involving systemic lymph nodes. The differential diagnoses included LCH, Rosai-Dorfman disease (RDD), ECD, and benign xanthogranulomatous inflammation. The possibility of LCH or RDD was considered low for the following reasons: (1) all spindle cells

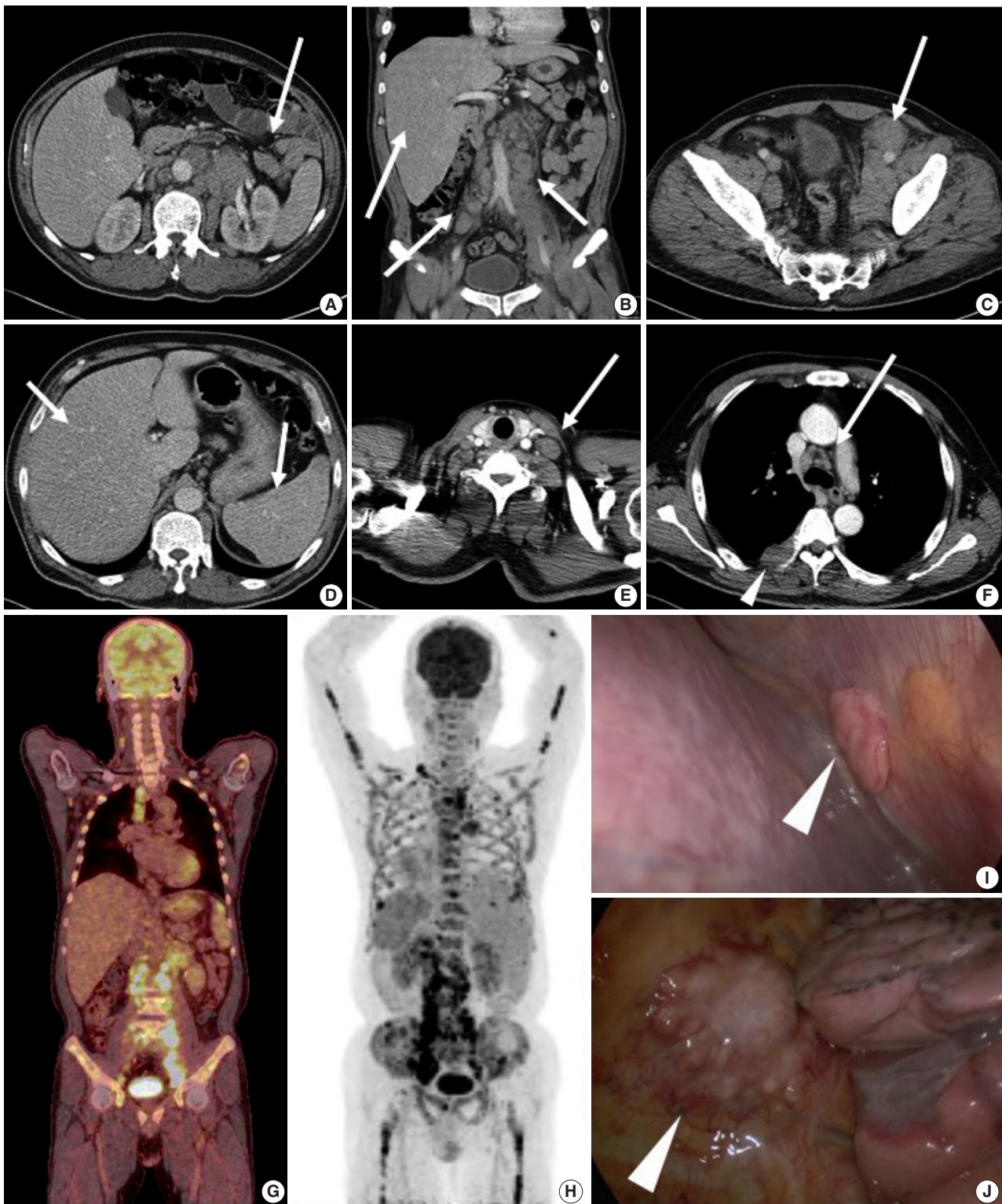


Fig. 1. (A–C) Abdominal computed tomography (CT) scan shows multiple enlarged paraaortic, aortocaval, common iliac, and inguinal lymph nodes (arrows). (B, D) Hepatomegaly and splenomegaly are also suspected (arrows). (E, F) Chest CT scan shows supraclavicular lymph node enlargement (E, arrow) and mediastinal lymph node enlargement (F, arrow). (F) Pleural mass is detected on chest CT (arrowhead). (G) Positron emission tomography–CT scan shows enlargement of multiple mediastinal and retroperitoneal lymph nodes. (H) Diffuse axial and appendicular skeletal involvement was suspected. (I, J) Video-assisted thoracosurgery showed multiple pleural nodules attached to the parietal pleura (arrowhead).

from biopsied sites were negative for CD1a and S-100; (2) characteristic histologic findings of LCH, such as large oval cells with complex grooved and folded nuclei, were not observed; (3) even in the lymph node, a frequent site of RDD involvement, the characteristic morphology of RDD including expansion of sinuses by large histiocytes and emperipolesis, was not identified. In addition, proliferation of similar cells was not confined to a particular organ or site, suggesting a systemic condition rather than localized reaction or inflammation. In conclusion, the patient was diagnosed with ECD with systemic involvement.

Additional testing for the *BRAF*^{V600E} mutation by real-time polymerase chain reaction was performed with the pleural biopsy tissue and was negative. Brain magnetic resonance imaging (MRI) was negative for disease involvement. MRI of the heart was not performed, but an echocardiogram showed negative

findings for pericardial involvement, cardiac wall involvement, valve involvement, or major vessel involvement. Furthermore, serial chest CTs for follow up of the pleura, lymph nodes, and bone lesions revealed no ECD involvement of the aorta or heart.

Interferon- α (IFN- α) was administered 3 times a week (3×10 IU subcutaneous injection). After 1 month of treatment, the patient complained of whole-body myalgia, general weakness, and depressed mood. The authors considered these symptoms signs of an adverse response to IFN- α , and the injection was delayed for 2 weeks. During this rest period, a response evaluation was performed. Chest and abdominal CT scan showed stable disease based on Response Evaluation Criteria in Solid Tumors ver. 1.0. After 1 additional month of IFN- α administration, the patient revisited the hospital complaining of anorexia, nausea, and sustained general weakness. WBC, hemoglobin, and platelet

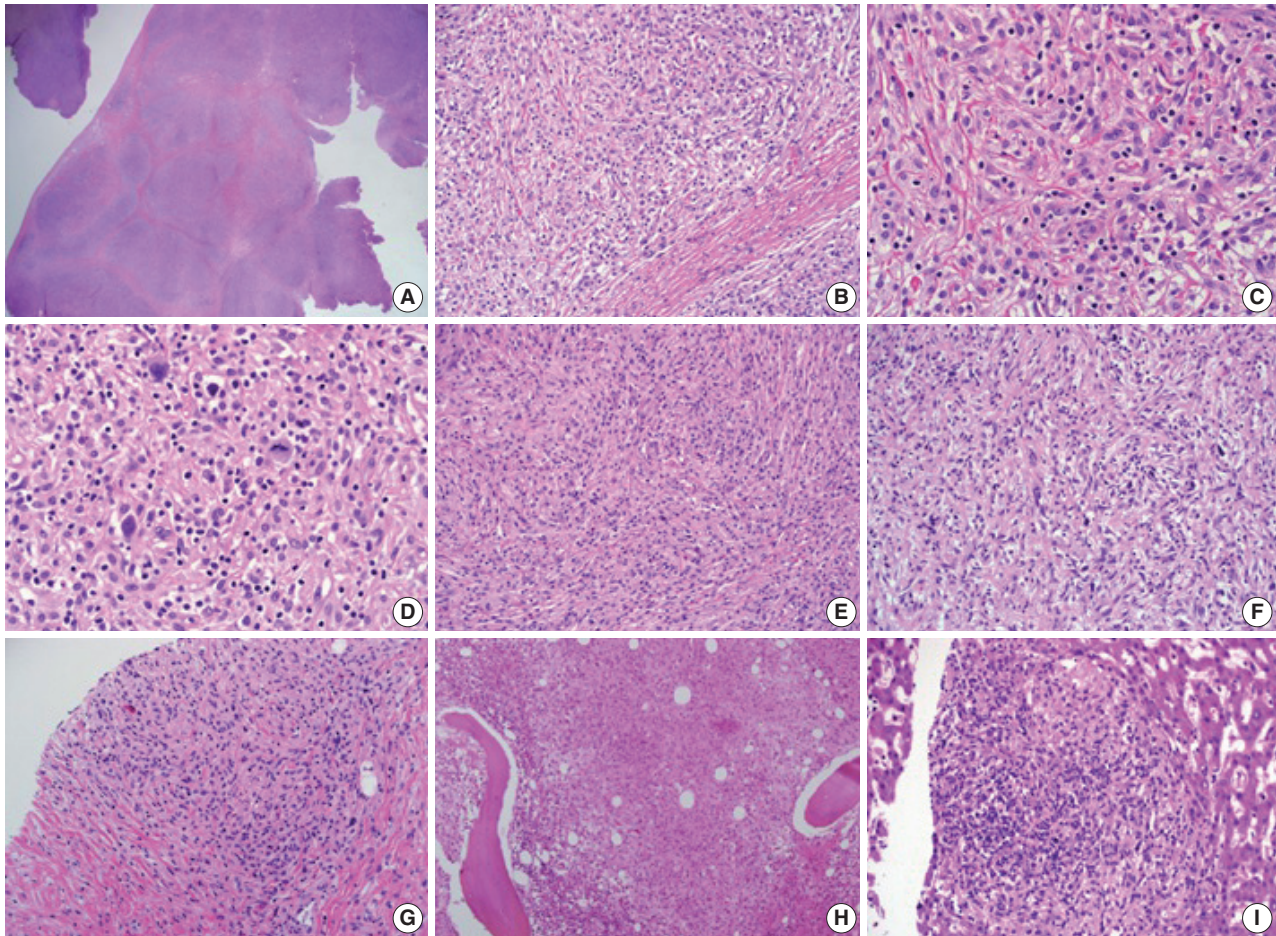


Fig. 2. (A, B) Histopathologic examination of pleural biopsy revealed a proliferating lesion of spindle to oval-shaped cells with a fibrous background. (C) Some cells showed vacuolated or focal clear cytoplasm. Otherwise, they had abundant eosinophilic, fine, granular cytoplasm. (D) A few cells with hyperchromatic and pleomorphic nuclei were noted, and mitosis was rarely found ($< 1/10$ high-power field). (E, F) In some areas, tumor cells showed marked spindle shape with the impression of randomly arranged fascicles. (G, H) External iliac lymph node (G) and bone marrow (H) biopsy showed similar tumor cells to the previous pleural biopsy. (I) Subsequent liver biopsy also revealed the same type of cells aggregating with fibrosis in the liver parenchyma.

counts were 6,290 cell/mm³ (normal range, 4,000 to 10,000 cell/mm³), 7.5 g/dL (normal range, 13.0 to 18.0 g/dL), and 250,000/mm³ (normal range, 150,000 to 450,000/mm³), respectively, and aspartate transaminase, alanine transaminase, total bilirubin, and direct bilirubin were 11 U/L (normal range, 14 to 40 U/L), 14 U/L (normal range, 9 to 45 U/L), 5.49 mg/

dL (normal range, 0.47 to 1.58 mg/dL), and 4.41 mg/dL (normal range, 0.13 to 0.47 mg/dL). Abdominal CT showed progression of multiple lymphadenopathy and hepatomegaly without biliary obstruction. With findings indicating progressive disease, high-dose steroids (dexamethasone 40 mg) were administered for 3 days. However, total bilirubin and direct bilirubin levels consis-

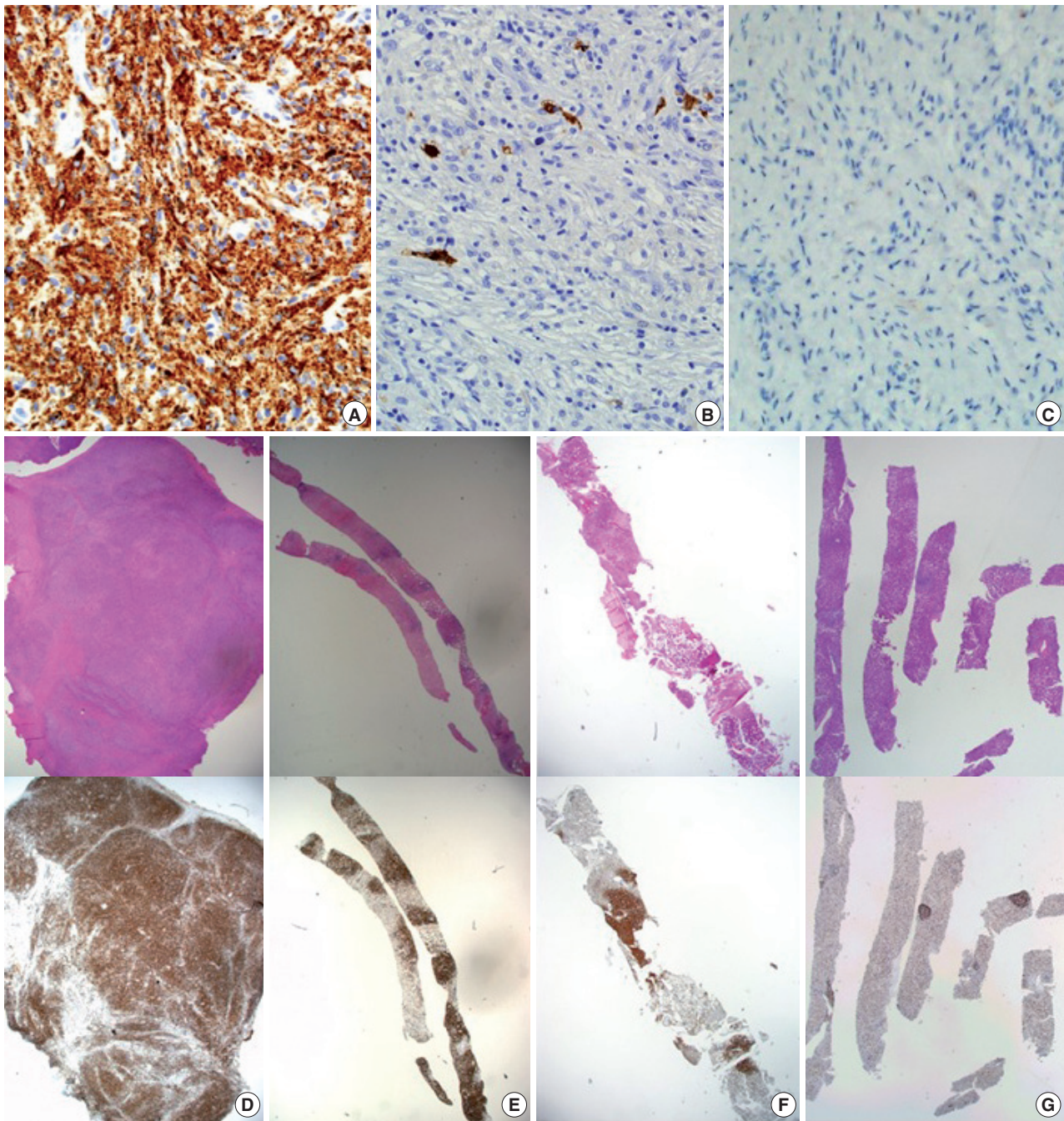


Fig. 3. CD68 immunohistochemical stain is positive in tumor cells (A); S-100 (B) and CD1a (C) are negative. Low-power view of hematoxylin and eosin stain and CD68 immunohistochemical stain of pleural mass excision (D); external iliac lymph node biopsy (E); bone marrow biopsy (F); liver biopsy (G).

tently increased up to 16.91 mg/dL (normal range, 0.47 to 1.58 mg/dL) and 14.36 mg/dL (normal range, 0.13 to 0.47 mg/dL), respectively. Subsequent liver biopsy and histological findings revealed multifocal aggregations of CD68 (+), S-100 (-), and CD1a (-) tumor cells with fibrosis in the liver parenchyma (Figs. 2I, 3G), identical to the previous biopsies of the pleura (Fig. 3D), lymph node (Fig. 3E), and bone marrow (Fig. 3F). Despite subsequent high-dose steroid treatment, the patient experienced rapid progression and hepatorenal syndrome and died due to hepatic failure.

This study was approved by the Institutional Review Boards of the Catholic Medical Center Office of the Human Research Protection Program (KC16ZISE0433), which included review of the patient's informed consent.

DISCUSSION

In this case, a 53-year-old male patient presented with constitutional symptoms and multiple enlarged lymph nodes mimicking malignant lymphoma. He was diagnosed with ECD based on histological findings and immunohistochemical studies. ECD is a rare disorder of unknown etiology characterized by CD68 (+), S-100 (-), and CD1a (-) non-Langerhans histiocytosis most commonly involving long bones such as the femur, tibia, and fibula.¹ Clinical manifestations of ECD vary greatly depending on the site of histiocytic infiltration.^{1,5}

Despite various clinical manifestations of ECD, patients almost always show long bone involvement detected by bone scan or PET-CT scan.¹ In addition to skeletal involvement, neurological, retroperitoneal, pulmonary, cutaneous, and cardiovascular involvement of ECD have been found in more than 20% of patients over the course of the disease. Characteristic imaging findings such as “coated aorta” or “hairy kidney” appear with cardiovascular and renal involvement, respectively.⁵ Such findings did not exist in this case, except for FDG uptake and signal increases in both femurs on PET-CT and bone scan. These findings were also identified in nearly all vertebrae (cervical, thoracic, lumbar, and sacrum), the skull, both scapulae, the sternum, and both humerus bones. In contrast with LCH, which usually involves the craniofacial bones,⁸ the axial skeleton is classically spared in ECD, with predominant involvement of the lower limbs, suggesting that this case is unusual. In addition, extensive involvement of the lymph nodes, liver, and spleen is also very rare in ECD. Few cases of ECD with lymph node involvement have been reported.^{2,6} This atypical manifestation obscured the clinical diagnosis of ECD. Extensive lymph node enlarge-

ment, involvement of the liver and spleen, and constitutional symptoms gave the clinical impression of malignant lymphoma.

The histopathological findings of ECD are characterized by xanthogranulomatous tissue infiltration with lipid-laden histiocytes,¹ which characteristically express an immunoprofile of CD68 (+), CD1a (-), and S-100 (-).^{1-4,8} However, specific or strict histopathological criteria for ECD are not established, such as the degree of “lipid-laden” features or characteristics including nuclear pleomorphism and arrangement pattern. In this case, cells of many foci were spindle-shaped with a fascicle pattern, and most nuclei were relatively large, oval, and plump with fine granular chromatin and nucleoli. A few cells were pleomorphic with hyperchromatic nuclei and mitosis, although they were very sparse. Most cells had fine, granular, abundant eosinophilic cytoplasm and clear foamy cytoplasm on high-power examination. With these findings, possible diagnoses included dendritic cell sarcoma, as well as histiocytic infiltrating lesions such as LCH, RDD, and ECD.⁹ Nuclear grooving, prominent eosinophilic infiltration, and definite emperipolesis were hard to identify, although there were abundant lymphocytes and a few eosinophils. Malignant lymphoma was initially suspected, but eventually deemed an unlikely possibility. Immunohistochemistry was negative for CD45RB, CD30, and CD15, excluding malignant lymphoma. Likewise, negativity for CD21, CD23, S-100, CD1a, and calretinin along with low Ki-67 index excluded dendritic cell sarcoma, LCH (commonly CD1a [+]), RDD (commonly S-100 [+]), and other possible diagnoses such as undifferentiated pleomorphic sarcoma and sarcomatoid mesothelioma.

In this case, disease progression with hepatic involvement was suspected due to increases in total bilirubin and direct bilirubin level, which were proven by liver biopsy. The patient died four months after initial presentation. Previous literature has reported that ECD presenting with central nervous system (CNS) and cardiovascular involvement has a poor prognosis.^{10,11} Data are lacking for ECD prognosis with lymph node or hepatic involvement, but our patient showed a poor prognosis over the course of treatment.

According to recently suggested revised classification, histiocytic disorders are grouped as L, C, R, M, and H by a system that incorporates histology, phenotype, molecular alterations, clinical findings, and imaging characteristics.¹² The “L” (Langerhans) group includes LCH, ECD, and indeterminate cell histiocytosis.¹² More than 80% of LCH and ECD cases express clonal mutations involving genes of the mitogen-activated protein kinase pathway.¹² In one study, about 20% of patients with ECD were found to also have LCH lesions.¹³ Although no biopsy

sites of our patient showed characteristic LCH morphology and were all negative for CD1a immunohistochemistry, the possibility of overlapping LCH histology cannot be ruled out, if other sites such as the vertebrae were also biopsied.

The largest cohort study to date identified *BRAF*^{V600E} mutations in 46 of 80 ECD patients (57.5%) with multiple orthogonal methodologies.¹⁴ In addition, some of the remaining *BRAF* wild-type patients had N/KRAS, PIK3CA, and AKT1 mutations.¹⁴ Therefore, although our patient was negative for *BRAF*^{V600E} mutation, the possibility of other genetic alterations found in previous studies of ECD cannot be ruled out. Unfortunately, further studies for other possible genetic alterations could not be performed due to the patient's rapid disease progression and death.

There are few prospective therapeutic studies on ECD and no randomized controlled trials on ECD. Therefore, therapeutic guidelines have not been established. In general, IFN- α has been the drug of choice since the first report of its efficacy in 2005.⁸ Multivariate retrospective analysis suggested increased survival with IFN- α .¹⁵ Although the optimal dose of IFN- α has not been established, 3 million units (mIU) 3 times per week were initially recommended.¹⁵ Several studies recommended long-term (up to 3 years) treatment with high-dose IFN- α (9 mIU 3 times/wk) in cases of CNS or cardiac involvement.^{8,15} In 2012, a somatic gain-of-function mutation (V600E) in the protooncogene *BRAF* was detected in 54% (13 of 24) of patients with ECD.¹⁵ This mutation leads to activation of the tumorigenic RAS-ERK pathway and is thought to play a key role in the pathogenesis of the disorder.¹⁶ Treatment targeting this mutation has been tried, and the results of four ECD patients treated with *BRAF* inhibitors vemurafenib or dabrafenib have been reported.^{8,16,17} There are no larger studies addressing several remaining questions, such as the optimal drug dose, treatment duration, and possible long-term effects. However, long-term treatment with *BRAF* inhibitor can eventually lead to treatment resistance based on alteration of the RAS-MEK-ERK pathway. Recently, there was a report of a patient who developed resistance to dabrafenib and showed additional clinical response after adding the MEK inhibitor trametinib.¹⁷ This report implies the promising role of target inhibitors in treatment of ECD. Other than RAS-ERK pathway alterations, several studies found that proinflammatory cytokines such as interleukin (IL)-1, IL-6, and tumor necrosis factor α (TNF- α) are increased in ECD lesions.¹⁸ A recombinant IL-1R antagonist anakinra, an anti-TNF- α antibody infliximab, and a humanized monoclonal antibody against the IL-6R tocilizumab have been suggested as

second-line treatments.⁸ The treatment effects of proinflammatory cytokine inhibitors have been reported as case reports with positive efficacy in clinical response. However, there is a recent report of 12 patients treated with anakinra after IFN- α failure who showed variable treatment response without partial response of measurable tumors.¹⁸ Based on prior case series, further modulation cytokine inhibitors should be considered as second line treatment. Imatinib mesylate, a tyrosine kinase inhibitor, has been successfully used in case reports.¹⁹ Imatinib selectively targets KIT, BCR-ABL, and platelet-derived growth factor. Haroche *et al.*¹⁰ found abundant expression of platelet-derived growth factor receptor (PDGFR- β) in some histiocytic lesions of ECD and related disorders, and they successfully treated six patients with ECD positive for PDGFR- β with imatinib. They suggest that tyrosine kinase inhibitors more specific for PDGFR- β could be promising drugs for treating patients with severe forms of ECD resistant to IFN- α therapy. In addition, corticosteroids and cytotoxic drugs such as vinca alkaloids, anthracyclines, and cyclophosphamide can be administered conventionally, but the effects of those drugs are not significant.^{8,15} Radiotherapy and debulking surgery for patients with ECD have been reported, but the effects are unclear.⁸ In our case, INF- α was administered for first-line treatment but showed no treatment response. After IFN- α , high dose steroids were applied for symptomatic control, but hepatic dysfunction progressed. Due to rapid progression of hepatic failure, other agents were not attempted. *BRAF*^{V600E} mutation was not detected in our patient, so vemurafenib was not applied as a systemic treatment.

Although the etiology of ECD had been veiled for decades, recent advances in genetic understanding of the disease have provided important clues. There is abundant evidence that, in patients with ECD and "L" LCH,¹² *BRAF*^{V600E} mutations exist in both histiocytes and bone marrow cells.²⁰ An animal experiment with mice also strengthened the hypothesis that ECD and LCH are forms of inflammatory myeloid neoplasia.²⁰ Histopathological findings of ECD appear benign, but when involving critical organs, numerous previous studies have shown poor prognoses and high mortality rates. Because ECD can involve any organ, clinicians should be aware of the disease and include it on differential diagnoses in suspicious clinical settings, even when the likelihood is low. The final diagnosis can be confirmed by identifying histiocytic lesions via histological and immunohistochemical studies in the context of a fitting clinical presentation and radiologic findings.

In this report, we present a unique case of ECD with an unusual presentation characterized by involvement of systemic lymph

nodes, axial and appendicular skeleton, liver, and pleura. More data and investigation regarding the cells of origin are necessary to further understand this disease and establish effective treatment for patients, particularly those with critical organ involvement, rapid progression, and high mortality, as in this case.

Conflicts of Interest

No potential conflict of interest relevant to this article was reported.

REFERENCES

- Campochiaro C, Tomelleri A, Cavalli G, Berti A, Dagna L. Erdheim-Chester disease. *Eur J Intern Med* 2015; 26: 223-9.
- Lim J, Kim KH, Suh KJ, *et al.* A unique case of Erdheim-Chester disease with axial skeleton, lymph node, and bone marrow involvement. *Cancer Res Treat* 2016; 48: 415-21.
- Bindra J, Lam A, Lamba R, VanNess M, Boutin RD. Erdheim-Chester disease: an unusual presentation of an uncommon disease. *Skeletal Radiol* 2014; 43: 835-40.
- Pavlidakey PG, Mohanty A, Kohler LJ, Meyerson HJ. Erdheim-Chester disease associated with marginal zone lymphoma and monoclonal proteinemia. *Case Rep Hematol* 2011; 2011: 941637.
- Haroche J, Amoura Z, Wechsler B, Veyssier-Belot C, Charlotte F, Piette JC. Erdheim-Chester disease. *Presse Med* 2007; 36: 1663-8.
- Sheu SY, Wenzel RR, Kersting C, Merten R, Otterbach F, Schmid KW. Erdheim-Chester disease: case report with multisystemic manifestations including testes, thyroid, and lymph nodes, and a review of literature. *J Clin Pathol* 2004; 57: 1225-8.
- Ivan D, Neto A, Lemos L, Gupta A. Erdheim-Chester disease: a unique presentation with liver involvement and vertebral osteolytic lesions. *Arch Pathol Lab Med* 2003; 127: e337-9.
- Diamond EL, Dagna L, Hyman DM, *et al.* Consensus guidelines for the diagnosis and clinical management of Erdheim-Chester disease. *Blood* 2014; 124: 483-92.
- Cha YJ, Yang WI, Park SH, Koo JS. Rosai-Dorfman disease in the breast with increased IgG4 expressing plasma cells: a case report. *Korean J Pathol* 2012; 46: 489-93.
- Haroche J, Amoura Z, Charlotte F, *et al.* Imatinib mesylate for platelet-derived growth factor receptor-beta-positive Erdheim-Chester histiocytosis. *Blood* 2008; 111: 5413-5.
- Arnaud L, Hervier B, Néel A, *et al.* CNS involvement and treatment with interferon-alpha are independent prognostic factors in Erdheim-Chester disease: a multicenter survival analysis of 53 patients. *Blood* 2011; 117: 2778-82.
- Emile JF, Ablu O, Fraitag S, *et al.* Revised classification of histiocytoses and neoplasms of the macrophage-dendritic cell lineages. *Blood* 2016; 127: 2672-81.
- Hervier B, Haroche J, Arnaud L, *et al.* Association of both Langerhans cell histiocytosis and Erdheim-Chester disease linked to the *BRAFV600E* mutation. *Blood* 2014; 124: 1119-26.
- Emile JF, Diamond EL, Hélias-Rodzewicz Z, *et al.* Recurrent *RAS* and *PIK3CA* mutations in Erdheim-Chester disease. *Blood* 2014; 124: 3016-9.
- Munoz J, Janku F, Cohen PR, Kurzrock R. Erdheim-Chester disease: characteristics and management. *Mayo Clin Proc* 2014; 89: 985-96.
- Tzoulis C, Schwarzlmuller T, Gjerde IO, *et al.* Excellent response of intramedullary Erdheim-Chester disease to vemurafenib: a case report. *BMC Res Notes* 2015; 8: 171.
- Nordmann TM, Juengling FD, Recher M, *et al.* Trametinib after disease reactivation under dabrafenib in Erdheim-Chester disease with both *BRAF* and *KRAS* mutations. *Blood* 2017; 129: 879-82.
- Cohen-Aubart F, Maksud P, Saadoun D, *et al.* Variability in the efficacy of the IL1 receptor antagonist anakinra for treating Erdheim-Chester disease. *Blood* 2016; 127: 1509-12.
- Janku F, Amin HM, Yang D, Garrido-Laguna I, Trent JC, Kurzrock R. Response of histiocytoses to imatinib mesylate: fire to ashes. *J Clin Oncol* 2010; 28: e633-6.
- Haroche J, Cohen-Aubart F, Rollins BJ, *et al.* Histiocytoses: emerging neoplasia behind inflammation. *Lancet Oncol* 2017; 18: e113-25.

Post-transplant Amputation Traumatic Neuroma of the Hilum and Extrahepatic Duct in a Liver Donor

Na Rae Kim · Hyun Yee Cho · Dong Hae Chung · Keon Kuk Kim¹ · Jae Hee Cho² · Seung Joon Choi³

Departments of Pathology and ¹General Surgery, ²Division of Gastroenterology, Department of Internal Medicine, ³Department of Radiology, Gachon University Gil Medical Center, Incheon, Korea

Traumatic neuromas develop after injury to nerve fibers encased in Schwann cells. They occur mainly in the amputated stump of the extremities.¹ Biliary traumatic neuroma was first described in 1928 by Husseinoff.² Since then, less than 100 cases of biliary traumatic neuroma have been reported.^{3,4} Most occur at the cystic duct stump after cholecystectomy. It may also occur in the main biliary tract following any injury, even liver transplantation.^{5,6}

Herein, we report a case of post-transplant biliary traumatic neuroma in a donor after an 8-year interval. This rare biliary traumatic neuroma may be a risk factor for liver transplantation-related biliary stricture.

CASE REPORT

A 53-year-old woman visited the emergency room for abruptly developed pruritus and jaundice. She had a past history of undergoing right hepatectomy and closure of left hepatic duct as a living donor liver transplantation (LDLT) to her husband 8 years previously. A computed tomography of the abdomen showed an enhancing lesion in eccentric wall thickening of the proximal bile duct, suggestive of hilar cholangiocarcinoma (Fig. 1A). The preoperative carbohydrate antigen 19-9 and carcinoembryonic antigen levels were within normal ranges. Liver function tests revealed total bilirubin at 1.5 (reference < 1.2 mg/dL), gamma-glutamyl transferase at 258 (reference < 48 U/L), alkaline phosphatase at 177 (reference < 123 U/L), and alanine transaminase at 49 (reference < 40). Liver magnetic resonance images and cholangiopancreatography revealed an enhanced wall thickening in the common hepatic duct and dilated left proximal intrahepatic duct. An endoscopic ultrasonography revealed a mass-like heterogeneous echogenic lesion, measuring 15.6×11.4 mm, at the hilar level. A preoperative endoscopic retrograde cholangiopancreatography revealed the diameter of the proximal common bile duct dilated up to 9 mm. A biopsy was done, and a biliary stent was placed to relieve the biliary obstruction. The preoperative biopsy showed only normal duodenal epithelium. At surgery, a firm adhesion to the adjacent portal vein and duodenal wall was found. She had a fibrotic and hard mass-like lesion in the hilum and proximal common bile duct. An intraoperative frozen biopsy of the proximal bile duct resection margin was done. A caudate lobectomy with bile duct resection and hepatojejunostomy was done under a presumptive diagnosis of cholangiocarcinoma. A periportal lymphadenectomy was done and a biopsy was taken from the portal vein.

Grossly, the received specimen showed the common bile duct external circumference dilated up to 2.2 cm (Fig. 1B). The inner surface of the resected bile duct was thickened and fibrotic, measuring 2.2×1.8 cm.

Under light microscopy, the serial sections of the thickened bile duct revealed hyperplastic and disorganized nerve fibers surrounded and dissected by thick collagenous fibrous connective tissue (Fig. 1C). The bile duct was compressed by fibrotic tissue. Small foci of mature lymphoid cells and hemosiderin-laden macrophages were also found. (Fig. 1D) Immunohistochemical stains were positive for S-100 protein (1:600, polyclonal, Dako, Glostrup, Denmark) and Masson-Trichrome stain revealed marked

Corresponding Author

Dong Hae Chung, MD, PhD
Department of Pathology, Gachon University Gil Medical Center, 21 Namdong-daero 774beon-gil, Namdong-gu, Incheon 21565, Korea
Tel: +82-32-460-3866, Fax: +82-32-460-2394, E-mail: dhchung@gjihospital.com

Received: December 8, 2016 Revised: January 5, 2017

Accepted: January 19, 2017

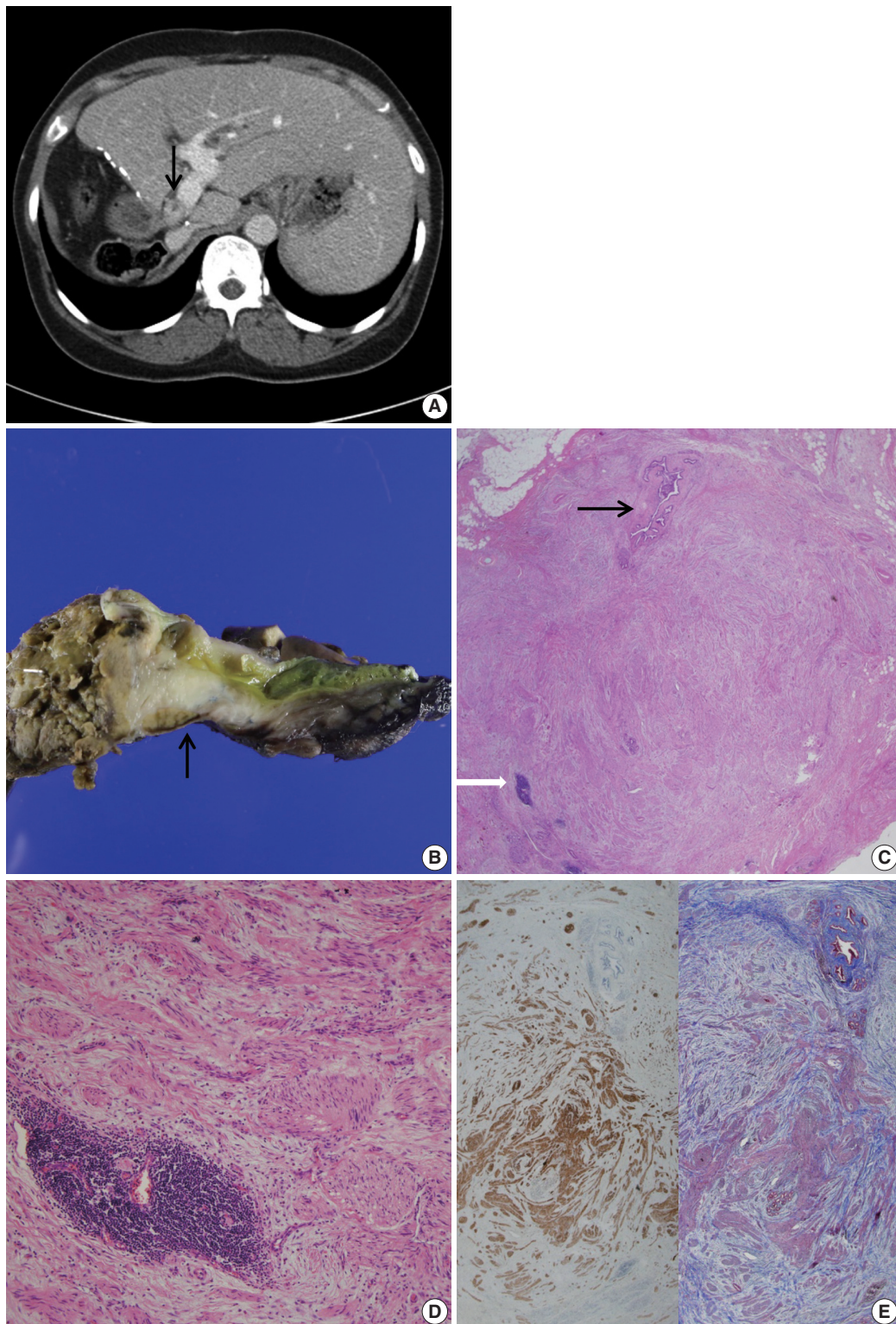


Fig. 1. (A) Abdominal computed tomography reveals an enhanced thickening (arrow) of the common bile duct wall. (B) Grossly, the resected common bile duct reveals a firm grayish mass-like lesion (arrow) at the proximal bile duct. (C) Microscopically, the thickened mass-like portion consists of abundant nerve fascicles mainly composed of axon fibers and Schwann cells, intermixed with collagen bundles. Note entrapped bile duct (black arrow) and focal lymphoid aggregates (white arrow). (D) Marked fibrosis and haphazard proliferation of nerve fascicles. Note lymphoid aggregates. (E) Marked collagen deposits are intervening in the perineurial and epineurial area of nerve fascicles (left: S-100 protein immunohistochemical stain, right: Masson-Trichrome stain).

perineurial and epineurial fibrosis (Fig. 1E). The diagnosis was amputation traumatic neuroma of the bile duct. Proximal and distal bile duct resection margins were free of fibrosis. Nerve fascicles were seen up to the tunica media of the biopsied portal vein. Enlarged, up to 1.2 cm, periportal lymph nodes showed reactive hyperplasia. On the fifth postoperative day, the serum bilirubin level was normalized. On the ninth postoperative day, the patient was discharged with an unremarkable course.

This study was approved by the Institutional Review Board of Gachon University Gil Hospital with a waiver of informed consent (GBIRB 2016-323).

DISCUSSION

LDLT was introduced in 1989, and the first Korean LDLT was done in 1994.⁷ According to the Korean Network of Organ Sharing, the number of adult LDLT (patients aged > 18 years) has increased annually, with 911 cases of adult LDLT performed in Korea in 2015. This number represents 67.4% of total adult liver transplantation in Korea, whereas LDLT comprises less than 3% in the United States.⁷ Therefore, this dramatic difference in clinical practice in Korea raises concerns and doubts about the long term well-being of donors.⁸ The immediate postoperative complications on the donor side are infections, portal vein or inferior vena cava thrombosis, and remnant cystic duct causing so-called post-cholecystectomy syndrome.⁹ Studies on recipients' postoperative morbidity report that biliary stricture due to traumatic neuroma occurs only after duct-to-duct biliary anastomosis following liver transplantation. The first report of transplantation-related biliary traumatic neuromas showed a 27.9% prevalence,⁵ but the risk of pathologically confirmed symptomatic biliary traumatic neuroma is about 0.5%.⁶

The biliary tract is richly innervated by the hepatic plexus, which is derived from the celiac plexus. Dissection of the biliary tract and dissected nerve fibers may induce inappropriate nerve regeneration, triggered by factors such as intraoperative thermal injury of the bile ducts and foreign bodies such as suture materials.⁴ Immunosuppressants of calcineurin inhibitors such as tacrolimus are also reported as another possible factor.¹⁰ However, not all sympathetic nerve fibers induce an amputation traumatic neuroma and the exact pathogenesis is still unknown.

Traumatic neuromas arising from bile duct after orthotopic liver transplantation have rarely been described.^{5,6} Previous articles have been focused on recipients of LDLT. However, the risk of biliary traumatic neuromas may be underestimated because they are usually asymptomatic even in severe stricture cases, like the

present case. These asymptomatic period ranges from several months up to 45 years after the biliary operation. There are no specific radiologic findings of biliary traumatic neuroma,³ and the diagnosis of biliary traumatic neuroma is not made unless it is pathologically confirmed after resection. Pathologic findings are characterized by disorganized haphazard proliferating nerve fascicles growing out in various directions, resulting in a bulb-shaped mass-like thickening, i.e., stump, resembling cholangiocarcinoma.⁴ Both end-to-end anastomosis and hepaticojejunostomy are most commonly advocated in symptomatic cases. Considering its possible pathogenesis, however, biliary traumatic neuromas can recur following the biliary operation.

Biliary traumatic neuromas represent a rare cause of biliary stricture in both donor and recipient after orthotopic liver transplantation. To avoid unnecessary wide resection, the physician should be aware of the possibility of biliary traumatic neuroma when facing unexplained anastomotic biliary stenosis, even when presenting with a mass-like lesion on radiology.

Conflicts of Interest

No potential conflict of interest relevant to this article was reported.

REFERENCES

1. Necmioglu S, Subasi M, Kayikci C, Young DB. Lower limb landmine injuries. *Prosthet Orthot Int* 2004; 28: 37-43.
2. Husseinoff D. Ueber einem Fall von Wucherung des Nervengewebes nach wiederholten Operationen der Gallenga: nge. *Zbl Allg Path* 1928; 43: 344-8.
3. Iannelli A, Fabiani P, Karimjee BS, Converset S, Saint-Paul MC, Gugenheim J. Traumatic neuroma of the cystic duct with biliary obstruction: report of a case. *Acta Gastroenterol Belg* 2003; 66: 28-9.
4. Pickens A, Vickers SM, Brown KL, Reddy VV, Thompson JA. An unusual etiology of biliary hilar obstruction and the potential role of acidic fibroblast growth factor in the development of a biliary neuroma. *Am Surg* 1999; 65: 47-51.
5. Colina F, Garcia-Prats MD, Moreno E, *et al.* Amputation neuroma of the hepatic hilum after orthotopic liver transplantation. *Histopathology* 1994; 25: 151-7.
6. Navez J, Golse N, Bancel B, *et al.* Traumatic biliary neuroma after orthotopic liver transplantation: a possible cause of "unexplained" anastomotic biliary stricture. *Clin Transplant* 2016; 30: 1366-9.
7. Jeon H, Lee SG. Living donor liver transplantation. *Curr Opin Organ Transplant* 2010; 15: 283-7.

8. Lee SG. Living-donor liver transplantation in adults. *Br Med Bull* 2010; 94: 33-48.
9. Ghobrial RM, Freise CE, Trotter JF, *et al.* Donor morbidity after living donation for liver transplantation. *Gastroenterology* 2008; 135: 468-76.
10. Sosa I, Reyes O, Kuffler DP. Immunosuppressants: neuroprotection and promoting neurological recovery following peripheral nerve and spinal cord lesions. *Exp Neurol* 2005; 195: 7-15.

Expression of CD34 and β -Catenin in Malignant Rhabdoid Tumor of the Liver Mimicking Proximal-Type Epithelioid Sarcoma

Woo Cheal Cho · Fabiola Balarezo

Department of Pathology and Laboratory Medicine, Hartford Hospital, Hartford, CT, USA

Malignant rhabdoid tumor (MRT) is a rare, aggressive malignant neoplasm often arising in the kidney in infants or young children. MRT was first described in 1978 as a rhabdomyosarcomatoid variant of Wilms tumor with unfavorable prognosis due to its morphologic resemblance to rhabdomyoblasts.¹ Since the first description outside the kidney, MRTs have been described in almost every conceivable location in the body, including the central nervous system where it is commonly referred to as atypical teratoid/rhabdoid tumor.² Involvement of the liver, however, is still exceedingly rare, with only fewer than 60 cases of primary MRT arising in the liver reported in the literature. Herein, we describe a rare case of MRT of the liver in a 1-year-old male infant with CD34 and β -catenin expression mimicking proximal-type epithelioid sarcoma (ES).

CASE REPORT

A 1-year-old male infant presented with a right-sided, non-tender abdominal mass. Imaging studies revealed a heterogeneously enhancing mass within the liver, measuring 10.0×10.0×7.9 cm, suspicious of hepatoblastoma. Liver biopsy showed a proliferation of malignant epithelioid cells with clear to amphophilic cytoplasm and small nucleoli (Fig. 1A–C). The tumor focally exhibited an organoid/trabecular growth pattern, and a rim of compressed non-neoplastic liver parenchyma was seen at

the periphery of the tumor (Fig. 1A). Necrosis was present (Fig. 1B) and numerous mitotic figures (7 mitoses/10 high-power field) (Fig. 1C) were identified. No definitive rhabdoid cells were seen. Immunohistochemical analysis revealed diffuse immunoreactivity to cytokeratin (CK) 19, CK MNF116, vimentin, and β -catenin (membranous) (Fig. 2A). The tumor was also focally positive for epithelial membrane antigen, glypican-3, and CD34 (Fig. 2B). Immunostains for CK7, CK20, hepatocyte paraffin (Hep Par) 1, arginase-1, α -fetoprotein, desmin, myogenin, human melanoma black 45, Melan-A, octamer-binding transcription factor 3/4, carcinoembryonic antigen, chromogranin, synaptophysin, calponin, smooth muscle actin, S100, and SRY-related HMG-box 10 (SOX10) were negative. Loss of nuclear INI1 expression (Fig. 2C) was seen. The diagnosis of INI1-negative neoplasm was entertained with differential diagnoses including extrarenal MRT, proximal-type ES, and small cell undifferentiated (SCUD) hepatoblastoma. Despite the lack of classic rhabdoid morphology and the presence of positive expression of CD34 and β -catenin, extrarenal MRT was favored over proximal-type ES given the patient's age and location of the tumor. In addition, the tumor lacked classic morphologic features of small round blue cell tumors, thereby making SCUD hepatoblastoma a less favored differential.

Formal written informed consent was not required with a waiver by the appropriate institutional review board of Hartford Hospital and/or national research ethics committee.

DISCUSSION

MRT is a rare, highly aggressive and lethal malignant neoplasm with poor prognosis. Histologically, MRT is classically characterized by sheets of large eosinophilic cells with eccentric

Corresponding Author

Woo Cheal Cho, MD
Department of Pathology and Laboratory Medicine, Hartford Hospital, 80 Seymour Street, Hartford, CT 06102-5037, USA
Tel: +1-860-972-2488, Fax: +1-860-545-2204
E-mail: woocheal.cho@hhchealth.org

Received: March 12, 2017 Revised: April 5, 2017

Accepted: May 15, 2017

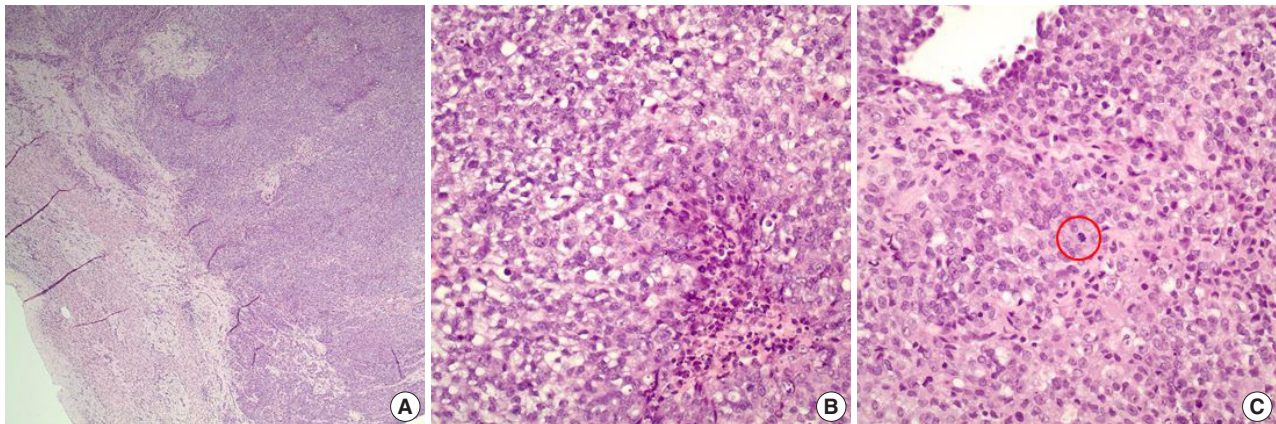


Fig. 1. Microscopic findings on liver biopsy. (A) The tumor displays malignant epithelioid cells with clear to amphophilic cytoplasm and small nucleoli with a focal organoid growth pattern. A rim of compressed non-neoplastic liver parenchyma is seen at the periphery of the tumor. (B, C) Areas of necrosis (B) and frequent mitoses (C, circle) within the tumor are also seen.

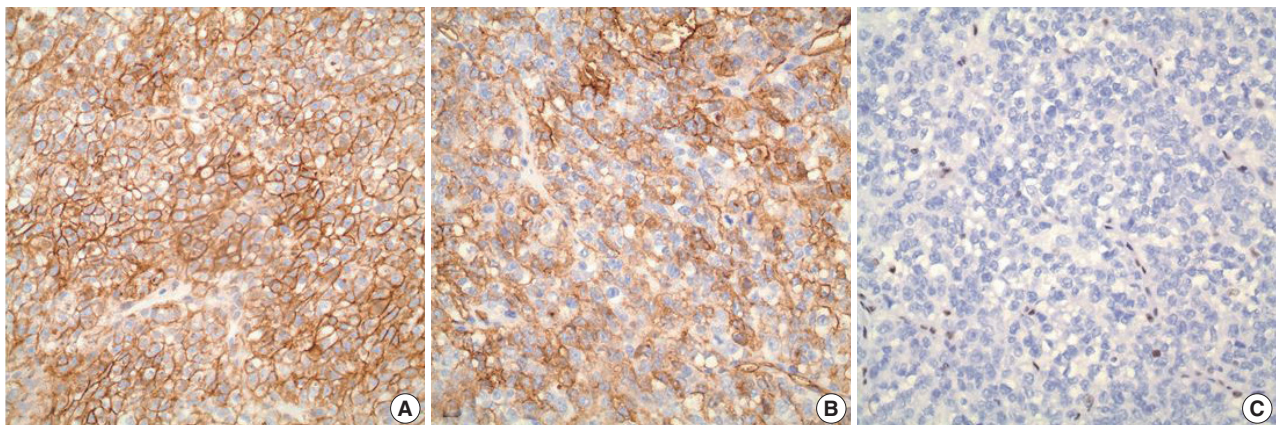


Fig. 2. Immunohistochemical analysis. (A) A diffuse and strong immunoreactivity (membranous) with β -catenin is seen in the tumor. (B) The tumor is also positive (patchy) for CD34. (C) Loss of nuclear INI1 expression is seen within the tumor.

vesicular nuclei, prominent nucleoli, and occasional intracytoplasmic inclusions of hyaline globules, reminiscent of rhabdomyoblasts. Loss of nuclear INI1 expression associated with deletions or mutations of the *SMARCB1/INI1* gene at 22q11.2 is the characteristic hallmark of MRT.^{3,4} This genetic alteration, however, is also seen in other rare neoplasms, including proximal-type ES⁵ and SCUD hepatoblastoma.⁶ In particular, distinction between extrarenal MRT and proximal-type ES can be problematic due to morphologic similarities between the two entities; proximal-type ES also shows large epithelioid cells, vesicular nuclei with prominent nucleoli, and rhabdoid cytoplasmic inclusions. Recently, CD34 and β -catenin have been suggested as potentially useful immunohistochemical markers for distinguishing extrarenal MRT from proximal-type ES. Proximal-type ES often exhibits positive expression of CD34 and β -catenin, while extrarenal MRT typically lacks immunoreactivity to these

markers. In the present case, however, the tumor was diffusely and strongly positive for β -catenin while showing patchy positivity with CD34 in the absence of nuclear INI1 staining, mimicking proximal-type ES. Nonetheless, extrarenal MRT was still favored over proximal-type ES in our case given the fact that proximal-type ES is predominantly seen in middle-aged or older adults, frequently occurring in axial or proximal regions, such as the pelvis, perineum, and genitalia.⁷ In contrast, MRT of the liver mainly occurs in infants.⁴ SCUD hepatoblastoma is a rare variant of hepatoblastoma known to show loss of INI expression, similar to MRT.⁶ In fact, some authors⁶ have recently postulated that SCUD hepatoblastoma may actually not be a hepatoblastoma but rather a form of MRT arising in the liver, although further study is needed. The tumor in our case, however, lacked small cell morphology compatible with SCUD hepatoblastoma, thus making it a less favored differential.

In conclusion, we report a case of MRT of the liver with unusual immunophenotypic features mimicking proximal-type ES and SCUD hepatoblastoma. To the best of our knowledge, this may be the first reported case of extrarenal MRT of the liver with CD34 and β -catenin expression.

ORCID

Woo Cheal Cho: <http://orcid.org/0000-0001-5867-1403>

Conflicts of Interest

No potential conflict of interest relevant to this article was reported.

REFERENCES

1. Beckwith JB, Palmer NF. Histopathology and prognosis of Wilms tumors: results from the First National Wilms' Tumor Study. *Cancer* 1978; 41: 1937-48.
2. Rorke LB, Packer RJ, Biegel JA. Central nervous system atypical teratoid/rhabdoid tumors of infancy and childhood: definition of an entity. *J Neurosurg* 1996; 85: 56-65.
3. Oita S, Terui K, Komatsu S, *et al.* Malignant rhabdoid tumor of the liver: a case report and literature review. *Pediatr Rep* 2015; 7: 5578.
4. Oda Y, Tsuneyoshi M. Extrarenal rhabdoid tumors of soft tissue: clinicopathological and molecular genetic review and distinction from other soft-tissue sarcomas with rhabdoid features. *Pathol Int* 2006; 56: 287-95.
5. Hornick JL, Dal Cin P, Fletcher CD. Loss of INI1 expression is characteristic of both conventional and proximal-type epithelioid sarcoma. *Am J Surg Pathol* 2009; 33: 542-50.
6. Vokuhl C, Oyen F, Haberle B, von Schweinitz D, Schneppenheim R, Leuschner I. Small cell undifferentiated (SCUD) hepatoblastomas: All malignant rhabdoid tumors? *Genes Chromosomes Cancer* 2016; 55: 925-31.
7. Armah HB, Parwani AV. Epithelioid sarcoma. *Arch Pathol Lab Med* 2009; 133: 814-9.

Secretory Carcinoma Arising in a Fibroadenoma: A Brief Case Report

Sharon Lim · Min Keun Shim¹ · Eun Yoon Cho² · Soo Youn Cho²

Department of Pathology, Hanyang University Guri Hospital, Hanyang University College of Medicine, Guri; ¹Foryou Pathology Laboratory, Gwangju;
²Department of Pathology and Translational Genomics, Samsung Medical Center, Sungkyunkwan University College of Medicine, Seoul, Korea

Secretory carcinoma is a rare subtype of breast cancer, accounting for less than 0.1% of invasive breast cancers.¹ It is characterized by distinctive intracellular and extracellular secretory material in solid, microcystic, and tubular growth patterns.

Recently, we experienced this rare tumor arising in a fibroadenoma (FA). Ductal epithelium within FA can undergo carcinomatous change. There have been several case reports of carcinoma arising in FA, usually in forms of lobular or ductal carcinoma *in situ*.²⁻⁴ However, there has been no reported case of secretory carcinoma arising in a FA.

CASE REPORT

A 20-year-old woman visited a local hospital with a palpable nodule in the right upper center breast. Her family history and past history were unremarkable. Also she denied the possibility of pregnancy or oral contraceptive use. She underwent excision of the mass under the clinical impression that it was benign. Seven months later, she visited Samsung Medical Center for a second opinion. Mammography and ultrasonography revealed no residual mass or abnormality.

At low power view, the tumor, measuring 0.7 × 0.6 cm, was multinodular with intervening fibrous septa. There were multifocal, less cellular, myxoid areas at the periphery (Fig. 1A). Tumor cells showed solid sheets or cribriform arrangement, and the tumor nests showed microcystic structures containing pale bluish secretory

material (Fig. 1B). The tumor cells were large and polygonal, displaying abundant vacuolated cytoplasm with intracellular secretory material. The secretory material was periodic acid Schiff-positive (Fig. 1C). Nuclei were small, showing mild to moderate atypia and small nucleoli. Bloom-Richardson histologic grade was grade II. There was no lymphovascular invasion. The tumor cells were diffusely positive for S-100 protein (1:5,000, polyclonal, Dako, Carpinteria, CA, USA) (Fig. 1D). At the periphery of the mass, bland tubular ducts were mixed with nests of tumor cells within myxoid stroma (Fig. 1E, F). The tumor cell nests within myxoid stroma showed diffuse strong positivity for S-100 protein, while the bland tubular components were negative (Fig. 1G). Calponin (1:200, clone CALP, Dako) and p63 (1:200, clone 4A4, Biocare Medical, Concord, CA, USA) staining confirmed the presence of myoepithelial cells in the bland tubular components (Fig. 1H). A few tumor cells expressed p63. This lesion corresponded to the pericanalicular pattern of FA. The invasive portion was confined within the FA with no extension to adjacent parenchyma. A few ducts with secretory type ductal carcinoma *in situ* were noted in and outside the boundary of FA (Fig. 1I, J). Estrogen receptor (ER; 1:200, clone 6F11, Novocastra Laboratories, Newcastle upon Tyne, UK), progesterone receptor (PR; 1:100, clone 16, Novocastra Laboratories, Newcastle upon Tyne, UK), and human epidermal growth factor receptor 2 (HER-2; clone 4B5, Ventana Medical Systems, Inc., Tucson, AZ, USA), epidermal growth factor receptor (1:100, clone EGFR.25, Novocastra Laboratories) were all negative in tumor cells, while cytokeratin (CK) 5/6 (1:100, clone D5/16B4, Dako) was expressed in 5% of the tumor cells. Ki-67 (1:200, clone MIB-1, Dako) labeling index was about 5%. *ETV6* rearrangement was confirmed by *ETV6* break-apart fluorescence *in situ* hybridization (Abbott Molecular, Chicago, IL, USA). We diagnosed this tumor as secretory carcinoma arising in a FA. Resection margin assessment was not feasible

Corresponding Author

Soo Youn Cho, MD, PhD
Department of Pathology and Translational Genomics, Samsung Medical Center, Sungkyunkwan University School of Medicine, 81 Irwon-ro, Gangnam-gu, Seoul 06351, Korea
Tel: +82-2-3410-2817, Fax: +82-2-3410-0025, E-mail: sooyoun.cho@samsung.com

Received: May 8, 2017 Revised: July 31, 2017

Accepted: August 1, 2017

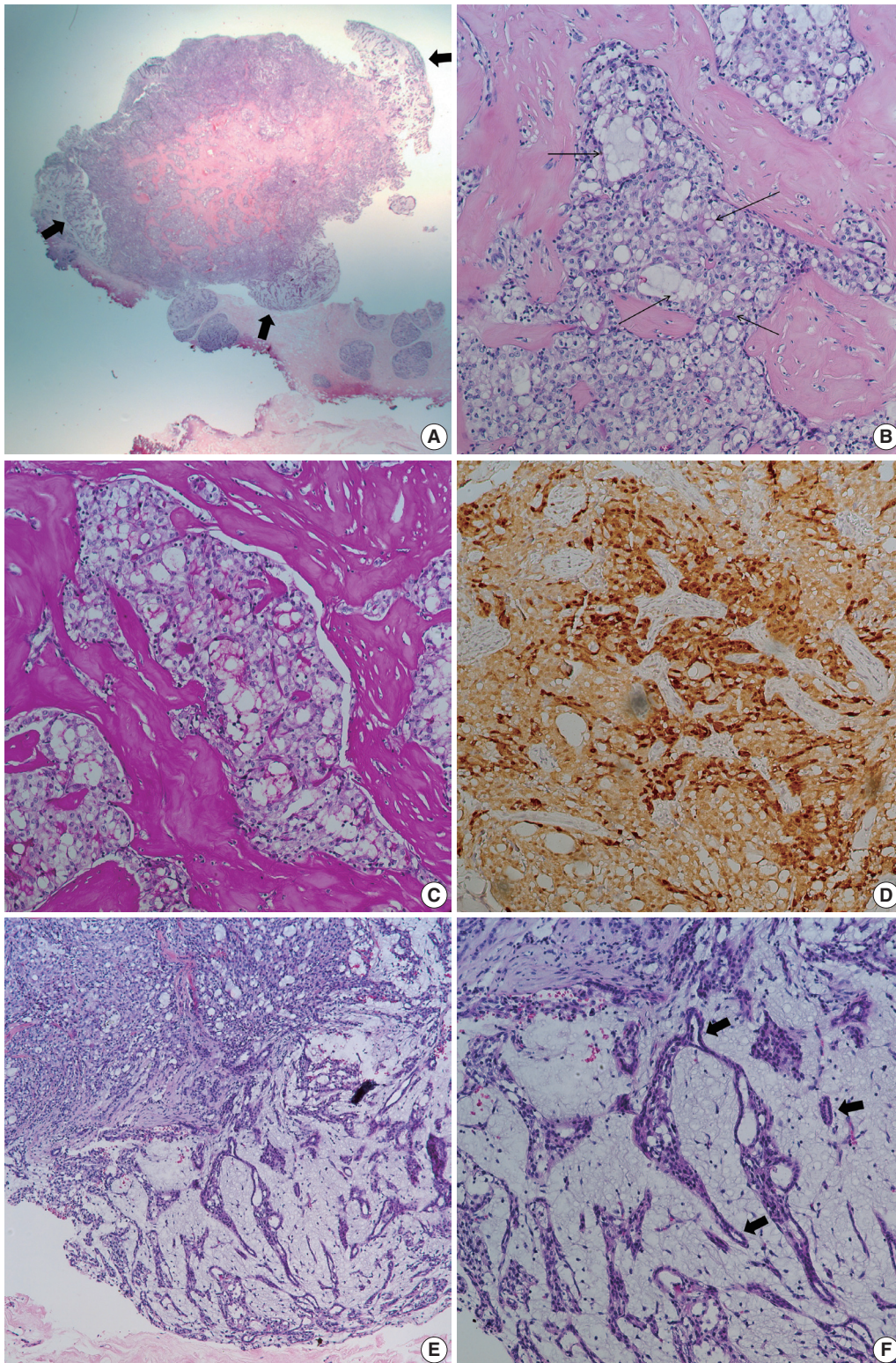


Fig. 1. Microscopic findings. (A) Low power field image shows fibrous septa within the tumor and peripheral hypocellular area (thick arrows). (B) Tumor shows solid or microcystic growth patterns within dense fibrous stroma. Cribriform tumor nests contain extracellular secretory material (thin arrows). Tumor cells have abundant, vacuolated cytoplasm. (C) Periodic acid Schiff staining highlights intra- and extracellular secretory material. (D) Tumor cells are diffusely positive for S-100 protein. (E) At the periphery of cellular tumor (left upper), hypocellular myxoid area is present (right lower). (F) Peripheral myxoid area shows mixture of bland tubules (arrows) and irregular tumor nests. (Continued to the next page)

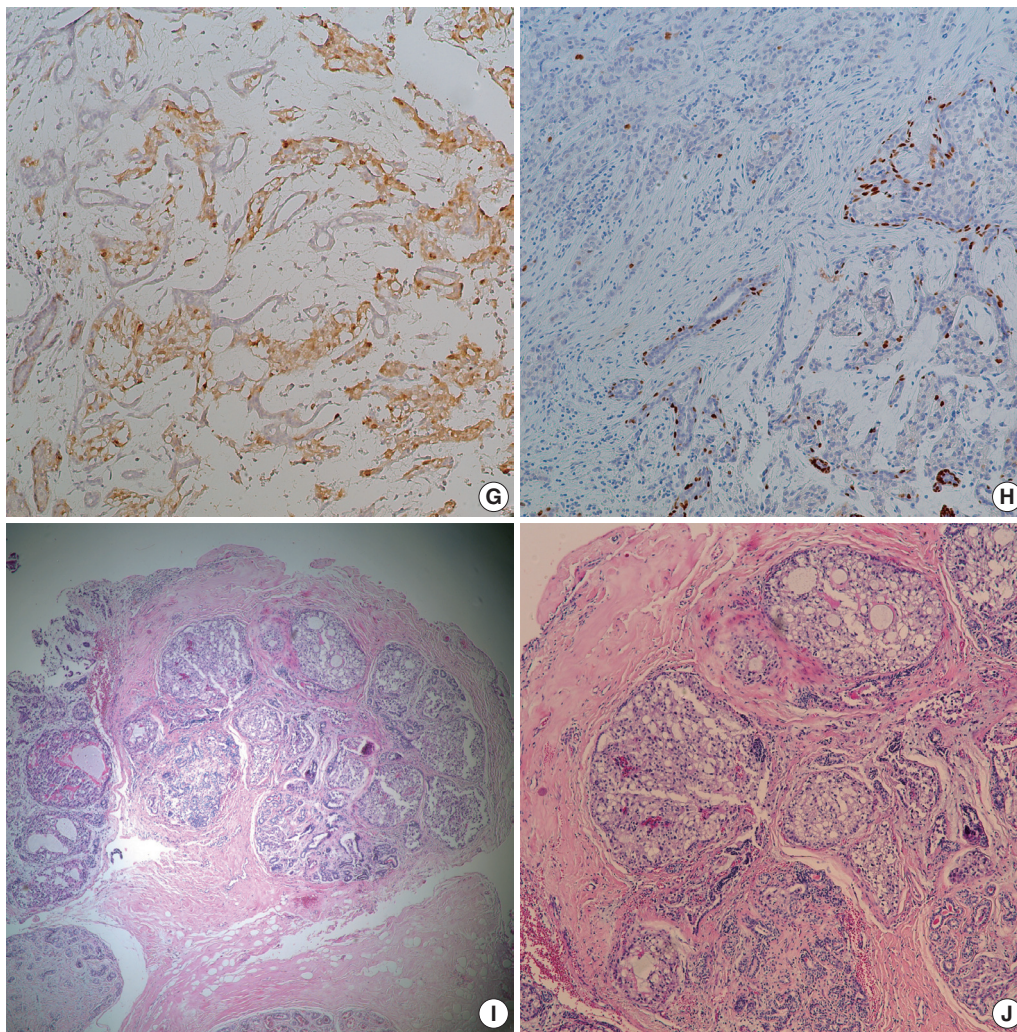


Fig. 1. (Continued from the previous page) (G) Tumor cells are positive for S-100 protein, while bland tubules are negative. (H) p63 staining highlights the presence of myoepithelial cells in the myxoid area. A few tumor cells express p63. (I) Ductal carcinoma *in situ* (DCIS) is noted in (left side) and outside the boundary of fibroadenoma. (J) DCIS also shows intracellular and extracellular secretory material.

due to tissue fragmentation. No further treatment was performed. The patient is well with no evidence of recurrence at 21 months after excision.

This study was approved by the Institutional Review Board of Samsung Medical Center, and informed consent was waived (2017-09-078).

DISCUSSION

Secretory carcinoma was initially described in 1966 as “juvenile breast carcinoma” by McDivitt and Stewart.⁵ Cases occurring in a wider age range were subsequently reported. Thus, the term “juvenile” was abandoned and the new title of “secretory carcinoma” was proposed by Tavassoli and Norris.⁶ Secretory carcinoma exhibits

typical microscopic features of solid, microcystic, and glandular growth patterns with intra- and extra-cellular secretory material. Immunophenotypically, secretory carcinoma usually belongs to the triple-negative, basal-like type, which is negative for ER, PR, and HER-2 with expression of basal (CK5/6 and CK14) markers.⁷ However, a recent large scale study from the National Cancer Data Base has reported that ER and PR are expressed in a considerable number of secretory carcinomas (64% and 44%, respectively).⁸ A balanced translocation, $t(12;15)$, that causes an *ETV6-NTRK3* fusion, also characterizes secretory carcinoma.⁹

Contrary to other basal-like type breast carcinomas, secretory carcinoma is a slowly growing, indolent disease with an estimated disease-specific survival of more than 90%.^{1,10} It has been shown that even patients with lymph node metastasis have excellent

prognosis.¹⁰ Distant metastasis is rare, but it is associated with large tumor size and multiple lymph node involvement.¹⁰

Breast cancer arising in a FA is an unusual presentation. Most reported cases have been lobular and ductal carcinoma *in situ*.² Some of the carcinomas were confined within the FA, while others showed extension beyond the FA.² In the case of carcinoma *in situ* arising in a FA, a more favorable prognosis has been suggested.² However, it is unknown whether the prognosis of carcinoma arising in a FA would differ from that of usual carcinoma because of the limited number of cases. It can be stated that in the case of carcinoma arising in FA, the FA attributes to a more favorable prognosis by enabling an earlier detection of the breast cancer due to mass effect.²⁻⁴

We described an unusual case of secretory carcinoma arising within a FA. To our knowledge, this is the first report of secretory carcinoma arising in a FA. Recognizing the FA component might be important for patient management.

Conflicts of Interest

No potential conflict of interest relevant to this article was reported.

REFERENCES

1. Horowitz DP, Sharma CS, Connolly E, Gidea-Addeo D, Deutsch I. Secretory carcinoma of the breast: results from the survival, epidemiology and end results database. *Breast* 2012; 21: 350-3.
2. Diaz NM, Palmer JO, McDivitt RW. Carcinoma arising within fibroadenomas of the breast: a clinicopathologic study of 105 patients. *Am J Clin Pathol* 1991; 95: 614-22.
3. Wu YT, Chen ST, Chen CJ, *et al*. Breast cancer arising within fibroadenoma: collective analysis of case reports in the literature and hints on treatment policy. *World J Surg Oncol* 2014; 12: 335.
4. Chintamani, Khandelwal R, Tandon M, *et al*. Carcinoma developing in a fibroadenoma in a woman with a family history of breast cancer: a case report and review of literature. *Cases J* 2009; 2: 9348.
5. McDivitt RW, Stewart FW. Breast carcinoma in children. *JAMA* 1966; 195: 388-90.
6. Tavassoli FA, Norris HJ. Secretory carcinoma of the breast. *Cancer* 1980; 45: 2404-13.
7. Laé M, Fréneaux P, Sastre-Garau X, Chouchane O, Sigal-Zafrani B, Vincent-Salomon A. Secretory breast carcinomas with *ETV6-NTRK3* fusion gene belong to the basal-like carcinoma spectrum. *Mod Pathol* 2009; 22: 291-8.
8. Jacob JD, Hodge C, Franko J, Pezzi CM, Goldman CD, Klimberg VS. Rare breast cancer: 246 invasive secretory carcinomas from the National Cancer Data Base. *J Surg Oncol* 2016; 113: 721-5.
9. Tognon C, Knezevich SR, Huntsman D, *et al*. Expression of the *ETV6-NTRK3* gene fusion as a primary event in human secretory breast carcinoma. *Cancer Cell* 2002; 2: 367-76.
10. Vasudev P, Onuma K. Secretory breast carcinoma: unique, triple-negative carcinoma with a favorable prognosis and characteristic molecular expression. *Arch Pathol Lab Med* 2011; 135: 1606-10.

Aberrant CD3 Expression in a Relapsed Plasma Cell Neoplasm

Jai-Hyang Go

Department of Pathology, Dankook University College of Medicine, Cheonan, Korea

Aberrant expression of CD3 is extremely rare in plasma cell neoplasm (PCN), and only a few cases have been reported.¹⁻⁶ Moreover, no studies have compared the expression pattern of CD3 between initial tumor and recurrent tumor in PCN. Herein, we describe an unusual case of PCN, which initially presented as CD3-negative plasmacytoma but exhibited aberrant CD3 expression at relapse. The tumor cells in both the initial tumor and relapsed tumor were positive for Epstein-Barr virus (EBV)-encoded RNA (EBER) *in situ* hybridization (ISH).

CASE REPORT

A 64-year-old man was admitted due to back pain of 2 months. Magnetic resonance imaging (MRI) showed pathologic fracture of the 12th thoracic vertebral body with anterior epidural and both paravertebral extensions (Fig. 1A). Histologic findings of bone biopsy showed differentiated PCN (Fig. 2A), which was positive for CD138 (Fig. 2B), MUM-1, and CD56 and weakly positive for CD10, but negative for CD20 or CD3 (Fig. 2C) and cyclin D1. The tumor cells were also positive for EBER ISH (Fig. 2D). The proliferation index (Ki-67) was approximately 50%. Bone marrow biopsy was negative. The patient was mildly anemic, and serum creatinine, blood urea nitrogen, and calcium levels were within the normal range. Serum immunoglobulin electrophoresis (EP) revealed a suspicious IgA λ monoclonal band. No M-proteins were detected in serum or urine protein EP. Serum levels of kappa (κ) and lambda (λ) free light chains (FLCs) were normal, and serum level of IgA

was mildly elevated to 473.0 mg/dL (normal range, 70 to 400). The patient was diagnosed with solitary plasmacytoma and received radiotherapy. Follow-up MRI at 4 months after initial diagnosis revealed multiple bone, muscle, and lymph node involvements (Fig. 1B). Physical examination revealed soft tissue masses in the right forearm, both thighs, and lower left abdomen. Histologically, tumors from the right forearm and lower left abdomen were composed of medium-sized and mononuclear blastic cells admixed with smaller cells showing plasmacytic differentiation, which was consistent with plasmablastic myeloma (PM) (Fig. 2E). The tumor cells were positive for CD138 (Fig. 2F), MUM-1, and CD56 and strongly positive for CD10 and CD3 (Fig. 2G), but negative for CD20 and cyclin D1. The proliferation index (Ki-67) was approximately 80%. The tumor cells were also positive for EBER ISH (Fig. 2H). At the time, the M-band was not yet detected in serum or urine protein EP, but the serum level of λ FLC was elevated to 117.2 mg/L (normal range, 5.71 to 26.3), and κ FLC was 13.8 mg/L (normal range, 3.3 to 19.4). Serum level of IgA was much more elevated at 1,230 mg/dL.

This study was approved by the Institutional Review Board of Dankook University Hospital, with informed consent waived (IRB No. 2017-09011).

DISCUSSION

We describe the first reported case of PCN in which aberrant CD3 expression is present only in the relapsed tumor, but not in the initial tumor, suggesting that CD3 expression is associated with disease progression and poor prognosis of PCN.

In the relapsed tumor in this case, plasmablastic lymphoma (PBL) should have been included in the differential diagnosis. A common histogenesis of PBL and PM is suggested with evidence linking these 2 tumors with morphological and immunophe-

Corresponding Author

Jai-Hyang Go
Department of Pathology, Dankook University College of Medicine, 119 Dandae-ro, Dongnam-gu, Cheonan 31116, Korea
Tel: +82-41-550-6972, Fax: +82-41-561-9127, E-mail: cyjy555@hanmail.net

Received: July 21, 2017 Revised: August 22, 2017

Accepted: September 5, 2017

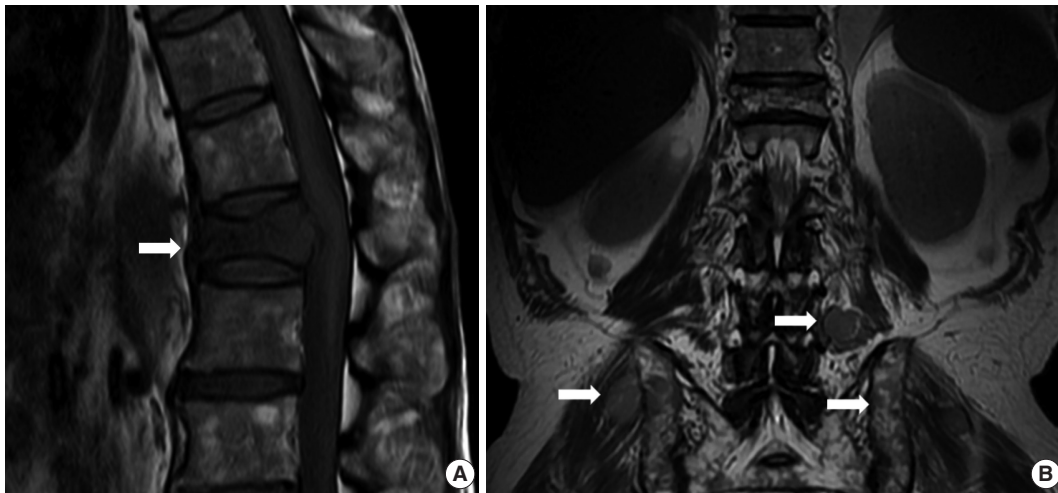


Fig. 1. Magnetic resonance imaging (MRI) showed pathologic fracture of 12th thoracic vertebral body with anterior epidural and both paravertebral extensions at initial presentation (A, arrow). Follow-up MRI at 4 months after initial diagnosis revealed multiple nodular masses in posterior paravertebral muscle, both gluteal muscles, and both iliac bones (B, arrows).

notypic similarities,⁷ including a high proliferation rate and expression of CD56 and CD10. These 2 markers are more often associated with PCN, but are positive in more than half of the cases of PBL,⁸ therefore, they cannot be used as definite criteria. Cyclin D1 is negative in PBL but positive in a subgroup of PCN.⁸ The distinction between PBL and PM is based largely on clinical presentation and the presence of EBV. PBL has a high association with EBV and is thought to lack the clinicopathological characteristics of PCN, which are monoclonal paraproteinemia, lytic bone lesions, and proliferation of plasma cells in the bone marrow, peripheral blood, or extramedullary sites.⁷ Therefore, high-grade lymphomas with plasmablastic morphology, occurring in an immunocompromised patient, localized primarily in extramedullary sites that are positive for EBV would be designated as PBL. In contrast, PM occurs in patients with preexisting or concurrent clinical evidence of PCN.⁷

Aberrant CD3 expression in B-cell neoplasm is relatively rare. Most cases have been EBV-associated malignancies including pyothorax- or immunodeficiency-associated lymphomas¹ and PBL.^{3,9} However, a recent study has revealed that EBV-negative tumors with plasmacytic differentiation including plasma cell myeloma and plasmacytoma were the main subset of CD3-positive B-cell tumors.¹ However, CD3 expression is still considered to be rare in PCN. Only 9 cases of PCN with aberrant CD3 expression have been reported in the literature (Table 1).¹⁻⁶

Lineage infidelity is uncommon in terminally differentiated B-cell lymphomas,⁹ and neoplastic plasma cells infrequently have aberrant phenotypic characteristics.² Myeloma cells have been found to express a wide array of early and late differentiation

markers pertaining to myeloid, monocytic, erythroid, megakaryocytic, and B-cell and T-cell lineages.⁵ However, these aberrant phenotypes have largely been limited to B-cell antigen expression including CD10 and TdT,² and neoplastic plasma cells very rarely express T-cell antigen.^{2,10} An aberrant phenotype is seen mostly in poorly differentiated or anaplastic myelomas associated with poor prognosis.¹⁰ Therefore, coexpression of non-lineage-restricted markers CD10, CD13, and CD33 on myeloma cells has been associated with poor prognosis.⁵

One study has reported that T antigen expression was present in 6 patients with multiple myelomas.² Among them, 5 cases were relapsed tumors, and the survival from demonstration of T antigen expression was very short in these cases,² suggesting that aberrant T antigen expression can be related to poor prognosis. Two additional relapsed PCN with CD3 expression have been reported.^{5,6} However, few reports have compared the expression patterns of CD3 between initial and recurrent tumors of PCN. In the present case, the initial tumor of CD3-negative plasmacytoma was relapsed to CD3-positive PM.

The reason for T antigen expression in PCN is not clearly understood. It might indicate that myeloma can arise from a normal minor subpopulation of B cells involved in immunoregulation. Aberrant T-cell antigen expression in B-cell lymphomas has been linked to host immunodeficiency.⁹ It has been suggested that EBV can promote T-cell antigen expression in B-cell tumors¹ or could be a coincidental aberrancy associated with malignant change in plasma cells.²

Several factors have been associated with prognosis of PCN. Plasmablastic and anaplastic cytologic types are correlated with

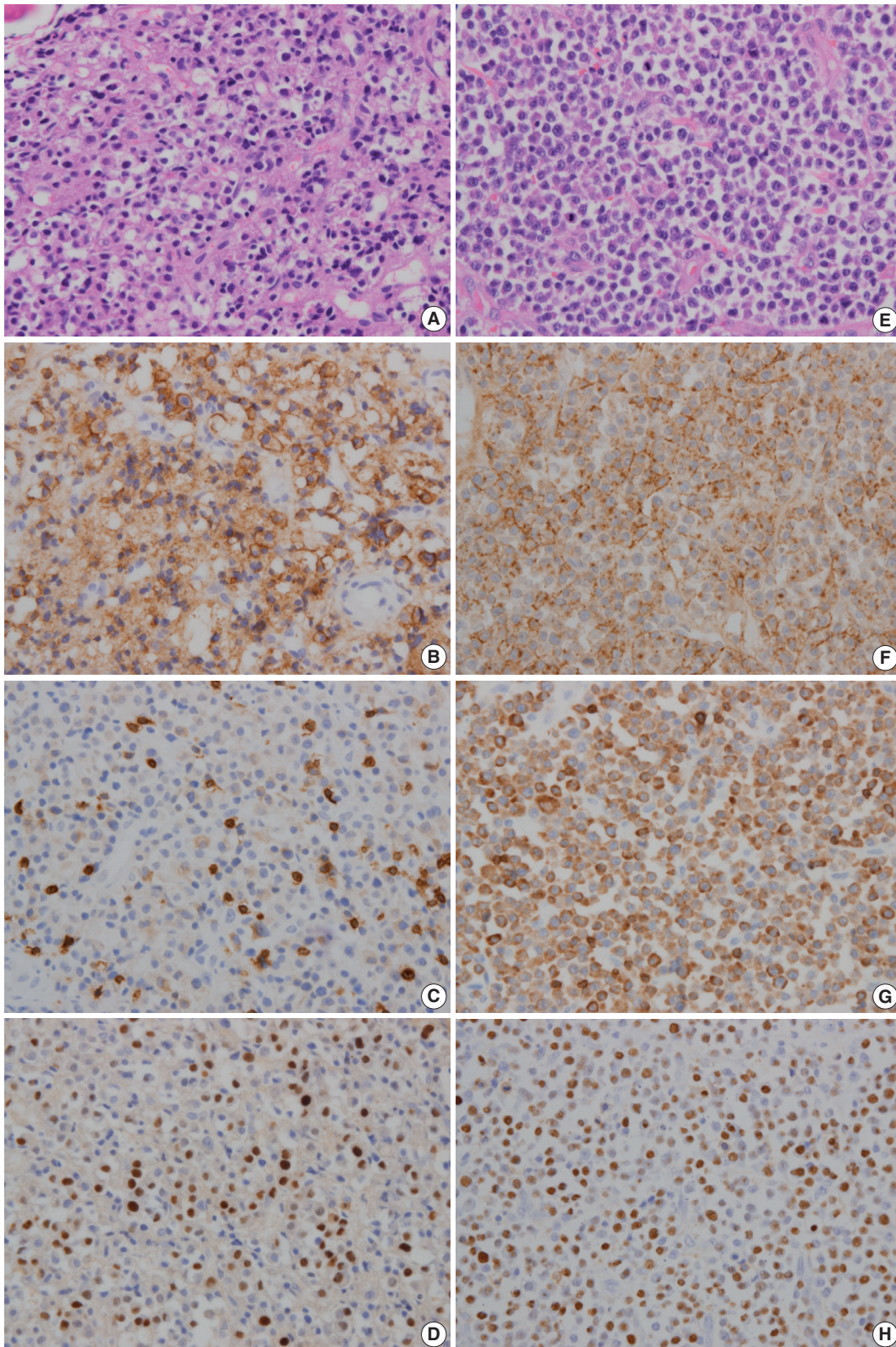


Fig. 2. In initial bone biopsy, the tumor was composed of differentiated plasma cells (A), which were positive for CD138 (B), but negative for CD3 (C). (D) The tumor cells were positive for Epstein-Barr virus-encoded RNA (EBER) *in situ* hybridization. (E) In relapsed soft tissue biopsy, the tumor was composed of medium-sized blastic cells admixed with smaller plasmacytic cells. Most of the tumor cells were strongly positive for CD138 (F) and CD3 (G). (H) The tumor cells were also positive for EBER ISH.

Table 1. Summary of previously published PCN cases with CD3 expression

| Case No. | Diagnosis | Sex | Age (yr) | Location | CD20 | CD10 | EBV | Reference |
|----------|-----------------------|-----|----------|--------------|------|------|-----|-------------------------------------|
| 1 | Myeloma | M | 62 | BM | +/- | + | ND | Spier <i>et al.</i> ² |
| 2 | Myeloma | M | 69 | BM | ND | ND | ND | Yagci <i>et al.</i> ⁵ |
| 3 | Plasmacytoma | M | 57 | Sacrum | - | ND | - | Oliveira <i>et al.</i> ¹ |
| 4 | Plasmablastic myeloma | M | 60 | Neck, thorax | - | ND | - | Oliveira <i>et al.</i> ¹ |
| 5 | Plasmacytoma | M | 48 | Sacrum | - | - | ND | Oliveira <i>et al.</i> ¹ |
| 6 | Anaplastic myeloma | M | 59 | BM | - | ND | - | Oliveira <i>et al.</i> ¹ |
| 7 | Myeloma | M | 67 | Radius, LN | - | - | - | Tang <i>et al.</i> ³ |
| 8 | Myeloma | M | 62 | Mandible, BM | - | - | - | Luo <i>et al.</i> ⁴ |
| 9 | Myeloma | F | 60 | Skin | - | ND | - | Mishra <i>et al.</i> ⁶ |

PCN, plasma cell neoplasm; EBV, Epstein-Barr virus; M, male; BM, bone marrow; ND, not done; LN, lymph node; F, female.

more aggressive disease.¹⁰ Change to more aggressive phenotype is seen in relapsed cases of PCN.¹⁰ However, an association with EBV has not been fully elucidated in previous cases of CD3-expressing relapsed PCNs. In the present case, both initial differentiated PCN and relapsed plasmablastic tumor were positive for EBER ISH. This suggested that a gain of CD3 in PCN is associated with tumor progression to high-grade morphology and aggressive clinical course, which might be attributable to EBV infection. In this context, aberrant expression of CD3 might be useful as a phenotypic marker for disease progression of PCN and could be a candidate to direct further treatment in relapsed PCN.

Conflicts of Interest

No potential conflict of interest relevant to this article was reported.

REFERENCES

- Oliveira JL, Grogg KL, Macon WR, Dogan A, Feldman AL. Clinicopathologic features of B-cell lineage neoplasms with aberrant expression of CD3: a study of 21 cases. *Am J Surg Pathol* 2012; 36: 1364-70.
- Spier CM, Grogan TM, Durie BG, *et al.* T-cell antigen-positive multiple myeloma. *Mod Pathol* 1990; 3: 302-7.
- Tang YL, Chau CY, Yap WM, Chuah KL. CD3 expression in plasma cell neoplasm (multiple myeloma): a diagnostic pitfall. *Pathology* 2012; 44: 668-70.
- Luo X, Kuklani R, Bains A. Dual CD3 and CD4 positive plasma cell neoplasm with indistinct morphology: a diagnostic pitfall. *Pathology* 2016; 48: 378-80.
- Yagci M, Sucak GT, Akyol G, Haznedar R. Hepatic failure due to CD3+ plasma cell infiltration of the liver in multiple myeloma. *Acta Haematol* 2002; 107: 38-42.
- Mishra P, Kakri S, Gujral S. Plasmablastic transformation of plasma cell myeloma with heterotropic expression of CD3 and CD4: a case report. *Acta Clin Belg* 2017; 72: 250-3.
- Taddesse-Heath L, Meloni-Ehrig A, Scheerle J, Kelly JC, Jaffe ES. Plasmablastic lymphoma with MYC translocation: evidence for a common pathway in the generation of plasmablastic features. *Mod Pathol* 2010; 23: 991-9.
- Vega F, Chang CC, Medeiros LJ, *et al.* Plasmablastic lymphomas and plasmablastic plasma cell myelomas have nearly identical immunophenotypic profiles. *Mod Pathol* 2005; 18: 806-15.
- Sun J, Medeiros LJ, Lin P, Lu G, Bueso-Ramos CE, You MJ. Plasmablastic lymphoma involving the penis: a previously unreported location of a case with aberrant CD3 expression. *Pathology* 2011; 43: 54-7.
- Gorczyca W. Atlas of differential diagnosis in neoplastic hematopathology. 3rd ed. Boca Raton: CRC Press, 2014; 359-81.

Merkel Cell Carcinoma Metastatic to Pleural Fluid: A Case Report

Ye-Young Rhee · Soo Hee Kim
Eun Kyung Kim¹ · Se Hoon Kim¹

Pathology Center, Seegene Medical Foundation, Seoul; ¹Department of Pathology, Severance Hospital, Yonsei University College of Medicine, Seoul, Korea

Received: October 11, 2017
Revised: November 7, 2017
Accepted: November 9, 2017

Corresponding Author

Se Hoon Kim, MD, PhD, FIAC
Department of Pathology, Severance Hospital,
Yonsei University College of Medicine, 50-1
Yonsei-ro, Seodaemun-gu, Seoul 03722, Korea
Tel: +82-2-2228-1769
Fax: +82-2-362-0860
E-mail: paxco@yuhs.ac

Merkel cell carcinoma (MCC) is a rare aggressive neuroendocrine carcinoma of the skin that shows locoregional or distant metastasis. Metastasis of MCC to body cavity effusion is extremely rare; only three cases have been reported so far. Metastatic MCC in effusion cytology shows small blue round cells with fine stippled chromatin like other small blue round cell tumors such as small cell lung carcinoma or lymphoma. The diagnosis of metastatic MCC can grant patients good chances at recently advanced therapeutic options. Here, we present a case of metastatic MCC to pleural effusion with characteristic single file-like pattern.

Key Words: Carcinoma, Merkel cell; Neoplasm metastasis; Pleural fluid; Liquid-based cytology

Merkel cell carcinoma (MCC) is an uncommon aggressive neuroendocrine tumor of the skin that occurs primarily in the elderly or immunosuppressed individuals and often shows locoregional or distant metastasis.¹⁻³ Toker first reported it as “trabecular carcinoma” in 1972,⁴ however, MCC has not been investigated as actively as other skin tumors due to its rarity and uncertain etiology until recently when diagnostic tools including immunohistochemistry have improved and polyomavirus has been identified to be associated with the tumor.^{2,5} Although the incidence of MCC is increasing and locoregional recurrence or metastasis has become common, distant metastases of MCC especially to body cavity effusions are extremely rare. There are only three case reports of metastatic MCC to effusions: two to pleural fluid and one to ascites.⁶⁻⁸ Here, we report the first case of metastatic MCC to pleural effusion in Korea.

CASE REPORT

This study was approved by the Institutional Review Board of Severance Hospital with a waiver of informed consent (IRB No. 4-2017-0634).

A 68-year-old female with a medical history of hypertension was diagnosed with MCC in the left buttock 2 years ago at an

outside hospital. The patient underwent excision of the tumor with inguinal lymph node dissection. Local recurrence occurred after one year, leading to additional left inguinal lymph node dissection. According to the positron emission tomography, metastases to the regional, intra-abdominal, and right axillary lymph nodes were identified. The patient was treated with three cycles of etoposide and cisplatin (EP) chemotherapy and radiotherapy in the left leg, para-aortic lymph node, and right inguinal lymph node. The patient was transferred to our hospital due to bone metastasis. Even after five cycles of cyclophosphamide, doxorubicin and vincristine (CAV), the disease progressed and the patient received first intraperitoneal chemotherapy. The patient was admitted to the hospital for fever, diarrhea, poor oral intake, and pancytopenia. Metastasis in a small-to-borderline sized lymph node in the left axilla and bilateral pleural effusion (Fig. 1) were identified.

Surgically excised specimen stained with hematoxylin and eosin presented blue round cell tumor with infiltrative growth, showing sheets, clusters, rows or balls of tumor cells with scanty cytoplasm, hyperchromatic nuclei, fine stippled or smudged chromatin and occasional mitoses (Fig. 2A–D). Immunohistochemical staining showed the tumor cells positive for cytokeratin 20 (CK20), CD56, chromogranin, and synaptophysin (Fig. 2C, D).

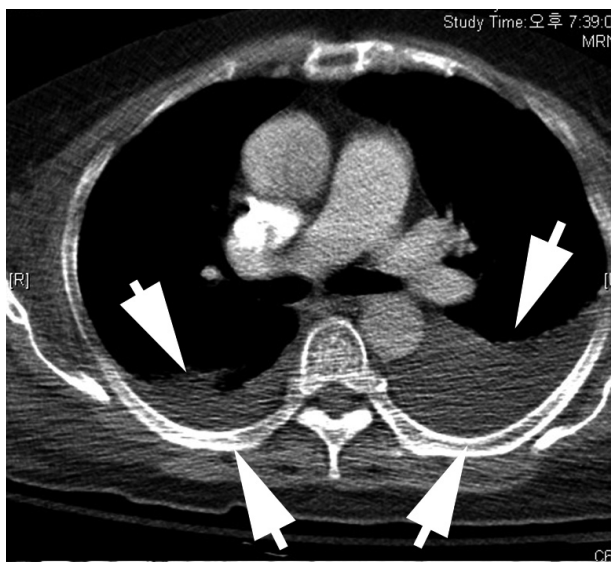


Fig. 1. Chest computed tomography (CT) with cell block findings. The chest CT shows marked pleural effusion (arrows).

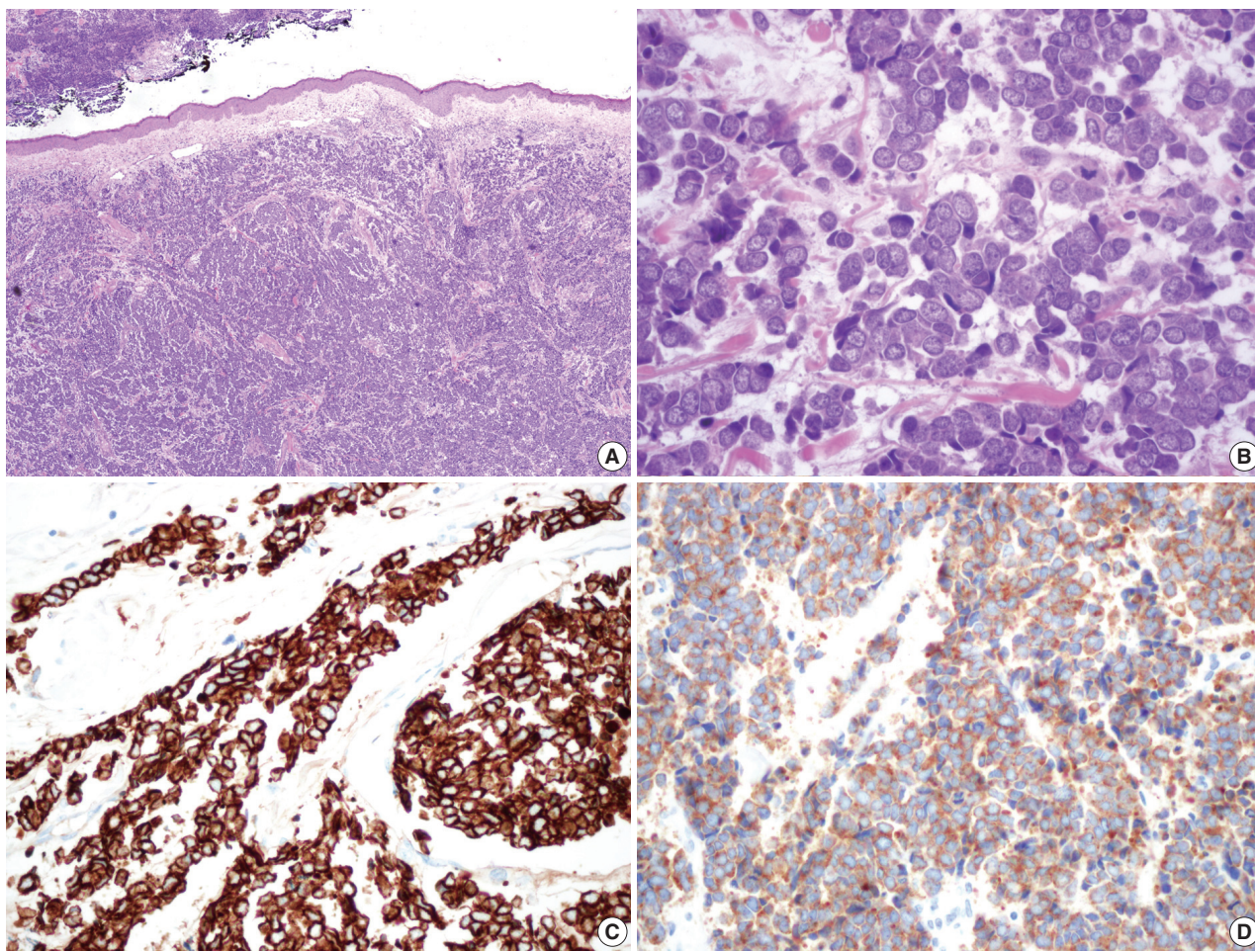


Fig. 2. Microscopic findings of the surgical specimen. Blue small round cell tumor with infiltrative growth (A) arranged in sheets, clusters, rows or balls, showing hyperchromatic nuclei, fine stippled or smudged chromatin and occasional mitoses (B). Immunohistochemical staining of cytokeratin 20 (C) and synaptophysin (D) show positive reaction in Merkel cell carcinoma cells.

Liquid based cytology (LBC; SurePath, BD Diagnostics, Burlington, NC, USA) (Fig. 3A) and cell block of pleural effusion (Fig. 3B) revealed malignant small blue round cells scattered, clustered, or arranged in a single file. Round to oval tumor cells showed hyperchromatic nuclei with fine granular salt and pepper chromatin, scant cytoplasm, occasional mitotic figures, and occasional nuclear molding (Fig. 3A). Immunohistochemical staining on the cell block also showed the tumor cells immunoreactive for CK20, CD56, chromogranin, and synaptophysin (Fig. 3C, D).

DISCUSSION

MCC is a rare and highly aggressive skin carcinoma often seen in the head and neck region.⁵ The increasing incidence^{1,9,10} and recent new findings about risk factors, especially the identification of polyomavirus infection,² stimulated the investigation of the etiology, pathogenesis and treatment options.^{3,5} Although

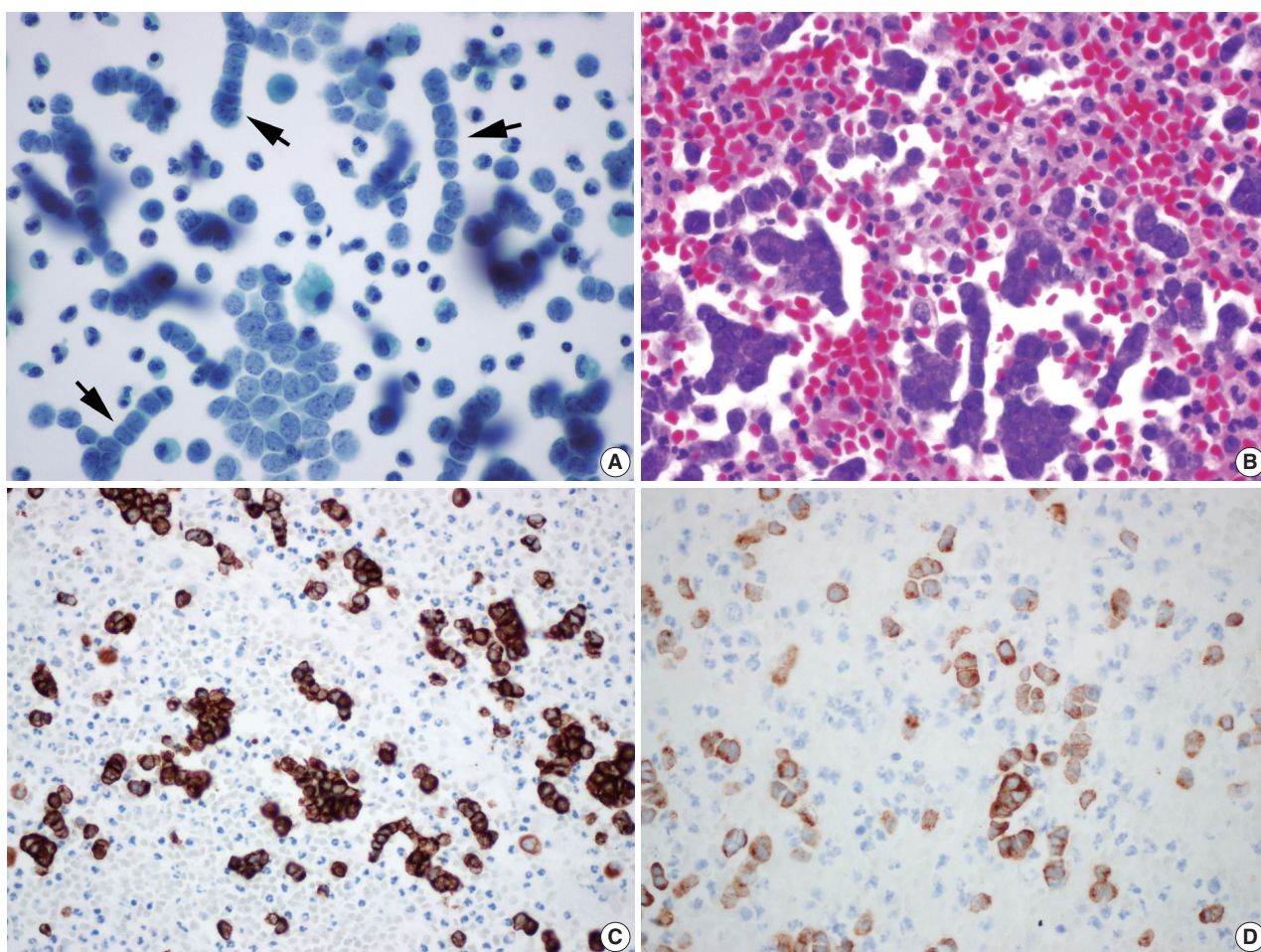


Fig. 3. (A) Liquid based cytology (BD Surepath) of the pleural effusion (Papanicolaou stain). Malignant small blue round cells are scattered, clustered or arranged with hyperchromatic nuclei, fine granular salt and pepper chromatin, scant cytoplasm, and occasional mitotic figures. Several single file patterns with nuclear molding are characteristic (arrows). (B) The cell block findings are similar to those in liquid based cytology's. Immunohistochemical staining of cytokeratin 20 (C) and synaptophysin (D) in the cell block of pleural effusion.

most patients present with localized tumors or with locoregional metastasis including lymph node metastasis without a primary MCC,¹¹ distant metastases have also been reported. According to a single institution data, the clinical stage III (positive regional lymph node) and IV (distant metastatic disease) were 24% and 6%, respectively.¹²

We reported a rare case of metastatic MCC to pleural effusion that had not been reported in Korea before. So far, only two cases of pleural metastasis of MCC have been reported worldwide. The first case was a metastasis of left great toe MCC to the pleural fluid, confirmed by electron microscopy.⁶ The second case was a metastasis of right buttock MCC to the pleural fluid, confirmed by immunohistochemical staining of CK20.⁷ Both cases showed small blue round cell clusters with fine granular chromatin in the pleural fluid as in our case. MCC stains positive for CK20 (a dot-like perinuclear positivity pattern), other epithelial

markers (AE1/AE3, epithelial membrane antigen, and CAM 5.2), and neuroendocrine markers (chromogranin, CD56, synaptophysin, and somatostatin).⁵ We confirmed our diagnosis by immunoreactivity of the tumor to CK20, CD56, chromogranin, and synaptophysin both in surgical specimen and cytology cell block.

The diagnosis of metastatic MCC to body cavity effusion is easy to be missed because of its rarity and similarity of morphology to other small round cell tumors. Microscopic findings of the pleural effusion cytology of metastatic MCC can be confused with metastasis of other malignant neoplasm showing small blue round cells: small cell lung carcinoma, lymphoma, malignant melanoma, etc. However, immunohistochemical markers such as CK20, CD56, chromogranin, and synaptophysin would be helpful.

In this case, multiple single file patterns with cytological

molding were dominant in both LBC and cell block. This identification of multiple single file patterns is a novel finding that has not been described in previous reports.^{6,7} It is more characteristic in LBC and may therefore be a helpful cytological clue in the era of LBC. The detection of hidden MCC presented only as distant metastasis in effusion could give patients good chances at cure because therapeutic options for MCC have increased recently: chemotherapy, immunotherapy, radiotherapy and targeted therapy.¹³

Conflicts of Interest

No potential conflict of interest relevant to this article was reported.

REFERENCES

- Hodgson NC. Merkel cell carcinoma: changing incidence trends. *J Surg Oncol* 2005; 89: 1-4.
- Feng H, Shuda M, Chang Y, Moore PS. Clonal integration of a polyomavirus in human Merkel cell carcinoma. *Science* 2008; 319: 1096-100.
- Pulitzer MP, Amin BD, Busam KJ. Merkel cell carcinoma: review. *Adv Anat Pathol* 2009; 16: 135-44.
- Toker C. Trabecular carcinoma of the skin. *Arch Dermatol* 1972; 105: 107-10.
- Pulitzer M. Merkel cell carcinoma. *Surg Pathol Clin* 2017; 10: 399-408.
- Watson CW, Friedman KJ. Cytology of metastatic neuroendocrine (Merkel-cell) carcinoma in pleural fluid: a case report. *Acta Cytol* 1985; 29: 397-402.
- Payne MM, Rader AE, McCarthy DM, Rodgers WH. Merkel cell carcinoma in a malignant pleural effusion: case report. *Cytojournal* 2004; 1: 5.
- Policarpio-Nicolas ML, Avery DL, Hartley T. Merkel cell carcinoma presenting as malignant ascites: a case report and review of literature. *Cytojournal* 2015; 12: 19.
- Fitzgerald TL, Dennis S, Kachare SD, Vohra NA, Wong JH, Zervos EE. Dramatic increase in the incidence and mortality from Merkel cell carcinoma in the United States. *Am Surg* 2015; 81: 802-6.
- Robertson JP, Liang ES, Martin RC. Epidemiology of Merkel cell carcinoma in New Zealand: a population-based study. *Br J Dermatol* 2015; 173: 835-7.
- Eng TY, Boersma MG, Fuller CD, *et al*. A comprehensive review of the treatment of Merkel cell carcinoma. *Am J Clin Oncol* 2007; 30: 624-36.
- Allen PJ, Bowne WB, Jaques DP, Brennan MF, Busam K, Coit DG. Merkel cell carcinoma: prognosis and treatment of patients from a single institution. *J Clin Oncol* 2005; 23: 2300-9.
- Barksdale SK. Advances in Merkel cell carcinoma from a pathologist's perspective. *Pathology* 2017; 49: 568-74.

